DISSERTATION

for the degree of

Doctor of Natural Sciences

submitted to the

Combined Faculties for the Natural Sciences and for Mathematics

of the Ruperto-Carola University of Heidelberg, Germany

presented by
Diplom-Biologin Sabine Katja Vogel
born in Heidelberg

Oral examination:

Mechanistic Studies on Transcription Activation via DNA Looping in a Prokaryotic Promoter-Enhancer System

Referees:
PD Dr. Karsten Rippe
PD Dr. Renate Voit

La raison fait l'homme,
mais c'est le sentiment qui le conduit.
Jean-Jacques Rousseau

Danke...

PD Dr. Karsten Rippe danke ich für die Überlassung des Themas und seine wissenschaftliche Unterstützung dieser Arbeit. Ich danke PD Dr. Renate Voit für die freundliche Übernahme des Koreferats.
Außerdem möchte ich meinen Kollegen Felix, Gerrit, Jacek, Kata, Malte, Thibaud und Tobi für die stets angenehme Arbeitsatmosphäre und den netten Umgang miteinander danken. Insbesondere möchte ich mich noch einmal ausdrücklich bei Kata, Karsten und Malte für das unermüdliche Korrekturlesen bedanken. Den namentlich nicht genannten Kollegen des Kirchhoff-Instituts für Physik danke ich ebenfalls für die angenehme Atmosphäre. Prof Dr. Peter Lichter und seinem 'Team' sei an dieser Stelle dafür gedankt, dass ich meine Radioaktivarbeiten in ihrem Labor machen durfte und ich trotz vorangeschrittener Stunde meist Gesellschaft hatte. Vielen Dank auch an Dich Margit für die Bearbeitung aller angefallenen Formalitäten. Andreas Hunziker sei gedankt für das schnelle und sorgfältige Sequenzieren der Transkriptionsplasmide. Bei Nick möchte ich mich für die aufopfernde Einarbeitung in LaTeX und die Versorgung mit Süßem bedanken. Ich danke Frau Dr. Wieland-Rigamonti, die mir gezeigt hat, die wirklich wichtigen Dinge im Leben zu erkennen und daran zu glauben. Außerdem danke ich allen meinen Freunden, die mir immer mit Rat und Tat zur Seite stehen, insbesondere Dir, Helmut. Danke!

Merci...

Je remercie surtout ma grand-mère Raymonde qui m'a toujours soutenue moralement et financièrement. Je dois surtout 'un grand merci' à Jean-Claude, Anna, Guillaume, Hélène et Felix. Je leur suis très reconnaissante de s'être occupés de ma grand-mère. Merci!

List of publication

- Binding affinity of *Escherichia coli* RNA polymerase·σ^{54} holoenzyme for the *gln*Ap2, *nif*H and *nif*L promoters, S. K. Vogel, A. Schulz and K. Rippe, *Nucleic Acids Research*, 30 (18):4094-101, 2002
- Modulating the transcription activity of NtrC with different combinations of enhancer elements, S. K. Vogel & K. Rippe (in preparation)

The work was done at the Deutsches Krebsforschungszentrum (division Biophysik der Makromoleküle) and the Kirchhoff-Institut für Physik (division Molekulare Biophysik) The project was funded by the Deutsche Forschungsgemeinschaft.

Zusammenfassung

In dieser Arbeit wurde die Aktivierung der Transkription in einem prokaryotischen Promotor-Enhancer-System untersucht. Es besteht aus der *E. coli* RNA-Polymerase, die mit der alternativen Sigma-Untereinheit σ^{54} assoziiert ist (RNAP·σ^{54}) und dem Transkriptions-Aktivatorprotein NtrC (Nitrogen regulatory protein C), das vom Promotor entfernt an die Enhancer-Region bindet. NtrC am Enhancer kontaktiert unter Schleifenbildung der DNA die RNA-Polymerase am Promotor (geschlossener Komplex) und induziert das Aufschmelzen der Promotor-DNA durch RNAP·σ^{54} (offener Komplex). Folgende Aspekte dieser Reaktion wurden untersucht:
(1) In Bindungsstudien und in *in vitro* Transkriptionsexperimenten wurden drei verschiedene σ^{54}-spezifischen Promotorsequenzen analysiert. Diese Promotoren waren, wie aus *in vivo* Expressionsstudien und DNA Schutzexperimenten bekannt, von unterschiedlicher Promotorstärke. Da die Initiation der Transkription aus verschiedenen nacheinander ablaufenden Schritten besteht (Promotorbindung der RNAP, Isomerisierung zum offenen Komplex und Bildung eines stabilen Elongationskomplexes) war bis dahin unklar, welches der geschwindigkeitsbestimmende Schritt der Gesamtreaktion ist. Für die Promotoren *gln*Ap2 und *nif*L war die Promotorbindung der RNAP·σ^{54} geschwindigkeitsbestimmend. Im Gegensatz dazu war für den *nif*H Promotor, der zwar eine starke Affinität zu RNAP·σ^{54} besitzt, aber nur schwach in vivo exprimiert, das Aufschmelzen der DNA bestimmend für die Gesamtreaktion der Transkription.
(2) Mittels Rasterkraftmikroskopie wurde festgestellt, dass die gebundene RNAP·σ^{54} die DNA krümmt und deshalb vorzugsweise in der Endschleife einer superhelikalen DNA lokalisiert wird, da dort die DNA stärker gebogen ist. Diese Lokalisation in der Endschleife erleichtert die Interaktion zwischen NtrC and RNAP·σ^{54} trotz der geringen Biegsamkeit der dazwischen liegenden DNA.
(3) Die Interaktion zwischen σ^{54} und NtrC wurde in einem ATPase-Test und in Gelshift-Experimenten analysiert. Es wurde festgestellt, dass σ^{54} die ATPase-Aktivität von NtrC unter den Versuchsbedingungen nicht beeinflusst, während die Bindung von NtrC an den Enhancer die Aktivität durch Oligomerisierung von NtrC stark stimuliert. Bindungsstudien, die mit Hilfe der analytischen Ultrazentrifugation und Gelshift-Experimenten durchgeführt wurden, haben außerdem gezeigt, dass σ^{54} allein den Promotor nur sehr schwach binden kann im Gegensatz zum RNAP·σ^{54}-Holoenzym. Dies unterstützt die Vorstellung, dass die Sigma-Untereinheit vor allem dazu dient, die Promotorsequenz zu erkennen, während das RNAP-Holoenzym die Bindungsenergie für eine hochaffine Promotorbindung liefert.
(4) In *in vitro* Transkriptionsexperimenten wurde gezeigt, dass NtrC je nach Position, Anzahl und Zusammenstellung seiner Bindungsstellen die Transkription verschieden stark aktiviert oder sogar als Repressor wirken kann. Es zeigte sich, dass der Promotor mit bestimmten Kombinationen aus starken und schwachen NtrC-Bindungsstellen bei sehr unterschiedlichen NtrC-Konzentrationen aktiviert wird. Dies ermöglicht die Regulation der Transkription in Abhängigkeit von der NtrC-Konzentration. Darüber hinaus konnte gezeigt werden, dass eine Transkriptionaktivierung auch ohne DNA-Schleifenbildung bei höheren NtrC-Konzentrationen stattfindet. Anhand dieser Ergebnisse wurde ein Modell der RNAP·σ^{54}-NtrC-vermittelten Transkriptionsaktivierung erstellt: Demnach erleichtern NtrC-Bindungsstellen nahe des Promotors die Interaktion zwischen NtrC und RNA-Polymerase im Loopkomplex bei niedrigen NtrC-Konzentrationen, während sie bei höheren Konzentrationen die Transkriptionsaktivierung auf ein bestimmtes Maximum limitieren. In diesem Fall wird eine andere NtrC-Spezies gebildet, die ohne DNA-Schleifenbildung mit der RNAP·σ^{54} interagieren kann.

Summary

In this thesis, transcription activation was studied in a prokaryotic promoter-enhancer system. It comprises the *E. coli* RNA polymerase, which is associated with the alternative sigma factor σ^{54} (RNAP·σ^{54}), and the transcription activator protein NtrC (nitrogen regulatory protein C), which binds to a remote enhancer region to the promoter. Enhancer-bound NtrC contacts the RNA polymerase at the promoter by means of DNA looping (closed complex) and induces DNA melting of the promoter DNA by RNAP·σ^{54} (open complex). The following aspects of this process were studied:
(1) Three different σ^{54}-specific promoter sequences were analyzed in binding studies and in *in vitro* transcription experiments. These promoters were known to have different overall promoter strength as determined by *in vivo* expression and DNA footprinting studies. Since initiation of transcription comprises different subsequent steps (promoter-binding by RNAP·σ^{54}, isomerization to the open complex and formation of a stable elongation complex) it was still unclear, which is the rate limiting step of the total reaction. For the *gln*Ap2 and *nif* L promoters, the promoter-binding by RNAP·σ^{54} was rate limiting. In contrast, for the *nif* H promoter with a high affinity to RNAP·σ^{54} but with a low *in vivo* expression level, the DNA melting step determined the overall speed of the transcription initiation reaction.
(2) By scanning force microscopy it was determined that promoter-bound RNAP·σ^{54} bends the DNA and is for this reason preferably localized in the end-loop of a supercoiled DNA, since the DNA is more bent in this region. The localization in the end-loop facilitates the interaction between NtrC and RNAP·σ^{54} in spite of the low flexibility of the intervening DNA.
(3) The interaction between σ^{54} and NtrC was studied in an ATPase assay and in gel shift experiments. It was shown that σ^{54} has no effect on the ATPase activity of NtrC under the experimental conditions whereas enhancer-binding of NtrC strongly stimulates the ATPase activity by facilitating the oligomerizaion of NtrC. Binding studies that were performed by analytical ultracentrifugation and gel shift experiments have also shown that σ^{54} alone only weakly bind sthe promoter DNA in contrast to the RNAP·σ^{54} holoenzyme. This supports the idea, that the sigma factor acts by recognizing the promoter sequence whereas the RNAP holoenzyme provides the binding energy for high affinity promoter binding.
(4) *In vitro* transcription experiments showed that NtrC activates with different efficiency and can even act as a repressor depending on the position, number and arrangement of its binding sites. Certain combinations of weak and strong NtrC binding sites were shown to activate transcription from the promoter at very different concentrations of NtrC. This enables a regulation of transcription in dependence of the NtrC concentration. From these results, a model of RNAP·σ^{54}-NtrC-mediated transcription activation was developed: Accordingly, the proximal NtrC sites very close to the promoter facilitate the interaction between activator and RNA polymerase in a loop complex at low NtrC concentrations, whereas at higher concentrations the transcriptional activation is limited to a maximum level. In this case, a NtrC species is formed, which can interact with the RNAP·σ^{54} without DNA looping.

Contents

List of Figures

List of Tables

Chapter 1

Introduction

Initiation of transcription is a central process for the regulation of gene expression. The proteins involved are typically parts of hetero-oligomeric complexes. The assembly of these complexes is often subject to regulation, since initiation of transcription depends strongly on the availability and the binding affinity of different proteins. After assembly and binding of the macromolecules at the promoter recognition sequence, interaction between the transcription complex at the promoter and other cis- or trans- regulating molecules can occur to initiate RNA synthesis.
In prokaryotic and eukaryotic organisms transcription of protein-coding genes is driven by a multi-subunit protein complex, the RNA polymerase (RNAP; 5 subunits in *Escherichia coli*, 12 subunits for RNAP II in *Saccharomyces cerevisiae* [1] and > 12 subunits in higher eukaryotic cells). The 'preinitiation' complex that forms prior to transcription is often referred to as 'closed' complex in which the DNA is fully double-stranded. The transcription initiation process consists essentially of three steps, all of which can be rate limiting:

1. **Closed complex formation**
   Assembly of the RNA polymerase-containing transcription machinery at the promoter site, also designated as the closed complex formation in which the DNA is not melted [2–5].

2. **Transition of closed to open complex (Isomerization)**
   Also designated as open complex formation where the promoter DNA is locally melted in order to expose the template strand [6].

3. **Transition to a stable elongation complex**
   After several cycles of dinucleotide synthesis, the open complex evolves to a stable elongation complex [7, 8].

Kinetic studies *in vivo* of enzyme assembly, transition from the closed to an open complex and elongation of the mammalian RNAP I and RNAP II complexes support the recruitment model where the assembly is a highly inefficient event. The closed complex is assembled stochastically by fast random exchange of the subunits at the promoter site [2,3]. It requires $\sim$ 75 % of the total transcription period compared to $\sim$ 25 % for elongation and very short intitiation and termination times. Formation of the closed complexes is promoted by the presence of an activator at the enhancer site which is the slowest step of the pathway [4]. Footprinting studies of mammalian RNA polymerase II showed similar results: after enhancer-mediated recruitment, open complex formation occurs then very rapidly when ATP is hydrolyzed by the activator [5]. In these examples, the formation of the closed RNAP complex at the promoter is the rate limiting step of the transcription pathway. Assembly of RNA polymerase proceeds in a stepwise manner with increasing stability as more subunits are incorporated which could explain this step to be the slowest of the overall reaction of transcription. A second possible regulation target is the isomerization of the closed to an open RNAP complex where the DNA at the promoter is locally melted [6]. In this case, the previous enzyme assembly is a fast step and DNA melting is rate limited. The rate of this isomerization step can be determined by the requirement of a additional regulatory factor or by the composition of the DNA sequence itself. A third model supports the idea that assembly and formation of the open complex are fast steps whereas the transition to a stable elongation complex is slow [7,8]. Only after several cycles of abortive initiation where the holoenzyme statistically falls off the template, the RNA polymerase evolves into a stable elongation complex. Regulation at each step seems to occur *in vivo* and allows fine tuning of gene expression in response to varying needs of the cell.

1.1 Transcriptional enhancers

Transcriptional enhancers were originally defined as *cis*-acting DNA elements located at a distance from promoter elements from which transcription is started. They function as positive control elements by increasing the transcription rate of RNA polymerase in eukaryotic as well as in prokaryotic organisms [9, 10]. These sequences function efficiently at large distances away from the promoter site that they regulate, both upstream and downstream [9–13].

The transcriptional machines in eukaryotes and the organization of enhancer elements are more complex than in prokaryotes: It has been shown that the activating

elements are often composed of multiple enhancer modules (Figure 1.1) which appear to perform a specific function, such as the activation of its cognate gene at a particular stage of development [9]. A core promoter binding region which maps the DNA region from – 40 to + 40 bp relative to the transcription start site comprises different recognition and binding elements that are sufficient to direct transcription initiation by the basal RNA polymerase transcription machinery. Adjacent upstream elements are recognized by DNA-binding transcription factors which enable regulated transcription. Additional DNA sequences which map at large distances from the transcription start site function as enhancer sites. These sites are known to be located up to 85 kb upstream and 69 kb downstream the promoter [9]. Eukaryotic and prokaryotic organisms share extensive homologies among the largest subunits of RNA polymerase as well as a similar composition of the promoter sequence [14].

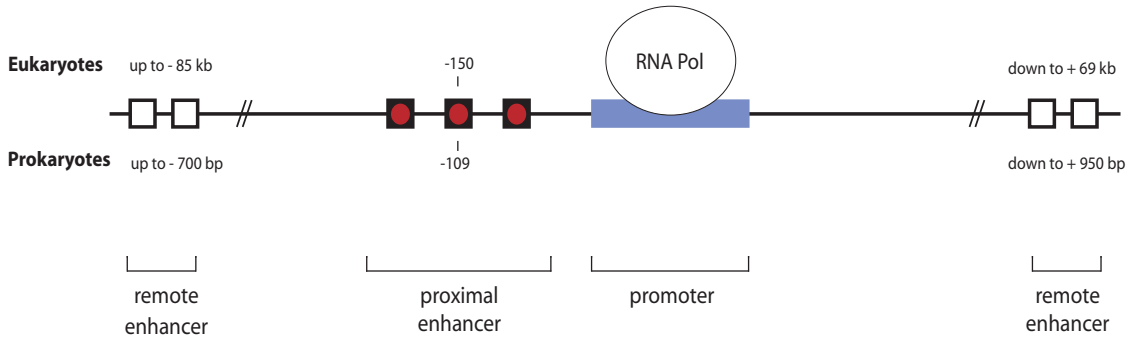

Figure 1.1: Schematic view of the architecture of an eukaryotic or prokaryotic promoter region with its surrounding upstream and downstream regulatory elements as reviewed in [9–13]. The preassembled multi-subunit transcription complex is bound to the cognate promoter region. The eukaryotic promoter is surrounded by additional characteristic cis-acting elements: Proximal specific binding sites for transcription factors — also designated as 'upstream elements' are located upstream the promoter. Enhancer sites which bind proteins activating transcription from this promoter were found to be located in both direction up to –85 bp upstream (wing margin enhancer from *D. melanogaster*) and –69 bp downstream (T cell receptor α-chain gene enhancer) the promoter [9]. Immediately upstream of the promoter site around –150 bp, there are multiple specific recognition sites for transcription factors such as Sp1 [9]. The prokaryotic promoter region is formed by similar modules. Upstream enhancer sites are known to reside from $\sim$ –80 to –700 bp such as the activator FhlA [15]. The activator NtrC studied here typically binds to 2 enhancer sites centered at –109 bp. It has been shown that these enhancer sites can be moved up to 3 kb away from the promoter site without losing the ability to activate transcription [16–19].

In prokaryotes, certain promoter sequences for so called 'house-keeping' genes direct efficient transcription initiation in the absence of an activator. In this case, transcription is performed by RNAP·σ^{70}. In 1986, enhancer-like elements were found

in bacteria and were shown to be binding sites for transcriptional activators that operate together with the bacterial RNA polymerase associated with an alternative sigma factor,σ^{54} [18]. These activators were shown to bind and function from remote enhancer sites [20, 21] and retain function when moved far away from the promoter site [16–19]. These enhancer sites allow no direct interaction between activator and RNAP and thus requires looping of the intervening DNA. A well-studied example for a bacterial enhancer binding protein is the nitrogen regulatory protein C (NtrC), an activator protein that stimulates transcription from σ^{54} dependent promoters [17]. In order to activate transcription the enhancer-bound regulatory proteins must somehow contact the RNA polymerase. There are different mechanisms by which transcription can be regulated from a distant site (Figure 1.2):

- **Alteration in the DNA conformation**
  Regulatory proteins can act by transmitting the signal via an altered DNA conformation [22]. The movement of RNA polymerase during elongation causes a temporal and local increase of superhelical density upstream and a reduction of superhelical density downstream of the enzyme [22]. Since partial uncoiling of the DNA stimulates transcription initiation, it is able to stimulate transcription from a second promoter. The coupled transcription from two promoters has been shown for the *E. coli leu*-500 promoter [23].

- **DNA tracking**
  The activating protein binds to its specific site and tracks along the DNA until it reaches the promoter-bound RNA polymerase from which it initiates transcription. This type of activation is realized for the late promoter of bacteriophage T4 [24].

- **DNA looping**
  DNA looping brings remote enhancer-bound activator and promoter-bound RNA polymerase into close proximity [11, 25–27].

DNA looping as a possible regulation mechanism for transcription appears to be very important in eukaryotes [4,9,28,29] but was also found in a number of prokaryotes [10, 15,19,30,31]. It acts by increasing the effective local concentration j_M in mol/l of one protein in the vicinity of another protein [11,25]. It is equivalent to the concentration of one species free in solution that would give the same contact probability in the absence of looping. Looping of the linker DNA between these two proteins depends on

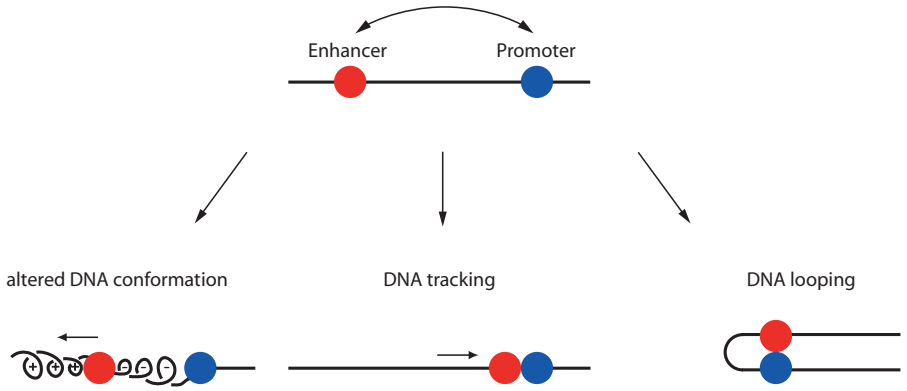

Figure 1.2: Different mechanisms of signal transduction between activator and RNAP

its flexibility and the presence of curvature within the DNA. Both DNA flexibility and DNA curvature are determined by structural features inherent to the DNA sequence and by the effect of bound proteins. DNA curvature can have two origins: Intrinsic curvature as a direct effect of the DNA sequence and extrinsic curvature induced by a bound protein. 'A-tracts' of four to six dA residues induce a strong intrinsic curvature of the DNA [32] whereas proteins that bind to specific sites on the linker DNA such as IHF (integration host factor) induce extrinsic DNA bending [33,34]. A further possibility to increase the local concentration of an enhancer in the proximity of the promoter is the superhelical conformation of the DNA. Theoretical and experimental work has been done to estimate the effect of the DNA conformation on the local concentration [11,25,35]. DNA curvature and superhelicity increase the value of j_M by one to three orders of magnitude under certain conditions [11,32,36]. Superhelical conformation of DNA alone increases j_M to 10^{-6} mol/l as compared to 10^{-8} mol/l for linear DNA for a separation distance of 150 bp between the two sites that interact [11]. This distance is comparable to the 109 bp distance between enhancer and promoter investigated in the NtrC system. DNA curvature on linear template has been shown to increase j_M by one order of magnitude [11]. Furthermore, an effective interaction between to proteins depends on the occupancies of the two protein binding sites [11]. In addition, the proteins need to have the correct torsional alignment to one another. Thus, unfavourable orientation of the proteins on the DNA reduces a functional protein-protein contact by 5- to 10-fold [37–40]. The dependence

on the helical periodicity of the DNA is only important for DNA shorter than 800 bp [11].

1.2 Transcription initiation in prokaryotes

All genes in prokaryotic organisms such as *Escherichia coli* (*E. coli*) are transcribed by the same RNA core polymerase composed of 4 subunits ($\alpha_2\beta\beta'$), which is reversibly associated with the σ subunit. Since the discovery of the σ^{70} factor in 1969, it has become clear that this protein is central to the function of bacterial RNA polymerase [41]. The RNA polymerase holoenzyme recognizes and binds specific promoter sequences located upstream of the transcription start site at +1 via the σ subunit. A prokaryotic organism usually encodes for a set of different σ, each of which directs RNAP to a different set of promoter sequences [42]. Seven different σ subunits (70, 54, 38, 32, 28, 24 and 18) are known by now which bind to promoters required for different cellular functions [43–51].
The major form of active RNA polymerase in procaryotic cells is the enzyme associated with σ^{70} (RNAP·σ^{70}). This complex transcribes the so called 'house-keeping' genes during exponential growth. Extensive work on the mechanism performed by RNAP·σ^{70} has revealed that the enzyme subsequently melts the DNA after promoter binding, in the simplest case without being regulated by an activator protein.
The overall transcription process can be divided into different subsequent reaction steps each of which can be subject to regulation:

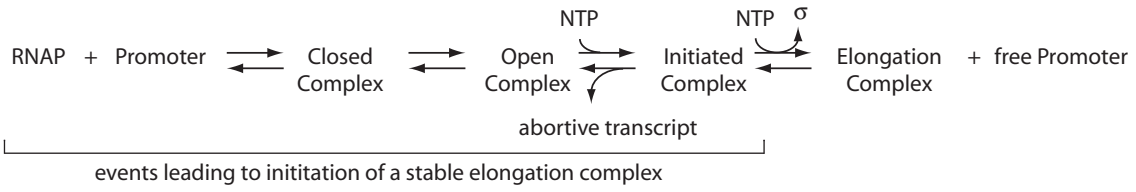

Figure 1.3: Steps in transcription initiation

The reversible binding of an alternative σ factor enables the bacterial cell to change the expression pattern required for different cellular functions which requires the presence of an activator protein [43–51]. It coordinates the transcription of functionally related genes which are often organized in operons and are coregulated by the

same σ subunit. Alternative σ factors coordinate distinct transport and metabolism pathways, flagellation and chemotaxis, the response to oxidative and osmotic stress, the response to heat and phage shock [43–51].

In 1985, a new σ factor, σ^{54}, was identified to be specifically required for the transcription initiation of nitrogen regulated promoters [52, 53]. Open reading frames potentially encoding σ^{54} have been revealed in a variety of bacteria such as extreme thermophiles, obligate intracellular pathogens, spirochetes and green sulfur bacteria [54]. Subsequently, it was discovered that σ^{54} does not only initiate the transcription of nitrogen-regulated promoters but also of some other genes whose products are not essential under all conditions of growth [55]. Based on structural and functional features, the σ^{54} factor is very different from the other σ subunits that share significant homology [41,53]. It is noteworthy that σ factors have several functional domains like two potential helix-turn-helix motifs in the C-terminal Region III that is responsible for DNA binding that resemble those of eukaryotic transcriptional factors in sequence composition and function [56]. After specific promoter recognition and binding, σ^{54} also regulates melting of DNA near the transcription start site. In addition, σ^{54} inhibits non-specific initiation of transcription [54]. Binding of alternate σ^{54} factor to the core RNA polymerase converts it to an enhancer-dependent enzyme [20, 21, 56, 57]. Sequence analyses of many different promoter [58] and footprint experiments [55,59] have revealed that σ^{54} promoters are characterized by a –24 and a –12 consensus sequence. In contrast to transcription initiated by RNAP·σ^{70}, transcription activation of RNAP·σ^{54} needs the direct interaction with an activator protein whose activating function requires nucleotide hydrolysis [50, 60]. RNA polymerase must be preassembled in a holoenzyme where the σ subunit mediates binding of the holoenzyme to the promoter sequence. The σ subunit tightly bound to the core enzyme is responsible for recognition of specific promoter sequences. The holoenzyme binds reversibly to the double-stranded promoter DNA, forming a closed complex. Melting of DNA requires energy and is a key event in transcription initiation. Reversible conformational changes within RNAP·σ^{54} convert the closed into the open complex. In the open complex the promoter DNA is partially melted within a region of 10 to 15 bp at the start site of transcription [61]. The open complex is typically short-lived and thus cannot be detected unless initiation is blocked [56,62]. Steps by which transcription can be regulated are the assembly of the closed complex at the promoter site, DNA melting (open complex formation or isomerization) and the synthesis of RNA (formation of the initiated complex, Figure 1.3).

1.3 The mechanism of activation of RNAP·σ^{54}

The closed complex of RNAP·σ^{54} on the promoter sequence and its activation upon binding of an activator protein is very similar to transcription initiation by eukaryotic RNA polymerase II [5,63]. Both RNA polymerases require ATP hydrolysis to drive DNA melting [64,65]. The regulatory systems of pro- and eukaryotes not only share the existence of different conformations of RNA polymerase while transcription initiation (closed/open complex) but also the formation of an intermediate loop complex [11, 25–27, 66, 67]. This productive interaction mediated by looping of the intervening DNA stimulates the isomerization of the closed complex into the open complex. The mechanism by which the RNAP·σ^{54} responds to enhancer-binding proteins has been addressed in a number of studies. σ^{54} alone specifically recognizes and binds the *nif*H promoter DNA [68] without the RNA core enzyme, whereas σ^{54} as well as the holoenzyme alone fail to melt DNA and thus transcription is not initiated [17, 62, 68, 69] until the activator abolishes this inhibition. The major functional aspect that differs strongly from transcription activated by σ^{70}-associated RNA polymerase is the energy requirement: The activator must hydrolyze ATP in order to activate the closed complex [60, 70]. Recently, the subunit σ^{54} was identified as the direct target of activation and it has been shown that ATPase activity which is characteristic for most σ^{54} activators is the necessary trigger of the conformational change of σ^{54} which involves its N terminus (region I) [71]. The N-terminal region I of σ^{54} is bifunctional: It is required for inhibiting the isomerization of the closed to the open complex in the absence of the activator and helps the RNA polymerase to melt DNA. With the usage of σ^{54}, another potential point of regulation exists in the process of transcription regulation: σ^{54}-bound RNA polymerase is preassembled as transcriptionally silent closed complex at the promoter site. Activation of RNAP·σ^{54} requires an activator that binds at remote enhancer sequences upstream the promoter site [55]. A variety of such activating proteins have been identified that are involved in different cellular processes. One of the best-studied activators is the nitrogen regulatory protein C (NtrC, also designated nitrogen regulator I or NRI) from enteric bacteria which is involved in nitrogen metabolism [64, 72]. NtrC acts as an transcriptional activator under conditions of NH_4^+ starvation and as repressor under conditions of NH_4^+ excess. The distal location of the binding sites for NtrC requires the intervening DNA to loop for interaction with the RNAP·σ^{54} at the promoter site [10, 18, 19, 26, 73–76]. Alignment of σ^{54} dependent promoters indicates conservation of two sequence elements, although the consensus sequence is

not the strongest promoter [77]. For example, the *gln*Ap2 promoter is regulated by an enhancer element which is centered *in vivo* at position –109 bp relative to the site of transcription initiation [18, 53].
This relatively simple prokaryotic enhancer system that was found to be comparable to that of eukaryotes and was used to investigate the mechanism of enhancer dependent transcription.

1.4 The NtrC-RNAP·σ^{54} model system for enhancer mediated transcription initiation

The preferred nitrogen source of *E. coli* and most other bacteria is ammonia which is the most important and sometimes the only substrate to synthesize glutamine. In nitrogen starved cells different promoters are activated sequentially which are involved in a variety of pathways to use alternative nitrogen sources. The activated genes are organized in different operons that make part of the Ntr regulon. The first operon of the Ntr regulon to be activated under nitrogen limited conditions is the *gln*ALG operon. NtrC, one of the products of this operon, plays a key role in this pathway. Phosphorylation turns NtrC in its activated form, NtrC-P. A change in the environmental nitrogen availability decides about the activation of the σ^{54} dependent genes.
The *gln*ALG operon consists of three structural genes: glnA, glnL and glnG whose products are the glutamine synthetase, the nitrogen regulatory protein C (NtrC) and the nitrogen regulatory protein B (NtrB), respectively (Figure 1.4) [78]. The transcription of these genes is regulated by three promoters: *gln*Ap1, *gln*Ap2 and *gln*Lp. It has been shown, that the promoters involved in using alternative nitrogen sources are activated with slightly increasing concentration of the activator NtrC [33, 79]. Two binding sites for NtrC are located upstream the *gln*Ap2 promoter, overlapping the *gln*Ap1 promoter. A third NtrC site overlaps the *gln*Lp promoter [80]. A key promoter in this signal transduction system is *gln*Ap2 which provides for expression of the most important enzyme of nitrogen assimilation, glutamine synthetase (GS), and for the two regualtory elements that control the regulon, NtrC and NtrB. The activation of expression of most of these genes depends on the rise in intracellular level of NtrC brought about by its increased expression, which is the immediate response to ammonia deficiency [80]. Figure 1.4 shows the composition of the *gln*ALG operon with the different promoters, encoding genes and the expression

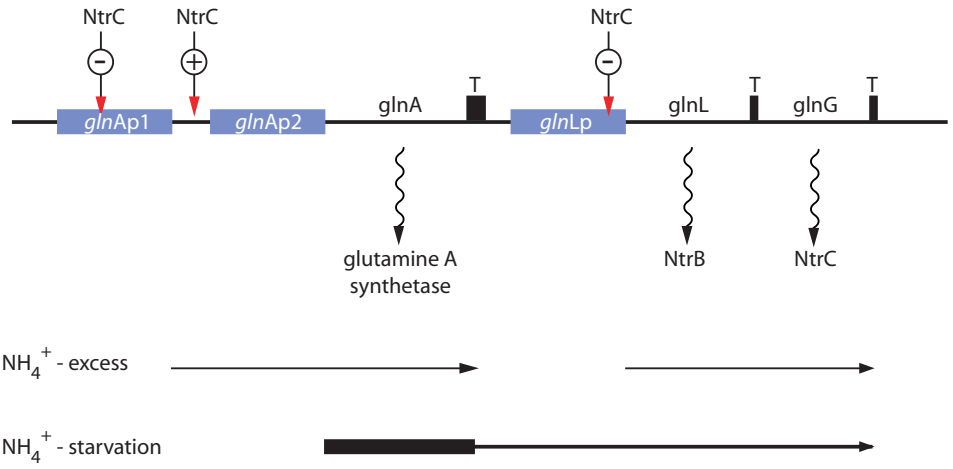

Figure 1.4: Scheme of the *gln*ALG operon. The promoters *gln*Ap1, *gln*Ap2 and *gln*L with the encoding sequences for the three major proteins involved in the usage of alternative nitrogen sources: glutamine synthetase (product of gene glnA), NtrC (glnG) and NtrB (glnL). T, termination sequences. Vertical arrows indicate NtrC binding sites (−: repressive, +: activating). Two NtrC sites overlap the *gln*Ap1 and *gln*Lp promoters. The horizontal arrows indicate the transcription from the different promoters at excess or deficiency of ammonia. When nitrogen is present the transcription is activated from the σ^{70} dependent promoters *gln*Ap1 and *gln*L yielding low levels of glutamine synthetase (GS), NtrB, and NtrC. Under nitrogen limited conditions transcription from the σ^{54} dependent *gln*Ap2 promoter is activated resulting in high levels of glutamine synthetase (heavy line) and the regulatory proteins NtrB and NtrC, whereas transcription of the other two promoters is blocked by binding of NtrC which functions as a repressor.

patterns at nitrogen excess or nitrogen limit. In an ammonia rich medium transcription is only activated from σ^{70} dependent promoters *gln*Ap1 and *gln*Lp [81]. This transcription is partially blocked by NtrC in order to maintain low levels of glutamine synthetase and the nitrogen regulatory proteins NtrB and NtrC [81]. Under these conditions, NtrC functions as an repressor of the σ^{70} depending promoter *gln*Lp by competitive binding of NtrC at the promoter (Figure 1.4) and regulates its own expression by partially blocking the *gln*Lp promoter [64]. This results in a concentration of about 5 NtrC dimers per cell, i.e., an intracellular concentration of about 5 nM for an *E. coli* volume of $\sim$1 μm^3) [82]. The σ^{70} dependent *gln*Ap1 promoter is a relatively weak promoter and provides a low level of glutamine synthetase during carbon limited growth. In addition, *gln*Ap1 needs the catabolite gene activator protein (CAP) and cyclic AMP for activation and is repressed by competitive

binding of NtrC under nitrogen limited conditions [81].
The σ^{54} dependent *gln*Ap2 promoter is a strong promoter and is activated by NtrC bound to the upstream enhancer [55]. NtrC-P catalyzes the isomerization of the closed to the open RNAP·σ^{54} complex and causes rapid initiation of transcription [17, 69]. Expression from *gln*Ap2 provides a high level of glutamine synthetase during nitrogen limited growth. A deficiency of ammonia in the direct environment of bacteria causes the start of a signal transduction pathway leading to the transcription of the *gln*ALG operon whose products are able to use alternative nitrogen sources. The interconversion of the inactive in the active phosphorylated form of NtrC (NtrC-P) is stimulated by NtrB, which is also transcribed from the *gln*ALG operon. NtrB in turn is stimulated by the products of the genes *gln*B and *gln*D etc. [49, 83–85]. Once the σ^{54} subunit has been produced in a previous step of signal transduction it can associate with core RNA polymerase and binds to its cognate promoter. The low level of intracellular NtrC is activated by phosphorylation carried out *in vivo* by NtrB. NtrC-P in turn stimulates the transcription from the σ^{54} dependent *gln*Ap2 promoter resulting in an increased intracellular level from 5 (5 nM) to approximately 70 dimers (70 nM) per cell causing the total block at *gln*Ap1 and *gln*L [82, 86]. The model system used here is derived from the *gln*ALG operon (Figures 1.4 and 1.5). The native upstream sequence of the *gln*Ap2 promoter consists of two enhancer sites with high affinity for NtrC which are located at a distance of 109 bp from the *gln*Ap2 promoter (center to center) [87]. These strong sites are essential and sufficient for transcription activation [18, 30, 64, 88]. In addition, three binding sites with low affinity for NtrC of unknown function are centered at –87, –66 and –45 bp from the transcription start site. Several lines of evidence indicate that activation of *gln*Ap2 is reduced at very high concentration of phosphorylated NtrC even *in vivo* [84, 89, 90]. It has been shown that an *in vitro* transcription system with RNAP·σ^{54}, NtrC, NtrB, and NTP yields a specific transcript. NtrB catalyzes the transfer of γ phosphate from ATP to NtrC. In the procaryotic model system used here, NtrB was replaced by carbamylphosphate, an anorganic phoshodonor [91]. This *in vitro* system was used to quantify the overall transcription activation process depending on different DNA templates with distinct compositions of NtrC binding sites and promoter sequences.

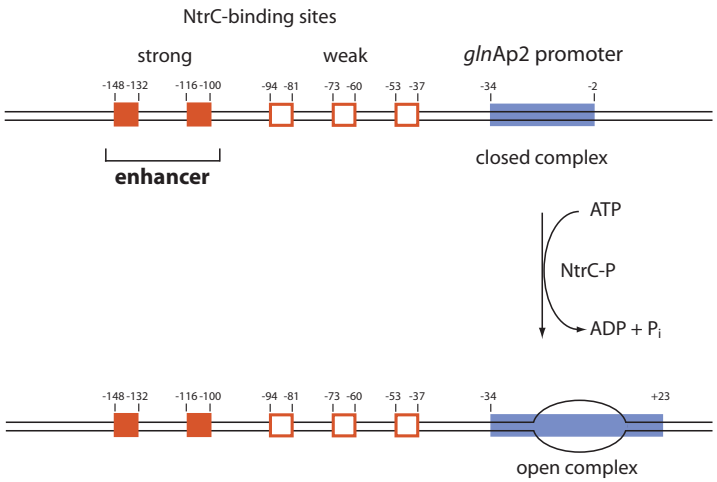

Figure 1.5: The isomerization of the closed RNAP·σ^{54} complex into the open complex is driven by the interaction of the enhancer-bound activator protein NtrC and the RNAP·σ^{54}. Strong NtrC binding sites (enhancer) with their position relative to the transcription start site are indicated by red boxes. Three additional NtrC binding sites of unknown function are indicated by open boxes.The activity of NtrC is an ATPase function which enables the RNA polymerase to melt DNA at the transcription start site (+1) after various conformational changes. DNA footprint by RNAP·σ^{54} is indicated by the stretched boxes and is increased downstream upon formation of the open complex [69, 92].

1.5 Aims of the thesis

Here, a relatively simple prokaryotic enhancer-promoter model system was used to investigate the molecular mechanism of transcription initiation activated by enhancers. The system consists of the strong *gln*Ap2 promoter, RNA polymerase bound to an alternative sigma factor, σ^{54}, (RNAP·σ^{54}) and the activator protein NtrC that binds to specific enhancer sites upstream the promoter sequence (Figure 1.5).

- In the first part of this work, the recognition and binding step of RNAP·σ^{54} to three different promoters of the σ^{54} family was examined. Previous *in vivo* and *in vitro* studies characterized them as strong (*gln*Ap2 promoter of *E. coli*) or weak promoters (*nif*H and *nif*L promoters of *K. pneumoniae*) [32, 59, 93–97]. Binding studies were conducted by measuring the rotational diffusion coefficient of free and RNAP·σ^{54}-bound promoter DNA over a broad range of ionic strength by fluorescence anisotropy. In addition, the effect of RNAP·σ^{54}-binding on the conformation of supercoiled DNA was investigated by scanning force microscopy (SFM). It was tested if RNAP·σ^{54} bound at the promoter is

preferably located in one of the two end-loops of a supercoiled plasmid.

- Interactions between σ^{54} and the activator NtrC, which is thought to be important to trigger the isomerization from the closed to the open complex of RNAP·σ^{54} were investigated by an ATPase activity of NtrC and by an electrophoresis mobility shift assay. Additionally, σ^{54} was tested for its binding ability without the core enzyme to two different promoter sites in order to determine the contribution of σ^{54} to the binding affinity of the RNAP·σ^{54} holoenzyme.

- Despite the apparent multifunctional role of enhancer sites of different affinities for the activation process, there have been no systematic studies of the effect of isolated or combined enhancer sites on transcription activity. Accordingly, a series of plasmids with different combinations of strong and weak enhancer sites were constructed and quantitatively analyzed by an *in vitro* transcription assay. The DNA templates can be divided into different groups: A series of templates contain two enhancer sites proximal to the *gln*Ap2 promoter with different distances to test if transcription activation without looping could occur. Other templates had enhancer sites overlapping with the promoter. Transcription activation by enhancer sites near the promoter was then compared to activation by the *in vivo* arrangement of two strong NtrC binding sites at a distance and three weak NtrC binding sites near the promoter. In addition, a similar DNA template with two strong NtrC binding sites at a distance and two strong NtrC binding sites near the promoter was examined.

The results provide new insight into the mechanism of transcription activation by enhancers. A model for the modulation of NtrC activation in response to activator concentration and position and affinity of enhancer sites was developed. Due to strongly related characteristics of this process, an improved model of the investigated prokaryotic enhancer system can be useful to understand the activation mechanism of eukaryotic enhancers.

Chapter 2

Methods

2.1 Chemicals and Enzymes

Buffers and salts were usually obtained from Sigma and Fluka and are not listed. All chemicals used were at the '*pro analysis*' degree. Working solutions were prepared using sterilized material and water.

Chemical	**Reference**
Acrylamide:bis	Roth, Karlsruhe, Germany
Agar	DIFCO laboratories, Detroit, MI, USA
Agarose, Seakem LE	Cambrex Bioscience, Rockland, USA
Ampicilline	Sigma, Deisenhofen, Germany
Bromphenolblue	Roth, Karlsruhe, Germany
BSA	New England Biolabs, Schwalbach, Germany
Carbamylphosphate	Sigma, Deisenhofen, Germany
Desoxynucleotides (dNTPs)	Amersham Bioscience
DNA molecular weight marker	Bio-Rad, München, Germany
Gel extraction kits	QIAGEN, Hilden, Germany
Glycerol	GIBCO/Invitrogen, Karlsruhe, Germany
NP-40	Boehringer Mannheim, Germany
Oligonucleotides	PE-Applied Biosystems and Thermohybaid
Radioactive nucleotides	Perkin Elmer, Life and Analytical Sciences, Boston, USA
Ribonucleotides (rNTPs)	Amersham Bioscience
ROX-labeled oligonucleotides	PE-Applied Biosystems, Weiterstadt, Germany and Thermo Electron GmbH, Ulm, Germany
Tryptone	Becton, Dickinson and Company

Xylencyanol	Roth, Karlsruhe, Germany
Yeast extract	DIFCO laboratories, Detroit, MI, USA

Enzymes	**Reference**
Alkaline phosphatase	New England Biolabs, Schwalbach, Germany
Core RNA polymerase	Epicentre Technologies via Biozym, Hess. Oldendorf
Klenow fragment	Boehringer Mannheim, Germany
Pfu Turbo DNA polymerase	Stratagene, La Jolla, CA, USA
Restriction endonucleases	Thermohybaid, Fermentas and New England Biolabs
T4 DNA Ligase	New England Biolabs, Schwalbach, Germany

2.2 Growth and Manipulation of *Escherichia coli*

Media and antibiotics

Any microbiological work such as cultivation of bacteria and the preparation of media was performed using sterilized material. Media, flasks and solutions were autoclaved for 30 min at 121°C. Some liquids such as solutions of $MgCl_2$ and glucose were sterile filtered (0.22μm syringe filter, Nalgene, Rochester, New York). Before addition of antibiotic, the medium was allowed to cool down to 50°C.

LB medium	10g/l tryptone + 5g/l yeast extract + 10 g/l NaCl, with NaOH to a pH = 7.5
LB agar for plates	LB medium + 1.5 %(w/v) agar
SOB medium	20 g/l tryptone + 5 g/l yeast extract + 0.5 g/l NaCl + 2.5 mM KCl with NaOH to a pH = 7.5 → sterilization → + 10 mM $MgCl_2$ (sterile filtered)
SOC medium	sterile SOB medium + 20 mM glucose (sterile filtered)
Ampicilline	in LB medium to an end concentration of 50-75 μg/ml for liquid medium and 50 μg/ml for plates out of a stock solution of 50 mg/ml in water aliquoted and stored at -20°C

Transformation of DNA into *Escherichia coli*

Transformation is the uptake of naked DNA into bacteria from the surrounding medium. Plasmids carrying origins of replications which are recognized by the host cell will be replicated. For transformation of recombinant plasmid DNA, the *E. coli* strain XL10-Gold from Stratagene was used. These cells exhibit a phenotype which increases the transformation efficiency of ligated and large supercoiled DNA molecules. The cells are deficient in all known restriction systems ($\Delta(mcrA)183\Delta mcrCB - hsdSMR - mrr173$), in endonuclease ($endA$) improving the quality of preparated DNA and in recombination ($recA$) which helps to ensure insert stability. The cells were previously aliquoted in prechilled tubes, immediately frozen in liquid nitrogen and stored at – 80°C until transformation.

Protocol

(1)	Thaw a 10 μl aliquot of cells on ice		
(2)	+ 0.4 μl of provided β-mercaptoethanol	$\mapsto$	Incubation for 10 min on ice, swirling gently every 2 min
(3)	+ 0.1 to 50 ng of DNA	$\mapsto$	Swirl the tube, incubate on ice for 30 min
(4)	Heat-shock the tubes for 30 sec at 42°C		
(5)	Incubation for 2 min on ice		
(6)	+ 190 μl of freshly prepared SOC medium	$\mapsto$	Incubation for 1 hour at 37°C with gentle shaking (expression of antibiotic resistance)
(7)	Plate on LB agar plates containing the appropriate antibiotic	$\mapsto$	Incubation at 37°C overnight ($\geq$16 hours)

To verify the transformed DNA, colonies of the selective plate were picked and grown in 1 to 5 ml of selective LB medium. The DNA was isolated and checked by restrictive digestion and/or sequencing of the region of interest.

Bacterial culture

Growth conditions were optimized to yield monomeric plasmid DNA at native superhelicity (σ=–0.05 to –0.06). It was found that bacteria produce highest amounts of monomeric DNA when cultured at lower temperatures until it reached an optical density at 600 nm (OD_{600}) of $\leq$ 1.0. For this purpose, 500 ml of ampicilline-containing LB medium was inoculated with an overnight preculture and was incubated at 30°C

and under rigorous shaking (220 rpm) in 1 l Erlenmeyer flasks until it reached the desired optical density. Under these conditions, about 100 % of the plasmids were monomers and naturally supercoiled. Growth at 37°C over an OD_{600} of 1.0 leads to a decreased yield of monomeric plasmids in favour of dimeric molecules. Bacterial cultures were stored at – 80°C in LB medium containing 15 % (v/v) of glycerol.

2.3 Manipulation of DNA

2.3.1 Oligonucleotides for binding studies

A: Sequences for binding of RNAP·σ^{54} holoenzyme

For RNAP·σ^{54} binding studies by fluorescence anisotropy (FA), short DNA fragments of 43 bp length were designed that contained the sequence of three different promoters. One of the two oligonucleotides of the DNA fragment was labeled with the fluorescent dye 6-carboxy-X-rhodamine (ROX) wich was covalently attached to the 5'–end via a C6 linker. The DNA oligonucleotides were HPLC-purified and purchased from PE-Applied Biosystems (Weiterstadt, Germany). The extinction coefficients of the single DNA strands were determined by the nearest neighbour method as previously described [98]. The following list contains the oligonucleotides required for RNAP·σ^{54} binding studies.

***gln*Ap2-top** [ε_{260}= 418.0 M^{-1} cm^{-1}]

ROX-GCA ATT TAA AAG TTG GCA CAG ATT TCG CTT TAT CTT TTT TAC G

***gln*Ap2-bottom** [ε_{260}= 440.0 M^{-1} cm^{-1}]

CGT AAA AAA GAT AAA GCG AAA TCT GTG CCA ACT TTT AAA TTG C

***nif*H-top** [ε_{260}= 394.0 M^{-1} cm^{-1}]

ROX-GCA ATG GCA CGG CTG GTA TGT TCC CTG CAC TTC TCT GCT GGC A

***nif*H-bottom** [ε_{260}= 426.9 M^{-1} cm^{-1}]

TGC CAG CAG AGA AGT GCA GGG AAC ATA CCA GCC GTG CCA TTG C

***nif*L-top** [ε_{260}= 418.8 M^{-1} cm^{-1}]

ROX-GCA ATG CCG ATA AGG GCG CAC GGT TTG CAT GGT TAT CAC CGT T

***nif*L-bottom** [ε_{260}= 414.5 M^{-1} cm^{-1}]

AAC GGT GAT AAC CAT GCA AAC CGT GCG CCC TTA TCG GCA TTG C

B: Sequences for binding of sigma factor σ^{54}

Promoters *gln*Ap2 and *nif*H were used to investigate the effect of isolated promoter-bound σ^{54} on activation by NtrC and for determination of the binding affinity to promoter DNA duplexes under certain conditions. It has been shown, that σ^{54} alone is able to bind the *nif*H promoter from *R. meliloti* when the bases –12 and –11 of the top strand were mutually exchanged [71]. Heteroduplexes of *gln*Ap2 and *nif*H were derived from homoduplexes that mismatch at position –12/11, a region that contributes to locking the holoenzyme in a conformation that makes it unable to melt the DNA prior to activation [77, 99]. Similarly, *E. coli gln*Ap2 promoter was modified by an exchange of base pairs at the same position from TT to GG. Each top-strand, homo or hetero, was annealed with the same ROX-labeled bottom-strand resulting in four different promoter DNA duplexes of 50 bp: *gln*Ap2-homo-ROX, *gln*Ap2-hetero-ROX, *nif*H-homo-ROX and *nif*H-hetero-ROX. The DNA oligonucleotides were HPLC-purified and purchased from Thermo Electron GmbH (Ulm, Germany). The following list contains the oligonucleotides used for σ^{54} binding studies.

***gln*Ap2-top for homoduplex** [ε_{260}= 478.2 M^{-1} cm^{-1}]

TTT AAA AGT TGG CAC AGA TTT CGC TTT ATC TTT TTT ACG GCG ACA CGG CC

***gln*Ap2 for heteroduplex** [ε_{260}= 483.6 M^{-1} cm^{-1}]

TTT AAA AGT TGG CAC AGA TTT CGC GGT ATC TTT TTT ACG GCG ACA CGG CC

***gln*Ap2-bottom** [ε_{260}= 506.9 M^{-1} cm^{-1}]

ROX-GGC CGT GTC GCC GTA AAA AAG ATA AAG CGA AAT CTG TGC CAA CTT TTA AA

***nif*H-top for homoduplex** [ε_{260}= 466.4 M^{-1} cm^{-1}]

TCA GAC GGC TGG CAC GAC TTT TGC ACG ATC AGC CCT GGG CGC GCA TGC TG

***nif*H-top for heteroduplex** [ε_{260}= 466.9 M^{-1} cm^{-1}]

TCA GAC GGC TGG CAC GAC TTT TGC CAG ATC AGC CCT GGG CGC GCA TGC TG

***nif* H-bottom** [ε_{260}= 472.2 M^{-1} cm^{-1}]

ROX-CAG CAT GCG CGC CCA GGG CTG ATC GTG CAA AAG TCG TGC CAG CCG TCT GA

C: Sequences for binding of the activator protein NtrC

The DNA oligonucleotides for NtrC binding were HPLC-purified and purchased from Thermo Electron GmbH (Ulm, Germany). Specific NtrC binding was analyzed with two different DNA fragments containing one (ES-1, 32 bp) or two (ES-2, 53 bp) strong NtrC binding sites:

ES-1-top [ε_{260}= 328.4 $M^{-1}cm^{-1}$]

TGA GAT CAG TTG CAC TAA AAT GGT GCA TAA TG

ES-1-bottom [ε_{260}= 308.9 $M^{-1}cm^{-1}$]

CAT TAT GCA CCA TTT TAG TGC AAC TGA TCT CA

ES-2-top [ε_{260}=599.1$M^{-1}cm^{-1}$]

TCA GTT GCA CTA AAA TGG TGC ATA ATG TTA ATG CAC TAA AAT GGT GCA ACA TG

ES-2-bottom [ε_{260}=579.1$M^{-1}cm^{-1}$]

CAT GTT GCA CCA TTT TAG TGC ATT GTT AAC ATT ATG CAC CAT TTT AGT GCA ACT GA

After hybridization of the complementary DNA-strands, the DNA duplexes were purified on a native 12 % polyacrylamide gel. The concentration of extracted ROX-labeled DNA was determined by using the averaged extinction coefficient of the ROX-label attached to DNA at 25°C (ε_{583}= 96.000). The synthesis and the reconstitution of the purified duplexes were analyzed on a native 20 % polyacrylamide gel with parallel loaded single-strands.

2.3.2 Construction of templates for *in vitro* transcription

The DNA templates used for the *in vitro* transcriptions experiments were either modified by subcloning different promotor and enhancer sequences or by introducing distinct mutations between enhancer and promoter in order to change the distance between these two sites. The plasmids constructed here were all derived from plasmid pVW7 [100] which is in turn derived from pTH8 [53]. Plasmid pTH8 contains the

in vivo enhancer sequence found upstream of the *gln*Ap2 promoter: The two strong NtrC binding sites (enhancer) resembling the consensus sequence are found *in vivo* at a distal location at –109 bp from the promoter site (Figure 3.15). The consensus sequence for a NtrC binding site is a perfect inverted repeat of 7 bp separated by 3 bp as shown in Figure 2.2. It has the highest affinity for NtrC. The three binding sites located directly upstream the *gln*Ap2 differ from the consensus sequence and have lower affinities (for site nomenclature see Hirschman *et al.* 1985 [52]). In contrast, plasmid pVW7 contains only the two strong NtrC binding sites at the distance, the weak sites are depleted and replaced by a random DNA sequence of the same length. In order to replace the *gln*Ap2 promoter from pVW7 by the *nif*H or *nif*L promoters, a single *Xho*I restriction site was created downstream by site-directed mutagenesis. Figure 2.1 shows the plasmid pVW7 with the new *Xho*I restriction site and the two DNA fragments which were inserted in the double-restricted plasmid to create plamids pVW7-*nif*H anf pVW7-*nif*L. Plasmid pES10 was derived from pVW7: Double restriciton with *Sal*I and *Hind*III eliminated a DNA-fragment containing the two enhancer sites at position –109 bp. The remaining plasmid was then ligated with a short DNA fragment containing the two enhancer sites resulting in a plasmid with a enhancer-promoter distance of 10 bp (Figure 2.2). Plasmid pProm contains no enhancer site and is also a derivative of pVW7. After double restriction of pVW7 with *Bam*H I and *Hind*III, the recessed 3' termini were filled with Klenow fragment to obtain cohesive ends and subsequently religated. After verification of the sequence by sequencing the modified sites, the plasmids were amplificated in *Escherichia coli* under moderate growth conditions to obtain monomeric and naturally plectonemic molecules.

Oligonucleotides for molecular cloning

The DNA oligonucleotides were HPLC-purified and purchased from Thermo Electron GmbH. They were diluted in TE buffer, pH 7.5 or water to a concentration of 100 pmol/μl and the concentration was checked by spectral analysis.

A: Changes of the promoter sequence

The *E. coli gln*Ap2 promoter of the plasmid pVW7 was replaced by two other prokaryotic promoter sequences from *Klebsiella pneumoniae*: *nif*H and *nif*L, that are *in vivo* involved in nitrogen fixation (as indicated by the abbreviation *nif*) and were shown to be also sensitive to regulation by NtrC.

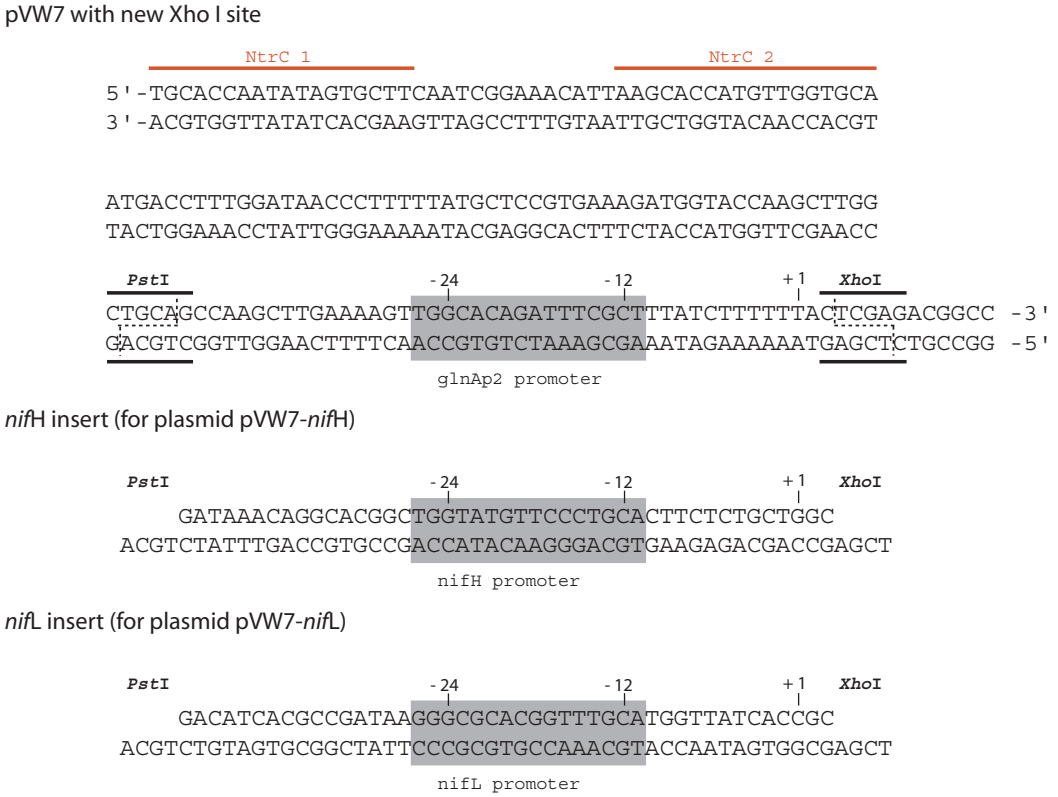

Figure 2.1: Construction of pVW7 (*gln*Ap2 promoter from *E. coli*) derivatives where the promoter region was cut off by DNA restriction (*Pst*I, *XhoI*) and replaced by DNA inserts containing the *Klebsiella pneumoniae* promoters *nif*H or *nif*L, respectively. The gray boxes indicate the σ^{54} recognition site with the highly conserved –24 and –12 regions of the promoter (see also Figure 3.1 for details).

nif H-top

GAT AAA CAG GCA CGG CTG GTA TGT TCC CTG CAC TTC TCT GCT GG

nif H-bottom

TCG AGC CAG CAG AGA AGT GCA GGG AAC ATA CCA GCC GTG CCT GTT TAT CTG CA

nif L-top

GAC ATC ACG CCG ATA AGG GCG CAC GGT TTG CAT GGT TAT CAC CGC

nif L-bottom

TCG AGC GGT GAT AAC CAT GCA AAC CGT GCG CCC TTA TCG GCG TGA TGT CTG CA

B: Insertion of enhancer sites

For the construction of pES10, double-digested pVW7 (*Sal*I x *Hind*III, eliminates strong NtrC binding sites at position –109 bp) was ligated with a short DNA fragment (hybridization of DNA oligonucleotides AS 9 and AS 10) containing two similar strong NtrC binding sites creating an *in vivo* enhancer-promoter distance of 10 bp as shown in Figure 2.2.

AS 9 CGA CTG CAC TAA AAT GGT GCA TAA TGT TAA CAT TAA TGC ACT AAA ATG GTG

AS 10 AGC TCA CCA TTT TAG TGC ATT AAT GTT AAC ATT ATG CAC CAT TTT AGT GCA GT

The construct pVW7-ES10 contained two strong NtrC binding sites at –109 bp upstream the promoter sequence and two strong NtrC binding sites adjacent to the *gln*Ap2 promoter with the native distance of 10 bp promoter as shown in Figure 2.2. It was formed by inserting two additional strong NtrC binding sites (DNA fragment created by hybridization of oligonucleotides ES-top and ES-bottom) comparable to those of pVW7 in the single restriciton site *Xba*I of pES10.

ES-top

CTA GAT TGC ACC AAT ATA GTG CTT CAA TCG GAA ACA TTA AGC ACC ATG TTG GTG CAA TGA T

ES-bottom

CTA GAT CAT TGC ACC AAC ATG GTG CTT AAT GTT TCC GAT TGA AGC ACT ATA TTG GTG CAA T

C: Oligos for site-directed mutagenesis

The plasmids with different distances between the strong NtrC sites very closed to the *gln*Ap2 promoter were derived from pES10 by site-directed mutagenesis. In the same way, replacement of the *gln*Ap2 promoter from pVW7 by the promoters *nif*H and *nif*L was performed by introducing a *Xho*I restriction site downstream the *gln*Ap2 promoter by site-directed mutagenesis.

*Xho*I-site in pVW7

SV 1 CGC TTT ATC TTT TTT ACT CGA GAC GGC CAA AAT AAT TGC

SV 2 GCA ATT ATT TTG GCC GTC TCG AGT AAA AAA GAT AAA GCG

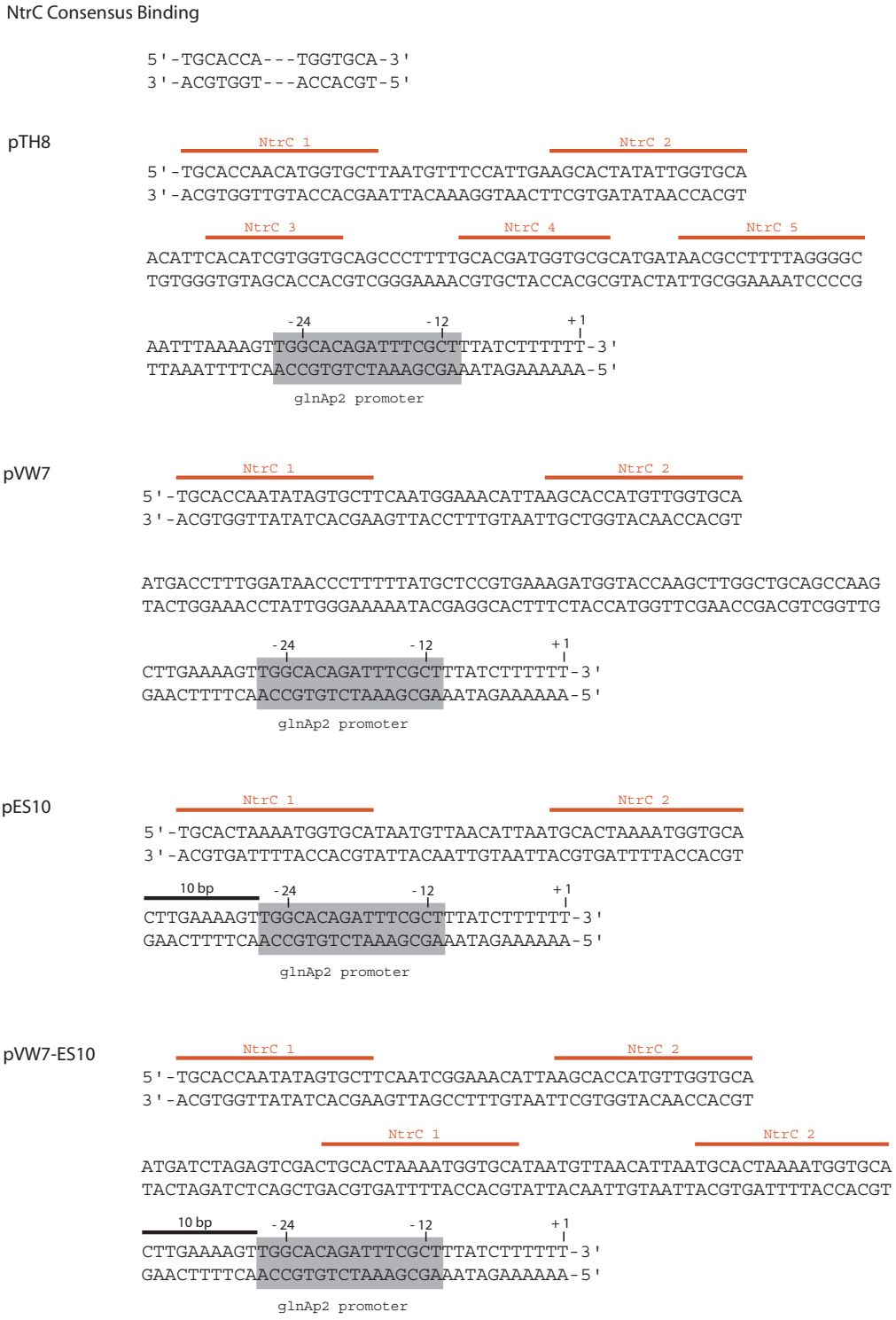
NtrC Consensus Binding
5'-TGCACCA---TGGTGCA-3'
3'-ACGTGGT---ACCACGT-5'
pTH8
NtrC 1
NtrC 2
5'-TGCACCAACATGGTGCTTAATGTTTCCATTGAAGCACTATATTGGTGCA
3'-ACGTGGTTGTACCACGAATTACAAAGGTAACTTCGTGATATAACCACGT
NtrC 3
NtrC 4
NtrC 5
ACATTCACATCGTGGTGCAGCCCTTTTGCACGATGGTGCGCATGATAACGCCTTTTAGGGGC
TGTGGGTGTAGCACCACGTCGGGAAAACGTGCTACCACGCGTACTATTGCGGAAAATCCCCG
-24
-12
+1
AATTTAAAAGTTGGCACAGATTTCGCTTTATCTTTTTT-3'
TTAAATTTTCAACCGTGTCTAAAGCGAAATAGAAAAAA-5'
glnAp2 promoter
pVW7
NtrC 1
NtrC 2
5'-TGCACCAATATAGTGCTTCAATGGAAACATTAAGCACCATGTTGGTGCA
3'-ACGTGGTTATATCACGAAGTTACCTTTGTAATTGCTGGTACAACCACGT
ATGACCTTTGGATAACCCTTTTTATGCTCCGTGAAAGATGGTACCAAGCTTGGCTGCAGCCAAG
TACTGGAAACCTATTGGGAAAAATACGAGGCACTTTCTACCATGGTTCGAACCGACGTCGGTTG
-24
-12
+1
CTTGAAAAGTTGGCACAGATTTCGCTTTATCTTTTTT-3'
GAACTTTTCAACCGTGTCTAAAGCGAAATAGAAAAAA-5'
glnAp2 promoter
pES10
NtrC 1
NtrC 2
5'-TGCACTAAAATGGTGCATAATGTTAACATTAATGCACTAAAATGGTGCA
3'-ACGTGATTTTACCACGTATTACAATTGTAATTACGTGATTTTACCACGT
10 bp
-24
-12
+1
CTTGAAAAGTTGGCACAGATTTCGCTTTATCTTTTTT-3'
GAACTTTTCAACCGTGTCTAAAGCGAAATAGAAAAAA-5'
glnAp2 promoter
pVW7-ES10
NtrC 1
NtrC 2
5'-TGCACCAATATAGTGCTTCAATCGGAAACATTAAGCACCATGTTGGTGCA
3'-ACGTGGTTATATCACGAAGTTAGCCTTTGTAATTCGTGGTACAACCACGT
NtrC 1
NtrC 2
ATGATCTAGAGTCGACTGCACTAAAATGGTGCATAATGTTAACATTAATGCACTAAAATGGTGCA
TACTAGATCTCAGCTGACGTGATTTTACCACGTATTACAATTGTAATTACGTGATTTTACCACGT
10 bp
-24
-12
+1
CTTGAAAAGTTGGCACAGATTTCGCTTTATCTTTTTT-3'
GAACTTTTCAACCGTGTCTAAAGCGAAATAGAAAAAA-5'
glnAp2 promoter

Plasmid	Primer	
pES2	SV 21	GCA CTA AAA TGG TGC ACT TGG CAC AGA TTT CGC
	SV 22	GCG AAA TCT GTG CCA AGT GCA CCA TTT TAG TGC
pES4	SV 19	GCA CTA AAA TGG TGC ACA GTT GGC ACA GAT TTC GC
	SV 20	GCG AAA TCT GTG CCA ACT GTG CAC CAT TTT AGT GC
pES5	SV 31	GCA CTA AAA TGG TGC ACG AGT TGG CAC AGA TTT CGC
	SV 32	GCG AAA TCT GTG CCA ACT CGT GCA CCA TTT TAG TGC
pES6	SV 17	GCA CTA AAA TGG TGC ACG AAG TTG GCA CAG ATT TCG C
	SV 18	GCG AAA TCT GTG CCA ACT TCG TGC ACC ATT TTA GTG C
pES7	SV 27	GCA CTA AAA TGG TGC ACG AAA GTT GGC ACA GAT TTC GC
	SV 28	GCG AAA TCT GTG CCA ACT TTC GTG CAC CAT TTT AGT GC
pES8	SV 15	GCA CTA AAA TGG TGC ACG AAA AGT TGG CAC AG
	SV 16	CTG TGC CAA CTT TTC GTG CAC CAT TTT AGT GC
pES9	SV 13	GCA CTA AAA TGG TGC ACT GAA AAG TTG GCA CAG
	SV 14	CTG TGC CAA CTT TTC AGT GCA CCA TTT TAG TGC
pES11	SV 9	GCA CTA AAA TGG TGC ACC TTG AAA AGT TGG CAC
	SV 10	GTG CCA ACT TTT CAA GGT GCA CCA TTT TAG TGC

Figure 2.2: DNA templates with different low- and high-affinity NtrC binding sites.
The shown DNA templates used for *in vitro* transcription assays all contain the *gln*Ap2 promoter. The σ^{54} recognition site (see also Figure 3.1 for details) is shaded in gray. pTH8 contains the *in vivo* sequences for NtrC binding. Two strong NtrC binding sites (enhancer) located with a distance of 109 bp from the promoter site (center to center) followed by three NtrC binding sites of low affinity. Plasmid pVW7 contains only the two distal enhancer sites. Plasmid pES10 contains the same two enhancer sites but positioned very close to the promoter at a distance of 10 bp. Plasmid pVW7-ES10 is a hybrid of pVW7 and pES10 and contains two distal enhancer sites (–109 bp) in combination with two proximal enhancers positioned at a distance of 10 bp from the *gln*Ap2 promoter. NtrC sites 1 and 2 refer to the *in vivo* enhancer sequences of plasmid pTH8 that are very similar to the consensus sequence. NtrC sites 3, 4 and 5 have less similarity with the consensus sequence and thus have low affinity to the activator protein NtrC.

pES12	SV 11	GCA CTA AAA TGG TGC ACG CTT GAA AAG TTG GCA C
	SV 12	GTG CCA ACT TTT CAA GCG TGC ACC ATT TTA GTG C
pES14	SV 23	GCA CTA AAA TGG TGC ACG CGC TTG AAA AGT TGG C
	SV 24	GCC AAC TTT TCA AGC GCG TGC ACC ATT TTA GTG C
pES16	SV 25	GCA CTA AAA TGG TGC ACG CGC TCT TGA AAA GTT GGC
	SV 26	GCC AAC TTT TCA AGA GCG CGT GCA CCA TTT TAG TGC

Plasmid	**Description**	**Reference**
pVW7	*gln*Ap2 promoter with enhancer for NtrC at a distance of 109 bp upstream the promoter site, 481 nt transcript	Weiss *et al.* [100]
pVW7-nifH	same as pVW7, *gln*Ap2 promoter is replaced by *nif*H	this work
pVW7-nifL	same as pVW7, *gln*Ap2 promoter is replaced by *nif*L	this work
pVW7-158	same as pVW7, but with a shorter transcript of 158 nt	Schulz *et al.* [32]
pTH8	contains the *in vivo* upstream sequence of *gln*Ap2: two enhancer for NtrC plus 3 weak NtrC binding sites	Hunt & Magasanik [53]
pProm	derivative of pVW7 without any specific NtrC site	this work
pESX series	*gln*Ap2 promoter with two enhancer sites adjacent to the promoter with a distance of X bp between enhancer enhancer and promoter	this work
pES2	distance of 2 bp	this work
pES4	distance of 4 bp	this work
pES5	distance of 5 bp	this work
pES6	distance of 6 bp	this work
pES7	distance of 7 bp	this work
pES8	distance of 8 bp	this work
pES9	distance of 9 bp	this work
pES10	derivative of pVW7 with *in vivo* distance of 10 bp	this work
pES11	distance of 11 bp	this work
pES12	distance of 12 bp	this work
pES14	distance of 14 bp	this work
pES16	distance of 16 bp	this work
pVW7-ES10	derivative of pES10 with two additional enhancer sites inserted at a distance of 109 bp upstream the promoter	this work

Table 2.1: DNA constructs for *in vitro* transcription

2.3.3 Sequencing of DNA

Sequencing of DNA was kindly performed by Andreas Hunziker (DKFZ).

2.3.4 Preparation of plasmid DNA

Isolation of plasmid DNA from *E. coli* was performed by alkaline lysis (Birnboim & Doly 1979 [101]) of the cells in combination with the detergent SDS followed by binding of the DNA to an appropriate matrix with subsequent washing and elution steps as provided by the DNA preparation kits from Qiagen.

Mini-preparation (for DNA amounts of $\sim 20 \mu$g)
Minipreparations were used to amplify small amounts of plasmid DNA. The resulting DNA preparation may be used for restriction endonuclease digestion, ligation, transformtion and sequencing. For minipreparation of plasmid DNA the QIAprep Spin Miniprep Kit from Qiagen was used. A selected colony was grown in 1 to 5 ml ampicilline supplemented LB medium at 37°C overnight. The cells were harvested by centrifugation at maximum speed (13.000 x g) in an Eppendorf table-top centrifuge. The cells were then lysed under alkaline conditions. The exposure of the bacterial suspension to the SDS-containing lysis buffer opens the cell membrane by solubilization of the phospholipid and protein components of the cell membrane while alkaline conditions denature the chromosomal and plasmid DNA, as well as proteins. Plasmid DNA is released into the supernatant. Although alkaline pH disrupts base pairing, the two strands of plasmid DNA are joined once again in their native form when the pH is returned to neutral. The neutralized solution is adjusted to high salt binding conditions which causes proteins, chromosomal DNA, cellular debris and SDS to precipitate, whereas renatured smaller plasmid DNA stays in solution. After centrifugation of the precipitated components the supernatant containing the plasmid DNA is loaded on the column (capacity: $\sim 20 \mu$g DNA/column) and eluted in 10 mM Tris-Cl, pH 8.5 (low salt buffer).

Maxi-preparation(for DNA amounts of $\sim 500 \mu$g)
The 500 ml cultures were harvested by centrifugation at 6000 x g for 15 min at 4°C (corresponds to 6000 rpm in Sorvall GSA rotor). The lysis of the cell pellet was performed with the appropriate Qiagen Plasmid Maxi Kit comparable to the minipreparation according to the manufactorers protocol. After alkaline cell lysis and subsequent precipitation of genomic DNA (centrifugation at 20,000 x g, corre-

sponds to 13,000 rpm in a Sorvall SS-34 rotor), cell debris proteins and SDS, the isolated DNA was bound onto an anion exchange resin column (capacity: $\sim$500μg DNA/column) under low salt conditions. DNA was eluted after several washing steps with high salt buffer (1.25 M NaCl, 50 mM Tris-Cl, pH 8.5, 15 % isopropanol (v/v)). The plasmid DNA was then concentrated and desalted by isopropanol precipitation. The DNA pellet was the redissolved in a suitable volume (250 to 400μl) of TE buffer, pH 8.0 or H_2O. Purified DNA is free of detectable RNase A activity and is suitable for *in vitro* transcription.

2.3.5 Concentration of DNA

Purines and pyrimidines in nucleic acids absorb UV light. The extinction coefficient ε of a polynucleotide depends on the sum of the extinction coefficients of each of their constituent nucleotides. The DNA concentration was determined from the absorbance (extinction E) at 260 nm using the Lambert-Beer relation:

$$E_{(260nm)} = log(\frac{I_0}{I_D}) = \varepsilon \cdot c \cdot d \tag{2.1}$$

with I_0 as the intensity of the monochromatic incident light with which the sample is irradiated and I_D as the light intensity of transmitted light. Given a path length of 1 cm the extincition E is called optical density (OD) at a given wavelength. At a given wavelength the absorbance is proportional to the optical path length d (in cm) and to the molar concentration c (in mole/liter). The molar extinction coefficient (ε) is numerically equal to the absorbance of a 1 M solution in a 1 cm light path and is therefore expressed in $M^{-1}cm^{-1}$.
For the determination of concentration of plasmid preparations, an average extinction coefficient of 6600 $M^{-1}cm^{-1}$ per nucleotide was used. 1 OD_{260} of a DNA solution corresponds to 50 μg/ml of double stranded DNA or 35 μg/ml of single-stranded DNA or RNA. For small nucleotides, it is best to calculate an accurate extinction coefficient with the nearest neighbor method [98]. Extinction measurements were measured using a spectrophotometer (JASCO, Model V-530).

ROX-labeled promoter-DNA duplexes

For the determination of ROX-labeled DNA duplexes after gel extraction, an averaged extinction coefficient of ε_{583} = 96000 $M^{-1}cm^{-1}$ at 25°C was used. The con-

centration used of the ROX-labeled DNA duplexes are summarized in the following Table 2.2.

DNA duplexes	**Stock concentration** [μM]
for RNAP·σ^{54} Binding	
*gln*Ap2-ROX	6
*nif*H-ROX	8
*nif*L-ROX	8.9
for σ^{54} Binding	
*gln*Ap2-homo-ROX	7.4
*gln*Ap2-hetero-ROX	5.9
*nif*H-homo-ROX	12.6
*nif*H-hetero-ROX	12.2
for NtrC Binding	
ES-1-Rho	5
ES-2-ROX	4
unlabeled ES-2	4

Table 2.2: Concentrations of used DNA duplexes used for binding studies

2.3.6 Hybridization of complementary DNA oligonucleotides

Equimolar amounts of complementary single strands were mixed in a buffer containing 10 mM Tris-HCl, pH 7.5, 10 mM NaCl, 0.1 mM EDTA and were annealed by 2 min heating at 70°C for ROX-labeled DNA or by 5 min at 95°C for unlabeled DNA. The reaction contained 1.4 to 1.9 μg of DNA per μl. Resulting ROX-labeled DNA duplexes for binding studies were further extracted from native polyacrylamide gels. DNA duplexes for molecular cloning were not purified.

2.3.7 Native polyacrylamide gels

Native polyacrylamide gels are used for the separation and purification of small fragments of double-stranded DNA. Binding of a protein i.e. to the DNA causes a shift to lower migration velocity as used in electrophoretic mobility shift assays. The percentage of acrylamide monomer to be used in preparing the gel is determined by the size of DNA fragments or DNA-protein complexes to be resolved. For migration of very small double-stranded DNA the usage of acrylamide-bisacrylamide premix with a ratio of 19:1 is suitable.

	Mobility Shift	Mobility Shift	Purification of ROX-labeled promoter duplexes and single strands	Analysis of ROX-labeled duplexes and
Percentage of gel	5 % (29:1)	6 % (37.5:1)	12 % (19:1)	20 % (19:1)
Volumes				
40 % Acrylamide:bis	6.25 ml	1.5 ml	15 ml	5 ml
10 x TBE	1 ml	200 μl	5 ml	1 ml
H_2O	42.25 ml	8.3 ml	30 ml	4 ml
10% (w/v) APS	500 μl	50 μl	250 μl	50 μl
TEMED	30 μl	30 μl	30 μl	30 μl
total	50 ml	10 ml	50 ml	10 ml
Running conditions				
Running buffer	0.2 x TBE	0.2 x TBE	1 x TBE	
Prerun	20 min at 70 volts	20 min at 70 volts	not necessary	not necessary
Run	1.5 hours at 70 volts	25 min 10 to 15 mA per gel	80 to 100 volts (30 mA per gel)	

The gels were casted and run with the Mini-PROTEAN 3 system from Bio-Rad (glass plate size: 8 x 10 cm (width x length), 0.75 mm well width, $\sim$ 5 ml of gel volume, slot volume of 20 μl)

10 x TBE electrophoresis buffer: 108 g of Tris base, 55 g of boric acid, 20 ml of 0.5 M EDTA, pH 8.0 (Storage at room temperature). TBE was used at a working strength of 0.2 or 1 x for polyacrylamide gels or of 1 x for agarose gels.

2.3.8 Ethidiumbromide staining

Agarose and Polyacrylamide gels were stained for 10 to 15 min in aqueous ethidium bromide solution (1 μg/ml). The solution was prepared from a stock solution of ethidium bromide of 10 mg/ml. The fluorescent dye ethidium bromide contains a tricyclic planar group that intercalates between the stacked bases of DNA. Its fixed position between the bases causes the dye to display an increased fluorescence compared to the dye free in solution. Ethidium bromide absorbs at UV radiation of 302 nm. It is also possible to radiate at 254 nm where the DNA absorbs and transmits the energy to the dye. In both cases, the energy is re-emitted at 590 nm in the red-orange region of the visible spectrum. Because of the high fluorescent yield of the ethidium bromide-DNA complexes, DNA amounts down to $\sim$ 50 ng/band can be detected.

2.3.9 Denaturing polyacrylamide gels (8 M Urea)

Denaturing polyacrylamide were used to resolve RNA transcripts of different length from *in vitro* transcription experiments. Addition of denaturing urea ensures that the RNA to separate remain apart and migrate the gel as linear molecules.

Ingredients for a 100 ml stock solution for 6 % denaturing gels
Volumes

15	ml	40% Acrylamide:bis solution (19:1)
10	ml	10 x TBE
35	ml	H_20
48	g	Urea
	$\mapsto$	dissolve while mixing and heating
add 100	ml	H_2O

The gels were poured and run with the Mini-PROTEAN 3 system from Bio-Rad (glass plate size: 8 x 10 cm (width x length), 0.75 mm well width, $\sim$ 5 ml of gel volume, well volume: $\sim$ 20 μl). Gels were used immediately or stored for up to 48 hours at 4°C.
Electrophoresis was carried out for 45 min in 1 x TBE (see above) and with a current of 25 mA per gel. The gel was dried for 20 to 40 min at 80°C (Bio-Rad Gel dryer 583) and the radioactive transcripts were visualized by audioradiography.

Formamide denaturation buffer
Approximately 500 mg of xylencyanol were diluted into 10 ml 1 x TBE and filtered (0.22 μm). 10 ml of formamide was then mixed with 200 μl of the xylencyanol solution. The buffer was stored at – 20°C.

2.3.10 Extraction of DNA from polyacrylamide gels

ROX–labeled DNA was extracted from the polyacrylamide gel by using the QIAEX II extraction kit. The extraction was performed as recommended by the manufacturer. After gelelectrophoretic separation of the duplexes from single-stranded DNA, the gel was ethidiumbromide stained (1 μl/ml), the desired gel band was localized with 366 nm UV-light and isolated. The gel slice was incubated overnight in diffusion buffer (0.5 M ammonium acetate, 10 mM magnesium acetate, 1 mM EDTA, pH 8.0, 0.1% SDS) at darkness. DNA adsorbs onto the silica-gel particles in the presence of

chaotropic salt. The binding capacity of the silica gel is $\sim 5\mu$g per 10 μl of suspension and the recovery is about 75 % for small DNA sizes up to 75 bp. Several washing steps remove salt impurities. The DNA was eluted by adding an appropriate elution buffer (10 mM Tris-Cl, pH 8.5) in two steps for increased yield. The extracted DNA was checked for purity and recovery by gelelectrophoresis (20 % native polyacrylamide gel (19:1)). Recovery was about 50 %.

2.3.11 Analytical agarose gels

Plasmid DNA was checked on 1 % (w/v) agarose gels in 1 x TBE. Gels were poured and run with the Sub-Cell GT Electrophoresis Cell system from Bio-Rad. The size rang of DNA fragments resolved by a 1 % agarose gel using low melting agarose is from 800 bp to 10 kb. The samples were mixed with 0.2 volume of the 6 x gel-loading buffer before loading into the slots. Electrophoresis was performed at 100 to 120 volts at room temperature. After electrophoresis, the gel was stained for 20 min in electrophoresis buffer containing 1 μg/ml ethidium bromide at room temperature.

10 x Electrophoresis Buffer (TBE): 108 g Tris base, 55 g boric acid, 40 ml of 0.5 M EDTA, pH 8.0 (Storage at room temperature)
Gel-loading Buffer (6 x): 0.25% bromphenol blue + 40% (w/v) sucrose + 1 x TBE in $H_2O \mapsto 0.2$ μm filtered (Storage at 4°C).

2.3.12 Extraction of DNA from agarose gels

Gelextraction of DNA fragments was performed with QIAquick Gel Extraction Kit from Qiagen according to the manufacturers protocol. This protocol is designed to extract and purify up to 10 μg of DNA (from 70 bp to 10 kb) from enzymatic reactions. The DNA can be then directly used for subsequent applications. DNA absorbs to a silica-membrane in the presence of high salt while contaminants and dissolved agarose pass through the column and are efficiently washed away. The pure DNA is eluted with Tris buffer (pH 8.5) or water.

2.3.13 Modifications of DNA

Site-directed mutagenesis

Site-directed mutagenesis is a suitable method to introduce and/or delete one or several base pairs at a concrete site. Primer are designed to mismatch with their

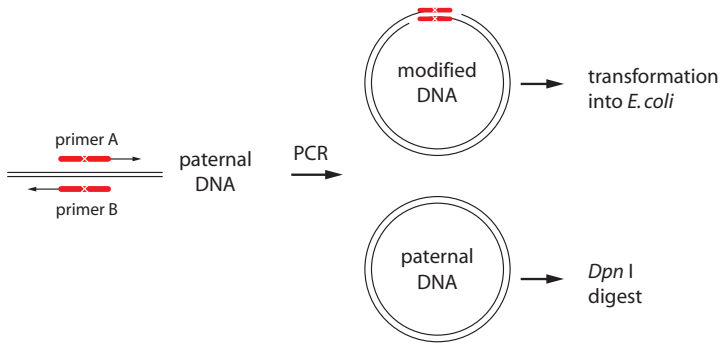

Figure 2.3: Scheme of site-directed mutagenesis. The desired mutation(s) (indicated by the white crosses) must be located within the DNA primers. After amplification by PCR, paternal DNA is digested by *Dpn*I, which specifically recognizes methylated DNA. DNA synthesized *in vitro* is not methylated and therefore resistant to cleavage.

target. Amplification by polymerase chain reaction thus introduces the new sequence in the amplified product (Figure 2.3). After amplification the target DNA will be degraded by the restriction enzyme *Dpn*I which is not specific for a distinct sequence but for methylated DNA. This increases the transformation efficiency of the altered but nicked plasmids. Nicks in the *Dpn*I-digested product were ligated for increased efficiency of transformation.

Primer design

Both of the mutagenic primers must contain the desired mutation and anneal at the same sequence on opposite strands of the plasmid. Primer length was between 25 and 45 bases, and for best results the primers were designed with a melting temperature greater than or equal to 78°C. The mutation(s) should be in the middle of the primer. The following formula was used to estimate the melting temperature T_m for primers that mismatch the DNA:

$$T_m(^\circ C) = 81.5 + 0.41(\%\ GC) - 675/N - \%\ mismatch \tag{2.2}$$

with the total length of the primer N and the content of G-C base pairs in %. For primers that introduce insertions or deletions the percentage of mismatches is considered to be equal to 0.

Polymerase chain reaction (PCR)

The polymerase chain reaction was conducted in a temperature cycler with top heating. The primer extension time is carried out near the optimal temperature for Pfu Turbo DNA polymerase (72°C) and depends on the length of the DNA to be synthesized: As a rule of thumb, extension is carried out for 2 min for every 1000 bp of product. The number of cycles was chosen to be 18 from step 2 to 4. The PCR product was checked on a 1 % agarose gel.

Reaction (50 μl)

5 - 50	ng	Template
125	ng	Primer A
125	ng	Primer B
1	μl	dNTP-mix (25 mM each from stock)
5	μl	10 x cloned Pfu buffer
1	μl	Pfu Turbo DNA Pol (2.5 units/μl)

10 x cloned Pfu buffer: 100 mM KCl, 100 mM (NH_4SO_4), 200 mMTris-Cl, pH8.75, 20 mM $MgSO_4$, 1 % Triton X-100, 1 mg/ml BSA

PCR program (18 cycles for steps 2 to 4)

Step	Temp [°C]	Time [sec]	
1	95	120	Initial denaturation
2	95	30	Denaturation
3	55	60	Primer annealing
4	68	420	Primer extension (120 sec/kB)
5	68	300	Final extension
6	4	∞	Storage

*Dpn*I digest

The restriction enzyme *Dpn*I cleaves double-stranded DNA specifically at the methylated sequence 5'-G^{m}6ATC-3' of methylated or hemi-methylated DNA. Plasmid DNA isolated from almost all commonly used strains of *E.coli* are fully methylated *in vivo* by endogenous *Dam* methylase and are therefore sensitive to cleavage by *Dpn*I (McClelland & Nelson 1988 [102]). *Dpn*I endonuclease is used to digest the parental DNA template. DNA synthesized *in vitro* by PCR using the four conventional deoxynu-

cleotides is unmethylated and therefore resistant to cleavage. *Dpn*I cleavage of the PCR reaction increases the transformation efficiency for the newly synthesized DNA.

Reaction

	40 μl	PCR reaction
+	0.5 μl	*Dpn*I (20 units/μl)
	$\mapsto$	Incubation at 37°C for 1 hour

Dephosphorylation

During ligation *in vitro*, DNA ligase catalyzes the formation of a phosphodiester bond between adjacent nucleotides only if one nucleotide carries a 5'-phosphate residue and the other carries a 3'-hydroyl terminus. Removal of terminal 5'-phosphate groups with alkaline phosphatase was therefore used to suppress self-ligation and recircularization of plasmid DNA. A DNA segment with intact 5'-residues can be ligated efficiently *in vitro* to the remaining 3'-hydroxyl group of the plasmid to generate an open circular molecule containing two nicks. This open circular DNA molecule is much more effective to transform into *E. coli*.

Ligation

DNA ligase from *E. coli* phage T4 catalyzes the formation of a phosphodiester bond between juxtaposed 5'-phosphate and 3'-hydroxyl termini in duplex DNA resulting in circular molecules. Additionally, this enzyme repairs single-strand nicks. Effective insertion of an insert into a vector depends on the molecular ratio of the insert over the vector. For a small insert length of i.e. 50 bp to be cloned in a vector of 3 to 4 kb length, the reaction should contain a 10 to 20-fold molar excess of insert.

Reaction (20 μl)

0.02	pmol	vector
0.2 - 0.4	pmol	insert
2	μl	10 x T4 DNA Ligase buffer
1	μl	T4 DNA Ligase (400 units/μl)

T4 DNA Ligase Buffer (1 x)

50mM Tris-Cl, 10 mM $MgCl_2$, 10 mM DTT, 1 mM ATP, 25 μg/ml BSA; pH 7.5

The ligation reaction was incubated overnight at 16°C and subsequently transformed directly into *E. coli* strain XL10 Gold or frozen at - 20°C.

Restriction of DNA

Analytical or preparative restrictions of DNA was performed by different restriction enzymes. Optimal restriction conditions such as pH and ionic strength of the reaction buffer and temperature were chosen as recommended by the manufacturer. For analytical restriction reaction, usually 10 μl of a mini preparation of DNA which is equivalent to an amount of $\sim$ 1 to 3 μg of DNA were mixed with 1 to 5 units of the chosen enzyme in an appropriate buffer. For best results, the amount of added enzyme did not exceed 10 % of the total volume. Double-digestion was performed in the same buffer at the same temperature. For preparative digestion an appropriate amount, e.g. 3 μg of plasmid DNA was cleaved with 10 units of the chosen enzyme for 2 to 4 hours. The restricted DNA was checked on an analytical 1 % agarose gel. The DNA fragments was then cleaned up from enzymatic reactions by extraction from an agarose gel.

2.4 Proteins

2.4.1 NtrC and σ^{54}

The activator protein NtrC and the σ^{54} subunit were provided by Dr. Alexandra Schulz. Expression and purification was as previously described [103, 104]. Briefly, N-terminal His-tagged proteins were purified on Ni^{2+} chelating resin with subsequent purification on a Mono Q column (anion exchange). Proteins were stored at – 80 °C in elution buffer supplemented with 50 % (v/v) glycerol containing 20 mM Tris/HCl pH 7.9, 180 mM KCl, 0.1 mM EDTA, 1 mM DTT and 5 % (v/v) glycerol for NtrC and 20 mM Tris/HCl pH 7.9, 350 mM KCl, 0.1 mM EDTA, 1 mM DTT and 5 % (v/v) glycerol for σ^{54}. The stock concentrations of NtrC and σ^{54} were 6 μM and 22 μM, respectively.

2.4.2 RNAP·σ^{54}

RNA polymerase core enzyme from *E. coli* (subunit composition: $\alpha_2\beta\beta'$) was obtained from Epicentre technologies (Madison, WI, via Biozym, Hess. Oldendorf,

Germany). RNAP·σ^{54} was prepared by mixing with σ^{54} in a ratio of 1:1.5 at a stock concentration of $\sim$ 1 μM. This preparation was stored at –20°C in a buffer with 50 mM Tris/HCl, pH 7.5, 250 mM NaCl, 0.1 mM EDTA, 1 mM DTT and 50% glycerol.

2.5 Characterization of proteins

The proteins used in this work were investigated with respect to their DNA binding affinities but also in their enzymatic activities with a variety of methods.

2.5.1 ATPase assay

ATPase activity of NtrC was tested with a test as previously described in [60]. The reaction buffer was slightly modified.

Reaction (25μl)

480	nM	NtrC (monomer)
0.1 to 1	μM	σ^{54} subunit or RNAP·σ^{54} holoenzyme
40	nM	ES-2 enhancer sequence
100	nM	heteroduplex *nif*H promoter
1	μl	radioactive ATP-Mix, freshly mixed
400	μM	ATP
25	mM	Carbamylphosphate
5	μl	1 x Reaction buffer

Radioactive ATP-Mix: (For 10 μl of freshly mixed reaction): 4.4 μl H_2O+5.5 μl 0.6 mM ATP+1.1 μl γ-^{32}P-ATP, Reaction buffer (5 x): 50 mM Tris-Cl, pH 8.0, 40 mM KCl, 10 mM $MgCl_2$,1 mM DTT, 0.1 mg/ml BSA, Chromatography solvent: 0.5 M LiCl, 1 M formic acid

The reaction was incubated for 15, 30 or 45 min at 37°C. 2 μl of the samples were applied to the origin of a 12 mm silica gel TLC (Thin Layer Chromatography) which was previously marked with a soft-lead pencil. After evaporation of the sample to dryness, the TLC plate was placed in the solvent chamber. The solvent was allowed to move $\sim$90 % of the distance to the top of the plate. The TLC plate was dried at 65°C and expose to a X-ray film (Kodak) for 15 min.

2.5.2 Electrophoretic mobility shift assay (EMSA)

Binding of RNAP·σ^{54} holoenzyme to promoter DNA

For gel shift analysis reactions (9μl) containing

245	nM	ROX-labeled promoter sequence
1	μl	RNAP storage buffer
x	nM	RNAP·σ^{54}

were mixed. A constant promoter DNA concentration (245 nM) was titrated with RNAP·σ^{54} in ratios (protein:DNA) of : 0:1 (0 nM), 0.25:1 (61.25 nM), 0.5:1 (122.5 nM), 0.75:1 (184 nM) and 1:1 (245 nM). The number in brackets refers to the concentration of added RNA polymerase. The reaction was incubated for 10 min at room temperature (~25°C). After addition of 1 μl of loading buffer the samples were loaded on a prerunned (20 min at 70 volts) native 5% polyacrylamide gel (29:1). Electrophoresis was conducted in 0.2 x TBE buffer for another 90 min at same voltage.

RNAP storage buffer: 50 mM Tris/Cl pH 7.5, 250 mM NaCl, 0.1 mM EDTA, 1 mM DTT and 50 % glycerol

Binding of sigma factor σ^{54} to promoter DNA

For gel shift analysis, reactions (27μl) containing

100	nM	ROX-labeled Promoter Sequence
x	nM	σ^{54} (0, 100, 500, 750, 1000, 2000, 5000)

in reaction buffer were mixed for 15 min at 30°C. Loading buffer was added 0.5 x (3 μl) and the samples were analyzed on a native 6% polyacrylamide gel (37.5:1, prerun for 25 min at 10 mA per gel). Electrophoresis was conducted in 0.2 x TBE buffer for 20 min at 10 to 15 mA per gel.

Reaction Buffer: 20 mM Hepes/KOH, pH 8.0, 5 mM magnesium acetate, 1mM DTT, 0.1 mg/ml BSA, 0.01 % NP-40 detergent, 50 mM potassium acetate, supplemented with 3.5 % (w/v) PEG 8000 (corresponds to Reaction Buffer from Anisotropy Measurements + 3.5 % (w/v) PEG 8000) Info: Addition of PEG stabilizes the formed interactions by 'Molecular Cageing'.

2.5.3 Analytical equilibrium ultracentrifugation

Analytical ultracentrifugation is a suitable method to determine molecular weights and stoichiometry of macromolecules. For this purpose, the sample is centrifuged at different rotational speeds (8, 13, 18 and 48 x 10^3 rpm). Absorption of the sample is measured during centrifugation and the wavelength can be chosen individually.
In sedimentation equilibrium experiments, a small volume ($\sim$ 120 μl) of an initially uniform solution is centrifuged at a lower angular velocity than is required for sedimentation of the particles to the bottom of the cell. First, there is a centrifugational force leading to a sedimentation of the particles. The process of diffusion opposes the process of sedimentation. After an appropriate period of time, the two opposing forces approach an equilibrium. The equilibrium concentration of the solution increases exponentially towards the cell bottom and is invariant with time. From measurement of the concentration at different radial positions, the molecular weight of the particles is determined.

Molecular weight determination

A good approach to analysis of the molecular weight is to consider that particles at different radial positions have different energetic states. After Boltzmann, the probability P_i to have a molecule with an energy E_i is

$$P_i \propto g_i exp(\frac{-E_i}{kT}) \tag{2.3}$$

where g_i is the number of possible energy states with the energy E_i, the Boltzmann's constant k and the absolute temperature T. Thus, the ratio of two probabilities which is equivalent to two concentrations is

$$\frac{c_j}{c_i} = exp(-\frac{E_j - E_i}{RT}) \tag{2.4}$$

The difference of energy at different radial positions i and j in the cell results from the work to perform for displacing a particle from i to j or vice versa. This energy arises from the integral of the force over . The difference of energy can be calculated for every position in the cell. To do so, the effective mass M_{eff} has also be taken into account. M_{eff} is calculated in consideration of the partial specific volume $\bar{\nu}$ of the particle and the density of the solvent ρ by $M_{eff} = M \cdot (1 - \bar{\nu} \cdot \rho)$. We get the following equation correlating concentration as a function of absorption and the radial position r:

$$A_r = A_0 \cdot exp(\frac{M \cdot (1 - \bar{\nu} \cdot \rho) \cdot \omega^2 \cdot (r^2 - r_0^2)}{2 \cdot RT}) + E \tag{2.5}$$

A_r and A_0 are the absorbance at a radial position r and at a reference position r_0. Thus, the absolute concentrations or extinction coefficients do not enter these equations and need not to be known for the determination of the molecular weight M. It is only required that the absorbance of a given component is proportional to the concentration given by the Lambert–Beer relation (A_r from 1.2 to 1.5).
For 2 components (A and B) in solution the above equation has to be expanded by an additional term relating to the second species

$$\begin{aligned} A_r \quad = \quad & A_{0,A} \cdot exp(\frac{M_A \cdot (1 - \bar{\nu}_A \cdot \rho) \cdot \omega^2 \cdot (r^2 - r_0^2)}{2 \cdot RT}) + \\ & A_{0,B} \cdot exp(\frac{M_B \cdot (1 - \bar{\nu}_B \cdot \rho) \cdot \omega^2 \cdot (r^2 - r_0^2)}{2 \cdot RT}) + E \end{aligned} \tag{2.6}$$

The indices A and B correspond to species A and B, respectively. The angular velocity ω is known from the rotor speed, R is the universal gas constant and T the absolute temperature. The parameter E is the baseline offset and was determined from the absorbance of the region close to the meniscus after sedimentation of the sample at 48,000 rpm for six hours. Parameter M is the molecular weight of the macromolecule studied which was derived from the fit, and $\bar{\nu}$ is the partial specific volume.

Sample preparation

Analytical sedimentation equilibrium ultracentrifugation was carried out in a Beckman Optima XL-A analytical ultracentrifuge equipped with absorbance optics and an An60Ti rotor. σ^{54} protein and DNA duplexes (*gln*Ap2 homoduplex, *gln*Ap2 heteroduplex, *nif*H homoduplex and *nif*H heteroduplex, each of 50 bp length with a molecular weight of 33 kDa) were mixed in a buffer containing 20 mM Hepes/KOH, pH 8.0, 5 mM magnesium acetate, 1 mM DTT, 0.01 % NP-40 detergent, 0.1 mM EDTA and 50 mM potassium acetate. The DNA duplex concentration was kept at 400 nM which is equivalent to an absorbance of 0.34 at 260 nm and a 12 mm path length of the cell. The σ^{54} protein concentration was kept at 3.05 μM. Centrifugation was carried out at 20°C at four different angular velocities: 8,000, 13,000, 18,000 and 48,000 rpm.

Data analysis

For determination of the molecular weight the data were analyzed with the software provided by Beckman which is based on the program Origin v.3.78 (MicroCal Software, Inc. MA) and performs either a single exponential (model ideal 1, equation 2.5) or two exponential fit (model ideal 2, equation 2.6) to the data. The partial specific volume $\bar{\nu}$ for the His-tagged σ^{54} studied here it was calculated from the amino acid sequence to be 0.7325 ml g^{-1} at 20°C. $\bar{\nu}$ for DNA duplexes were calculated with the program Bandit from the nucleic acid sequence at 20°C and values of 0.5519 cm^3g^{-1} (*gln*Ap2 homoduplex), 0.5505 cm^3g^{-1} (*gln*Ap2 heteroduplex) and 0.5466 cm^3g^{-1} (*nif*H hetero- and homoduplex) were determined. $\bar{\nu}$ for the protein-DNA mixture was calculated from the partial specific volumes and molecular weights of the free components to be 0.664 ml g^{-1}. The density ρ of the solvent was calculated with the software Sednterp to be 1.00336 g ml^{-1}at 20°C.

2.6 Fluorescence anisotropy measurements (FA)

Anisotropy measurements are based on the photoselective excitation of fluorophores or fluorescent-labeles molecules by polarized light. When a population of fluorescent labeled molecules is excited with polarized light those molecules with an absorptive dipole moment parallel to the plane of polarization light are preferentially excited. Other molecules are excited dependent on the angle to this plane of polarization. Provided that the molecule remains stationary the emitted light will also be polarized. Any movement of the molecule will results in a reduced polarization of the emitted light. Measuring the polarization or anisotropy of a molecule is a suitable method to yield information concerning its molecular motion. Binding of one molecule to another has direct effect on the rotation motion of each of the single molecules. This method permits acquisition of data under thermodynamic equilibrium conditions with variable salt concentrations or temperatures.

2.6.1 Definition of anisotropy

When polarized light passes through a sample, the emitted light is also polarized. In order to understand what happens with a population of fluorophores where every molecules has another spatial orientation to the plane of polarization it is useful to reduce the by following the pathway of the polarized light through the sample and the relation to the measured intensities in x, y and z direction (Figure 2.4).

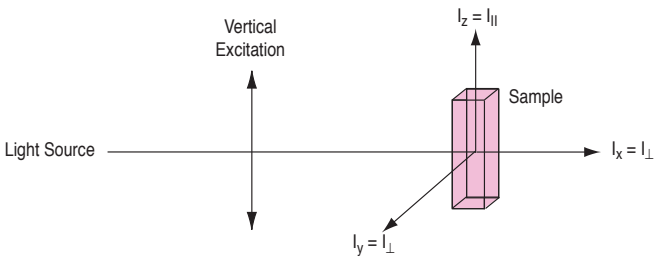

Figure 2.4: Pathway of vertically polarized light through the sample

The sample is excited with vertically polarized monochromatic light (z axis). Given by the geometry of the experimental set-up (Figure 2.5) the total intensity ($I_x + I_y + I_z$) of the vertically polarized light which travels along the x axis is divided into 2 fractions: an intensity which can be measured parallel to the initial plane of polarization ($I_{||} = I_z$) and an intensity perpendicular to the initial plane of polarization($I_\perp = I_y$). The anisotropy is defined as the ratio of the polarized component to the total intensity (I_{total}). Since light radiates by a dipole it is distributed equally along the x and the y axis and thus the total intensitiy is given by $I_{total} = I_{||} + 2I_\perp$ and equation (2.7) is obtained

$$r = \frac{I_z - I_y}{I_x + I_y + I_z} = \frac{I_z - I_y}{I_{total}} = \frac{I_{||} - I_\perp}{I_{||} + 2I_\perp} \tag{2.7}$$

2.6.2 Rotational Diffusion of a Fluoropohore

A dominant cause of depolarization is the rotational diffusion of a fluorophore during its fluorescence lifetime (t) which is described in the Perrin equation. A following derivation is based upon the fact that the time-resolved decay of anisotropy $[r(t)]$ for a spherical molecule is a single exponential function:

$$r(t) = r_0 e^t / \phi \tag{2.8}$$

ϕ is the rotational correlation time of the fluorophore, which is determined by the viscosity η and temperature T of the the solution and by the volume of the rotating molecule V, as described by

$$\phi = \frac{\eta \cdot V}{R \cdot T} \tag{2.9}$$

The time-resolved decay of the total fluorescence intensity $I(t)$ is given by $[I_{\parallel}(t) + 2 \cdot I_{\perp(t)}]$ (see above). Thus, the anisotropy of a steady state measurement is an average of $r(t)$ weighted by $I(t)$:

$$r = \frac{\int_0^\infty \mathrm{I(t)r(t)dt}}{\int_0^\infty \mathrm{I(t)dt}} \tag{2.10}$$

For a spherical fluorophore in a homogenous environment one expects $I(t)$ to decay as single expotential with a fluorescence lifetime τ

$$I(t) = I_0 e^{-t/\tau} \tag{2.11}$$

and after substitution of equations (2.8) and (2.11) we get the Perrin equation

$$r = \frac{r_0}{1 + (\tau/\phi)} \tag{2.12}$$

The Perrin quation describes the effects of rotational diffusion or the equivalent rotational correlation time (ϕ) and the fluorescence lifetime (τ) on the steady state anisotropy. In high viscous solution $\phi \gg \tau$ and the measured value is r_0. In the other case of very fluid solutions where $\tau \gg \phi$, the measured r is reduced to 0.
In order to investigate the binding of one molecule to a pre-labeled second molecule the changes in anisotropy depends no more on fluorecence lifetime since the latter is supposed to be constant upon complex formation. A change in anisotropy decay is no more dependent on fluorescence lifetime but depends now only on the rotational correlation lifetime τ (see equation (2.12)).

2.6.3 The L-format method

In the L-format method (= single channel method) used here, a single emission channel is used. Thus the parallel and perpendicular components of the total anisotropy are observed subsequently. The light passes through a monochromator to create a monochromatic light beam. The subsequent polarizer transmits the vertical plane of the light with respect to the electric component of the light. The emitted light passes then through a filter before it reaches the photodetection system. The objective is to

measure the actual intensities in parallel and perpendicular direction unbiased the detection system. A monochromator usually has different transmission efficiencies for vertically or horizontally polarized light. Hence, rotation of the emission polarizer leads to wrong intensities. To take this effect into account, the measured intensities have to be corrected. The factor G is the ratio of the sensitivities for vertically and horizontally polarized light depending on the detection system (see equation (2.16)).

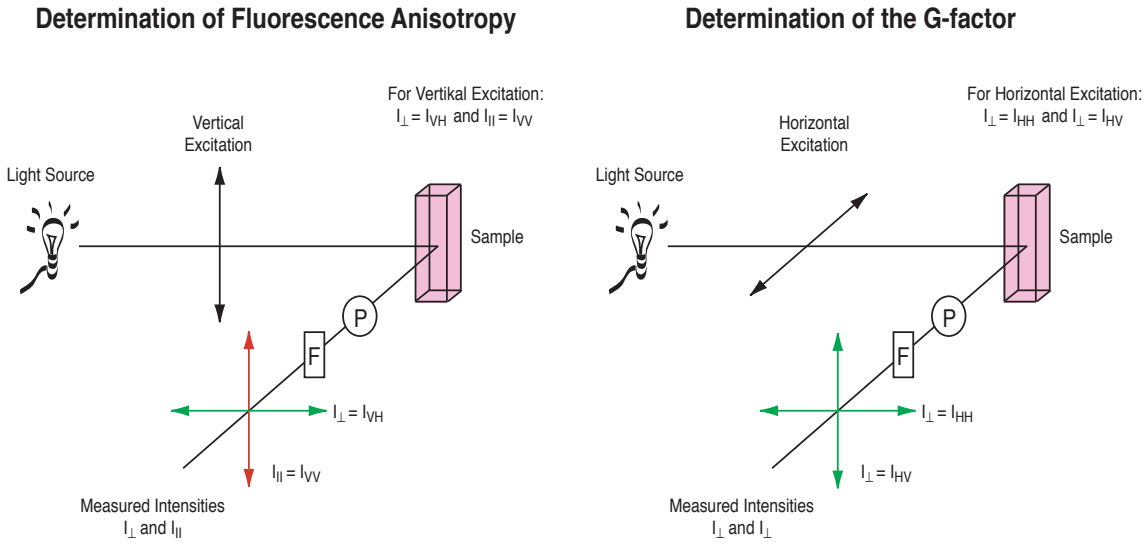

Figure 2.5: Experimental setup of aniostropy measurements
Schematic diagram for two different L-format measurements, P, polarizer, F, filter: At the left side: For determination of fluorescence anisotropy the excitation is vertically polarized and the measured intensities are perpendicular and parallel to the initial plane of polarization as defined. At the right side: For determination of the G-factor the excitation is horizontally polarized and the measured intensities are both perpendicular to the initial plane of polarization. Hence, any measured difference in the intensities I_{HV} and I_{HH} must be due to the properties of the detection system.

Determination of the G-factor

For the derivation of G two subscripts are used to indicate the two different orientations of the polarizers according to the order in which the light passes through the two polarizers: The first subscript indicates the orientation of the excitation polarizer the second subscript indicates the orientation of the emission polarizer in a horizontal (H) or vertical (V) orientation. Given the sensitivities of the emission polarizer for the different orientation of the latter S_V and S_H. For vertically polarized

excitation, the observed intensities are

$$I_{VV} = kS_V I_{\parallel} \tag{2.13}$$

$$I_{VH} = kS_H I_{\perp} \tag{2.14}$$

where k is the proportionality factor to account for the quantum yield of the fluorophore and other instrumental factors. Division of (2.13) by (2.14) leads to

$$\frac{I_{VV}}{I_{VH}} = \frac{S_V}{S_H}\frac{I_{\parallel}}{I_{\perp}} = G\frac{I_{\parallel}}{I_{\perp}} \tag{2.15}$$

Hence, the G-factor is

$$G = S_V/S_H \tag{2.16}$$

It depends upon the chosen emission wavelength and, to some extent, the bandpass of the monochromator. G is measured using horizontally polarized excitation. Under this condition, both the horizontally and the vertically polarized components of the emission are equal because both components are perpendicular to the polarization plane of the excitation. Any difference in the intensities must now be due to the properties of the detection system and G is defined by

$$\frac{I_{HV}}{I_{HH}} = \frac{S_V}{S_H}\frac{I_{\perp}}{I_{\perp}} = \frac{S_V}{S_H} = G \tag{2.17}$$

It can be easily measured by determination of the intensities I_{HV} and I_{HH} (Figure 2.5). Once the G-factor is determined, the ratio of $I_{\parallel}/I_{\perp}$ can be expressed by the intensities measured with vertically polarized light (equation (2.18)).

$$\frac{I_{VV}}{I_{VH}}\frac{1}{G} = \frac{I_{\parallel}}{I_{\perp}} \tag{2.18}$$

The corrected formula for anisotropy is then given by equation (2.19)

$$r = \frac{(I_{\parallel}/I_{\perp}) - 1}{I_{\parallel}/I_{\perp} + 2} = \frac{I_{VV} - GI_{VH}}{I_{VV} + 2GI_{VH}} \tag{2.19}$$

Magic angle conditions

Since the efficiency of a monochromator depends on the polarization of the light, one does not observe the total intensity, but rather some other combination of $I_{\parallel}$ and $I_{\perp(t)}$ (see above). By the use of the emission polarizer with an orientation of 54.7° ($\cos^2(45.7°)$=0.333 and $\sin^2(45.7°)$=0.666) with respect to the vertically excited light, $I_{\perp}$ is enhanced twofold over $I_{\parallel}$, forming the correct sum for the total intensity ($I_{total} = I_{\parallel}+2I_{\perp}$). At this angle the anisotropy is equal to zero and thus the intensities are only dependent on the orientation of the polarizers. This setup was used in this work to determine if the quantum yield of the ROX-dye changed upon binding to RNAP·σ^{54}.

2.6.4 Determination of binding affinities

Preparation of the sample

For titration, cuvettes (Hellma, quartz, pathlength: 3 x 3 mm) were used. The measurements were conducted at 25°C in a buffer containing 20 mM Hepes/KOH, pH 8.0, 5 mM magnesium acetate, 1 mM DTT, 0.1 mg/ml BSA, 0.01% NP-40 detergent, supplemented with potassium acetate at a concentration from 50 to 350 mM. To 60μl of a pre-diluted solution of ROX-labeled promoter-DNA in the given buffer, the protein was added stepwise which was diluted in the same buffer. During the experiment the protein stock solutions were kept on ice. The decrease in DNA concentration during the titration was taken into account in the analysis of the data. For stoichiometric titrations DNA concentrations of 10 nM were used.

Measurements of RNAP·σ^{54}-promoter DNA binding activity by stoichiometric titration

The RNAP·σ^{54}-promoter DNA binding activity was determined by stoichiometric titrations at a DNA concentration of 10 nM ROX-labeled duplex in low salt binding buffer (50 mM potassium acetate) for high affinity binding. In the case of a stoichiometric titration, the added molecule, RNAP·σ^{54}, binds quantitatively to the predeposited DNA until a fractional binding degree of 1 is reached. From the linear increase at low protein concentration and the plateau region obtained at saturation of the binding sites the equivalence point for the formation of a 1:1 complex was determined. The binding activity for different RNAP·σ^{54} holoenzyme preparations were determined.

Measurements of NtrC-enhancer binding activity by stoichiometric titration

The NtrC-enhancer binding activity under phosphorylating and non-phopshorylating conditions was determined by stoichiometric titration at a DNA concentration of 10 nM DNA duplex containing one (ES-1) or two (ES-2) strong NtrC binding sites (enhancers) in low salt binding buffer (50 mM potassium acetate) for high affinity binding. When needed carbamylphosphate as a chemical phospho-donor was added to an end concentration of 25 mM. The DNA was titrated with a pre-diluted solution of NtrC in the same buffer of a concentration of 200 or 300 nM until a plateau level was reached.

Determination of RNAP·σ^{54} binding affinities to different promoters

For the determination of dissociation constants a DNA solution with 25 to 200 pM was titrated with a RNAP·σ^{54} protein solution diluted into the same buffer. After addition of the protein the sample was equilibrated for ∼3 min before measuring the the equilibrium anisotropy value. For each anisotropy value the average of 20 measurements with an integration time of 5 sec was determined.

Dependence of the binding affinity on the ionic strength

Interaction between protein and DNA are electrostatic and therefore depend strongly on the ionic strength and pH used in the experiment. Since working solutions may be composed of different kations and anions of different valencies the relative ionic strength can be expressed in K^+ equivalents. Ionic strength of a solution with the concentration C with respect to one species of ion and z as the valency of the ion is calculated by [105]

$$I = \frac{1}{2} \sum_i C_i {z_i}^2 \tag{2.20}$$

The dependance of binding affinity on the ionic strength expressed as a concentration of monovalent ion has been derived by Record and co-workers [106, 107].

$$\frac{\partial log K_d}{\partial log[M^+]} = z\Psi \tag{2.21}$$

According to this equation, a double-logarithmic plot of the dissociation constant K_d

versus the salt concentration $[M^+]$ is linear. The slope of the plot yields the number of ion pairs z that form upon binding. Using 0.88 for the parameter Ψ for double-stranded B-form DNA one obtains a value for z by linear regression analysis [106].

Estimation of the quantum yield

The use of the fit function (2.25) is only correct for a constant quantum yield of the ROX dye upon binding of RNAP·σ^{54}. To check whether the quantum yield of the ROX dye changed upon binding of the polymerase the fluorescence intensity of the free promoter DNA and the intensity after saturation of the DNA binding sites was recorded under polarization independent 'magic angle' conditions (vertically polarized excitation and emission polarizer oriented at 54.7°C) for every titration.

Data acquisition

Fluorescence anisotropy measurements were performed with a SLM 8100 fluorescence Spectrometer (SLM Aminco Inc.) using an L-format setup [108]. The ROX excitation wavelength of 580 nm was selected with a double grated monochromator using an 8 or 16 nm slit width for high intensity. In the emission channel scattered light was suppressed with a 610 nm cut off filter. Intensity variations of the light source were corrected by normalization to a reference channel with a rhodamine quantum counter.

Data analysis

The data of anisotropy were converted to a binding degree Θ which describes a ratio of bound to free molecules. Θ adopts values between 0 (only free molecules) and 1 (100 % of bound molecules). Equation (2.22) describes the formation of the closed complex from the promoter P and the RNA polymerase R with a single step binding model.

$$R + P \rightleftharpoons RP_c \tag{2.22}$$

Equation (2.22) can be converted following the mass action law in equation (2.23). The forward and backward rate constants k_1 and k_{-1} of the part reactions can be combined to the dissociation constant k_d. Since the total fluorescence anisotropy

depends on the respective concentrations of free promotor-DNA and RNAP·σ^{54}-promoter complexes the resulting equation on which a fit function would be based on is

$$K_d = k_{-1}/k_1 = \frac{[R] \cdot [P]}{[RP_c]} \tag{2.23}$$

at a given point of titration, i.e. under stoichiometric conditions.
The promoter concentration $[P]$ was chosen so that $10[P] \leq K_d$ and hence the reduction of the total amount of the RNA polymerase is neglectable. Under these conditions the concentration of free RNAP·σ^{54} $[R]$ can be approximated by the total polymerase concentration $[R_{total}]$, i.e. $[R] \cong [R_{total}]$.

Derivation of the fit function

The fit function is based on the mass action law which describes the formation of the closed RNAP·σ^{54}-DNA complex accordingly to equation (2.23). The fractional saturation Θ of the promoter duplex with RNAP·σ^{54} is given by

$$\Theta = \frac{[R_{total}]}{[R_{total}] + K_d} = \frac{r - r_P}{r_{RP} - r_P} \tag{2.24}$$

In equation (2.24) r is the measured anisotropy at a given polymerase concentration, r_P and r_{RP} are the minimal and maximal anisotropies as estimated from the fit which reflects the anisotropies of the free promoter duplexes $[r_P]$ and the closed complexes $[r_{RP}]$, respectively. Rearrangement of equation (2.24) leads to equation (2.25), which was used to determine K_d from a least squares fit of the binding curve obtained by plotting the measured r values versus the added RNA polymerase concentration $[R_{total}]$ with r_P and r_{RP} as additional fit parameters.

$$r = \frac{r_P \cdot K_d + [R_{total}] \cdot r_{RP}}{[R_{total}] + K_d} \tag{2.25}$$

The least squares fit was computed with the program Kaleidagraph v.3.5 (Synergy Software, PA).

2.7 *In vitro* transcription assay

The product of the *in vitro* transcription assay, the RNA transcript, displays the total process of transcription activation involving promoter binding of the RNAP·σ^{54} and enhancer binding of the activator NtrC, DNA melting, elongation and finally termination. Any change of template composition such as altering the promoter sequence or changes in the upstream region of the promoter containing activator binding sites may lead to a change in the amount of transcript. The transcription experiments were carried out in the presence of a second plasmid, the reference plasmid pVW7-158 which produces a shorter transcript of 158 nt which can be easily discriminated from the 481 nt transcript of the test plasmid.

2.7.1 Sample preparation

Sample preparation was performed in small (500 μl) siliconized Eppendorf cups from Biozym (Hess. Oldendorf, Germany) at room temperature (~25°C).

Determination of transcription activity of RNAP·σ^{54}

Transcriptional activity of RNAP·σ^{54} was determined to get a maximum of transcription rate for the following experiments (Figure 3.18). The experiments were carried out as described below. The binding mix was prepared with a constant concentration of NtrC dimer of 50 nM and RNAP·σ^{54} was titrated in steps of 10 nM from 0 to 80 nM. The preparation of the elongation mix as well as the incubation times were the same as in the following section.

Titration of RNAP·σ^{54} to the *gln*Ap2, *nif*H and *nif*L promoters

The templates of interest which differ in the promoter sequence were investigated in transcription activity at partially and fully occupied promoters with an excess of activator protein NtrC. The concentration where a maximum of transcription activity can be expected was chosen to be 100 nM, owing to the results of NtrC titration. The working mixtures were prepared in a low salt buffer (0.5 x HS buffer, see below). The binding mix contained the following ingredients supplemented with different concentrations of RNAP·σ^{54} from 0 to 80 nM.

Binding Mix (9 μl)

0-80	nM	RNAP·σ^{54}
50	nM	NtrC dimer
5	nM	test plasmid
5	nM	reference plasmid pVW7-158
0.5	x	HS buffer
1	mM	DTT
0.1	mg/ml	BSA

The elongation mix was prepared andthe experiment was performed as described in Subsection 'Titration of NtrC'.

Transcription activity in dependence of the NtrC protein concentration

For the single-round *in vitro* transcription experiments a binding mix and an elongation mix were prepared. The binding mix contained 50 nM RNAP·σ^{54}, which was determined as described above to give nearly maximal amounts of open complexes or transcript.

Binding Mix (9 μl)

50	nM	RNAP·σ^{54}
0-200	nM	NtrC dimer
5	nM	reference plasmid pVW7-158
5	nM	test plasmid
0.5	x	HS buffer
1	mM	DTT
0.1	mg/ml	BSA

Elongation Mix (80 x 2 μl= 160μl)

96	μCi	α-^{32}P-CTP
0.08	mM	CTP
1.77	mM	GTP
1.77	mM	UTP
0.5	x	HS buffer
1	mM	DTT
0.08	mg/ml	heparin

4 x HS buffer

40	mM	Hepes/KOH, pH 8.0
80	mM	Mg acetate
400	mM	K acetate

The elongation mix was aliquoted to 2 μl. The binding mix was aliquoted and supplemented with the given concentration of NtrC-dimer. While the 5 min at 37°C incubation time, the proteins can bind to their specific binding sites on the DNA. After addition of 0.5 μl of a 400 mM stock solution of carbamyl phosphate to an end concentration of 20 mM the binding mix the latter was incubated for further 5 min at 37°C. NtrC is phosphorylated by carbamylphosphate, oligomerizes at the enhancer site and is now able to activate RNAP·σ^{54}. Addition of 0.5 μl of a 100 mM solution of ATP to an end concentration of 5 mM enables DNA looping between the activated NtrC at the enhancer and the promoter-bound RNAP·σ^{54}. The interaction between NtrC and the RNAP·σ^{54} enables the polymerase to melt the DNA (open complex). After a 16 min incubation at the same temperature where the isomerization of the closed to the open complex takes place, 5 μl of the 10μl assay was added to the elongation mix and incubated for another 13 min and then stopped by adding 10 μl of formamide stopping buffer. Heparin is a polyanion which competes with DNA for binding of RNAP·σ^{54}. Addition of heparin destroys transcriptionally inactive RNAP·σ^{54} closed complexes whereas opne complexes are heparin resistent. Thus, after a first round of transcription, formation of new closed complexes at the promoter is inhibited. To ensure equal incubation times, the different steps of ATP addition, addition of the binding mix to the elongation mix and stop of the reaction were carried out in a time frame of 20 sec. 8 μl of each samples were loaded on a denaturing 6 % urea polyacrylamide gel.

Working solutions of NtrC

Activator protein NtrC was prediluted from a stock solution of 5.2 μM with respect to the protein monomer in a buffer containig 0.5 x HS, 1 mM DTT and 0.1 mg/ml BSA into dilutions of (1:2) (1:4) (1:6) and (1:18).

Data acquisition

For detection, the dry gels were exposed for 7 up to 25 h hours to phosphoimager plates (Molecular Dynamics, Krefeld, Germany). The data scan was performed with the setup best resolution and a resolution of 100 μm. The sensitive medium of the phosphoimager plates are constituted of fine BaFBr:Eu^{2+} cristals which are stabilized by an organic substrate. Energetic β radiation of the sample excites the Eu^{2+}-ion into its oxidated state Eu^{3+}. This oxidation state remains stable even

when the plate is removed from the gel and exposed to room light for a moment. A helium-neon laser with an emission wavelength of 633 nm scans the phosphoimager plate pixel by pixel. Absorption of the laser beam induces the release of an electron and the initial reduced state of Eu^{2+} is restored. The release of the electron is accompanied by the emission of light which is further detected and is transformed into a digital image of the gel. This image can be finally analyzed by the program ImageQuant vs 5.2 (Molecular Dynamics). The data were then exported into the program Kaleidagraph version (Synergy Software, Reading, PA, USA), quantified and plotted. Phosphoimager plates were erased by 12 min exposition on the Image Eraser (Molecular Dynamics).

2.8 Scanning force microscopy (SFM)

Scanning force microscopy (SFM also called AFM, Atomic force microscopy) is a versatile method for characterization of surfaces and has been developed 1986 by Binnig and coworkers [109]. The resolution of the SFM is comparable to conventional electron microscopy. However, SFM is a topographic technique, so that additional information is encoded in the height of the sample. It can be used to investigate the structure of biological samples such as DNA and proteins. Fixation of the negatively charged DNA can be done by using bivalent cations such as Mg^{2+} to bind the DNA to negatively charged surface of freshly cleaved mica.

Figure 2.6 schematically outlines the experimental setup of an scanning force microscope. Scanning of the sample across the investigated surface is achieved by means of a piezoelectric scanner which moves the sample. A scanning force microscope measures the forces between two macroscopic bodies, the tip and the sample. These force measurements are made by recording the deflection of the cantilever. The deflection of the cantilever is measured by reflecting a laser beam on the back-side of the tip. The change in the reflection angle is detected by a four-segment photodetector. A feed-back loop to the piezoelectric scanner maintains constant forces between sample and the tip. A scanning force microscope can be operated in many ways measuring different interactions between the tip and the sample.

Biological samples are mostly soft and tend to be destructed by small forces. They are usually scanned in the tapping-mode which reduces the destruction of these relatively soft samples. In this mode, the tip is vertically oscillating near its free resonant frequency ω_0 during scanning of the sample. Thus, the tip stays in contact only for a short period of time. When approaching the surface, the oscillation is damped

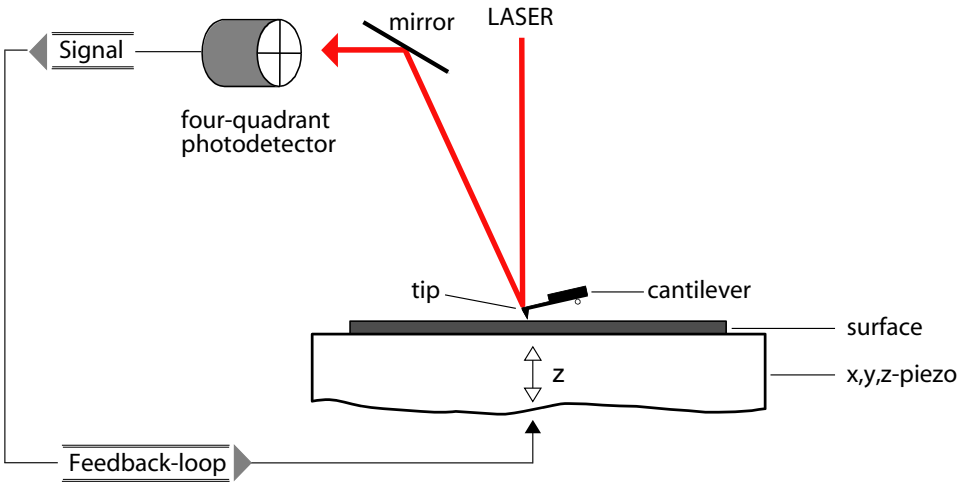

Figure 2.6: Experimental setup of the scanning force microscope (SFM).The setup uses the optical beam deflection method. A laser beam is focused on the back-side of the tip. When the tip interacts with the surface of the sample, the cantilever exhibits a deflection perpendicular to the surface and changes the direction of the laser beam which is reflected into a four-quadrant detector. A feed-back loop to the piezoelectric scanner that moves the sample maintains constant forces between sample and tip.

which results in an altered amplitude and frequency which in turn is recorded by the photodetector. Changes in amplitude and frequency contain information about the height of the sample and can be transformed in a topographic image of the sample (see Figure 2.7 as an example). The key advantage of the tapping mode are first, that the forces between tip and sample are minimized due to the sensitivity towards small variations in the amplitude when the tip encounters the sample. Thus the tapping mode is ideal for soft and fragile samples. In addition, this technique allows it to image the sample after drying on an appropriate surface as well as under physiological condititions in liquid [110]. The resolution is limited by the sharpness of the tip. The tips used in this study have an apex radius of 5 to 10 nm, which sets the lower limit in the resolution around a few nanometers. The tips used for scanning in air (Nanoprobe, type: RTESP7 from Veeco, Mannheim, Germany) had resonance frequencies around 300 kHz.

2.8.1 Image acquisition and analysis

The SFM images were obtained with a Nanoscope III (Digital Instruments, Santa Barbara, CA) operating in the tapping mode, where the cantilever is oscillated vertically while it is scanning over the surface. RNAP·σ^{54}-DNA complexes were formed by incubating 0.5 nM supercoiled 3314 bp long plasmid pVW7 with 1 nM RNAP·σ^{54} in a low salt buffer (10mM Hepes/KOH 8.0, 5 mM magnesium acetate, 20 mM potassium acetate) for 10 min at 37°C. After incubation, 20 μl of the mix were deposited onto a freshly leaved mica surface. After 10 to 15 seconds, the mica was washed right away by dropping 1 ml of distilled water onto the surface and then drying the sample in a stream of N_2. Images were recorded in air at ambient humidity using etched Si-probes (type Nanosensors) purchased from L.O.T. Oriel (Darmstadt, Germany) with a force constant of 17 to 64 N/m, a thickness of of 3.5 to 5.0 μm, a resonance frequency between 250 and 400 kHz, and a tip curvature radius of $\sim$ 10 nM (specifications as given by the manufacturer).
Only supercoiled DNA molecules with a single RNAP·σ^{54} holoenzyme were analyzed. In order to exclude open circular molecules, the number of crossovers had to be at least three. Measurements of the DNA contour length and the length of the end-loops were done with the program NIH image vs 1.58 (National Institutes of Health, Bethesda, MD). The total DNA contour length was determined from free relaxed DNA plasmids by measuring along the DNA. Figure 2.7 shows an image of a closed RNAP·σ^{54} complex bound to a supercoiled DNA.

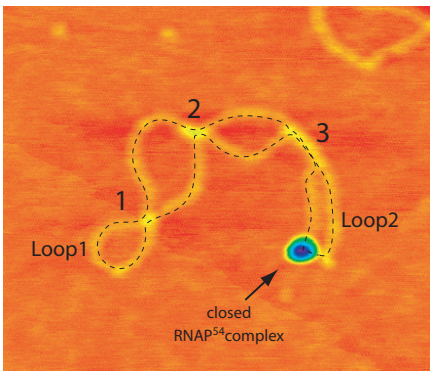

Figure 2.7: Data analysis of the images aquired by scanning force microscopy.
The height of the sample is color-coded, orange indicates the mica surface, yellow the DNA and blue the protein RNAP·σ^{54}. The image shows the supercoiled DNA plasmid pVW7 bound by a single RNAP·σ^{54} holoenzyme in a closed complex. The protein is localized in one of the end-loops. The total contour length is determined by the length of the dashed line. The length of the two end-loops was determined in the same way.

The molecule contains three crossovers and thus is classified as superhelical. The RNAP·σ^{54} is positioned in one of the two end-loops. The DNA molecule contains three crossovers. In order to determine the ratio of the end-loops to the total contour length, the length of the end-loops were also measured.

Chapter 3

Results

The initiation of transcription is a complex process. It involves different steps which are potential control points that enable the cell to change expression pattern in response to growth conditions. Studies with bacterial RNA polymerase have divided the transcription initiation into three steps each of which can be subject to regulation (Figure 1.3):

1. Promoter binding of RNA polymerase to form a closed complex (R_c)

2. Isomerization from the closed to the open complex ($R_c \mapsto R_o$)

3. Initiation of processive RNA synthesis

Experiments were performed to elucidate the mechanism of transcriptional activation by the NtrC protein. Binding affinities of closed RNAP·σ^{54} complexes to different promoter sequences were determined by fluorescence anisotropy measurements. The binding of NtrC and its active phosphorylated form NtrC-P to the enhancer was examined with the same technique. The topology of the closed RNAP·σ^{54} complex at the *gln*Ap2 promoter on superhelical DNA templates was investigated by scanning force microscopy. Isomerization from the closed to the open complex occurs by a conformational change in both σ and the core RNA polymerase triggered by a productive interaction between NtrC and the sigma factor σ^{54}. This interaction was investigated with a gel mobility shift assay. Furthermore it was tested wether the ATPase activity of NtrC-P was stimulated by σ^{54}. Finally, *in vitro* transcription assays were used to elucidate the relation between DNA binding of NtrC and the transcription activation process.

3.1 Protein-DNA interaction in the NtrC-RNAP·σ^{54} system

Binding of RNAP to the promoter leads to the formation of the closed complex as shown in equation (2.22) which could be rate limiting for transcription initiation. For the standard *E. coli* RNAP·σ^{70} it has been demonstrated that binding of the RNA polymerase to the promoter as well as the subsequent isomerization of the closed to the open complex can be rate limiting. For RNAP·σ^{54} no quantitative analysis of the promoter strength in terms of the relative contributions of the separate steps has been reported so far.

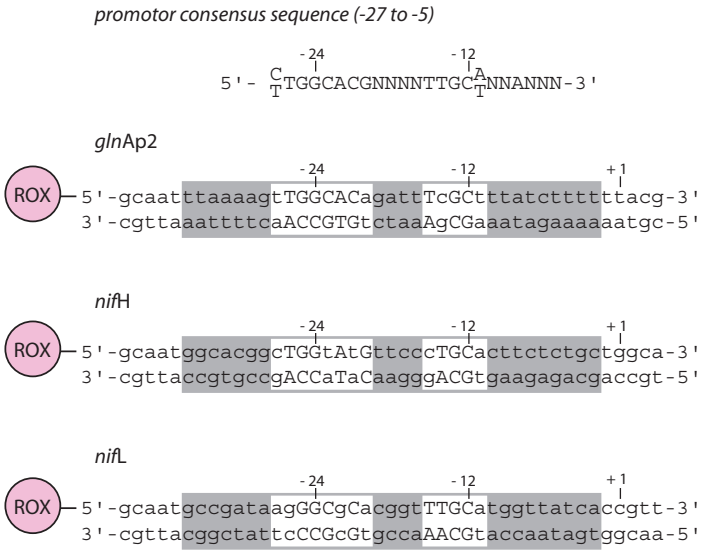

Figure 3.1: ROX-labeled DNA duplexes used in the binding studies.
The *gln*Ap2 promoter sequence from *E. coli* and the *nif*H and *nif*L promoter sequences from *K. pneumoniae* were studied. The nucleotides that fit the –24/–12 consensus sequence for RNAP·σ^{54}-specific promoters are in bold [58]. The RNAP binding region from about -34 close to the transcription start site at position -2 (shaded in gray) and has been derived from footprinting studies [69, 92]. Positions +1, –12 and –24 relative to the RNA transcript start site are indicated.

Three different oligonucleotide duplexes of 43 bp length were studied with respect to their binding affinity for RNAP·σ^{54}. The sequences correspond to the *gln*Ap2 promoter from *E. coli* and the *nif*H and *nif*L promoters from *K. pneumoniae*. All duplexes carried the fluorescent dye ROX at the 5'-end. The σ^{54}-dependent promoters are characterized by a consensus sequence. Two highly conserved motifs at position –25/24 and –13/12 allow recognition of the DNA in double-stranded

form [58]. The length of the promoter duplexes is too short to allow binding of a second holoenzyme. The sequences of the promoter DNA duplexes are depicted in Figure 3.1.

3.1.1 Binding of RNAP·σ^{54} to promoter DNA

Gel analysis of ROX-labeled promoter DNA and RNAP·σ^{54}-promoter complexes

The purified DNA duplexes and ROX-labeled single strands were analyzed on a 20% native polyacrylamide gel. Figure 3.2 shows the purified duplexes (three left lanes) in comparison to the ROX-labeled single strands (three right lanes), which displayed a higher electrophoretic mobility. Both the ROX fluorescence signal as well as ethidium bromide staining of the duplexes revealed only one single band demonstrating that the synthesis and the reconstitution of the promoter DNA sequences was successful.

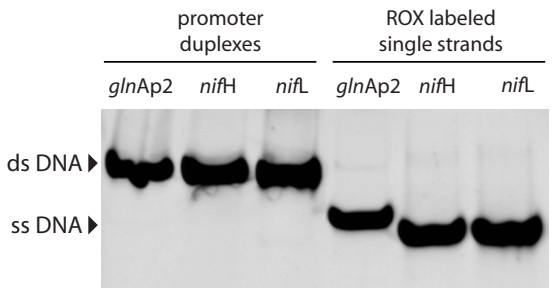

Figure 3.2: Native polyacrylamide gel of promoter DNA duplexes (three left lanes) and ROX-labeled single strands (three right lanes). Equal amounts of 1.5 μg of each sample was loaded.

The binding of RNAP·σ^{54} to these duplexes was qualitatively characterized in an electrophoretic mobility shift assay under conditions of stoichiometric binding. Both the RNAP·σ^{54} holoenzyme and the DNA promoter sequences were active with respect to binding to each other as indicated by the almost fully shifted DNA fraction at an approximate 1:1 ratio of protein and DNA (see Figure 3.3, highest concentrations). The gel shows qualitatively that the promoters *gln*Ap2 and *nif*H have similar binding affinities to RNAP·σ^{54}. The ratios of shifted closed complexes to free DNA are comparable in contrast to *nif*L where more DNA remains free in solution (see Figure 3.3, compare highest protein concentrations). However, the dissociation constant of the binding reaction cannot be precisely determined from the gel.

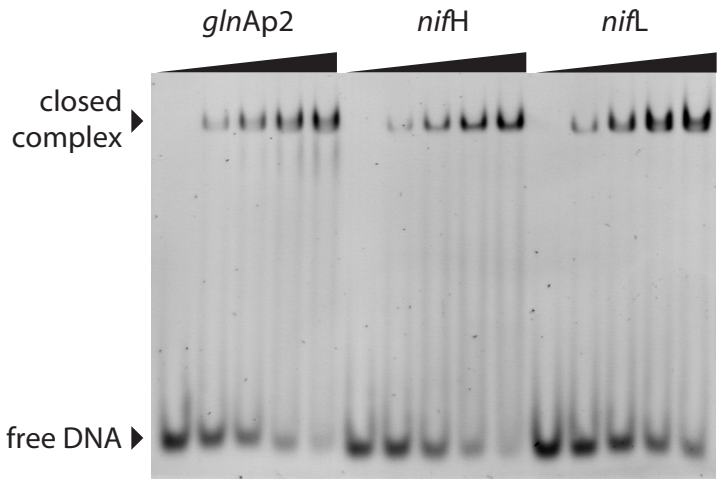

Figure 3.3: Gel shift analysis of RNAP·σ^{54} complexes with the three promoter DNA duplexes. The five lanes for each promoter sequence display an increasing ratio of RNAP·σ^{54} to the DNA duplex (245 nM concentration) from 0:1, 0.25:1, 0.5:1, 0.75:1 and 1:1.

RNAP·σ^{54}-promoter DNA binding studies by anisotropy

In order to measure the dissociation constant K_d of RNAP·σ^{54} with the three different promoters under true equilibrium conditions and at a defined ionic strength and pH the binding of RNAP·σ^{54} was followed by fluorescence anisotropy measurements. The assay used here is based on the rationale that the free DNA has relatively low fluorescence anisotropy due to a high rotational diffusion coefficient. Accordingly, the anisotropy of a fluorescent complex increases with its volume and reflects its rotational mobility. Upon binding of RNAP·σ^{54} anisotropy increases according to the Perrin equation (2.8) due to the reduced rotational diffusion time after formation of the protein-DNA complex. The same approach has been used successfully in a number of other studies (see for example [111–117]). The RNA polymerase was titrated into a solution of ROX-labeled DNA duplex at a given salt concentration. Protein was added until all binding sites were saturated and anisotropy reached a plateau value, which reflects the anisotropy of the 1:1 complex of RNAP·σ^{54} with the DNA. The resulting binding curve was fitted to equation (2.25) and K_d as well as the anisotropies of the free promoter DNA (r_P) and the protein-DNA complex (r_{RP}) were obtained. As expected, similar average values of both r_P (0.165-0.169) and r_{RP} (0.244-0.266) were obtained for the three promoters indicating similar rotational diffusion times for the free promoter DNA duplexes and its complex with the polymerase (Table. 3.1). The analysis of the binding curve according to equation

Binding parameters determined by fluorescence anisotropy

	*gln*Ap2	*nif*H	*nif*L
Anisotropy of free DNA (r_P)[a]	0.165 ± 0.02	0.169 ± 0.01	0.166 ± 0.01
Anisotropy of complex (r_{RP})[a]	0.244 ± 0.03	0.260 ± 0.01	0.266 ± 0.02
Quenching factor q[b]	1.13 ± 0.1	1.08 ± 0.1	1.0 ± 0.1

Table 3.1: Fluorescence anisotropy parameters for the binding of RNAP·σ^{54} to the *gln*Ap2, *nif*H and *nif*L promoters.
[a]The anisotropies of free (r_P) and complexed DNA (r_{RP}) were derived from fitting the binding curves to equation (2.24)
[b]The quenching factor q was determined for every titration under polarization-independent conditions and averaged

(2.25) is only valid if the quantum yield of the ROX dye does not change upon binding of the RNA polymerase [118].To test whether this was the case the fluorescence intensities of each sample before and after titration were measured. After correction for dilution these intensity ratios corresponded to quenching factors q of 1.13 ± 0.1 (*gln*Ap2), 1.08 ± 0.1 (*nif*H) and 1.02 ± 0.1 (*nif*L). Thus, within the acuracy of the measurements, the binding of RNAP·σ^{54} to the promoter DNA did not change the ROX quantum yield so that the analysis of the data according to equation (2.25) is valid. The resulting quenching factors (q) for the three different promoters as well as the anisotropies for free (r_P) and complexed DNA (r_{RP}) derived from the fit are summarized in Table 3.1.

Determination of RNAP·σ^{54} binding activity by stoichiometric titrations

The binding of the RNAP·σ^{54} stock solution purchased from the manufactorer was studied with the ROX-labeled DNA duplex carrying the *gln*Ap2 promoter. The 10 nM DNA solution in a low salt buffer (50 mM potassium acetate) was titrated with a solution of RNAP·σ^{54} in the same buffer. The initial linear increasing fluorescence anisotropy of the titration reflects the binding of added RNAP·σ^{54} to the DNA until the binding sites were saturated, i.e. the anisotropy reached a plateau value. The intersection point of the plateau with the initial linear part of the curve indicates the equivalence point where each molecule of promoter-DNA is bound by one molecule of RNAP·σ^{54} assuming a 1:1 stoichiometry of the complex. In these experiments, the DNA binding activity of RNAP·σ^{54} was calculated to be between 80 and 90 % for the same preparation with respect to the nominal core RNA polymerase concentration given by the manufacturer. These values were reproducible for different preparations of RNAP·σ^{54}. Figure 3.4 displays a representative stoichiometric binding curve.

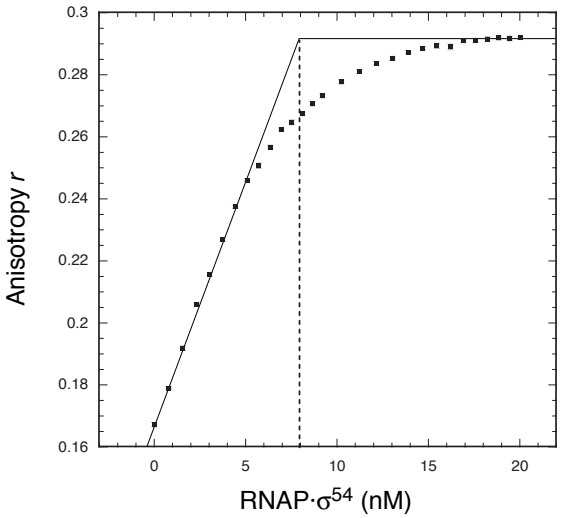

Figure 3.4: RNAP·σ^{54} binding activity was determined by stoichiometric titration of RNAP·σ^{54} on 10 nM of *gln*Ap2 promoter in low salt binding buffer (50 mM potassium acetate). Anisotropy values r are plotted versus the actual concentration of RNAP·σ^{54} at a given point of titration. The concentration of RNAP·σ^{54} at the equivalence point is indicated by the dotted line.

Binding affinity of RNAP·σ^{54} for *gln*Ap2, *nif*H and *nif*L promoters

The three different promoter DNA duplexes were examined with respect to their binding affinity for the RNAP·σ^{54} holoenzyme. Figure 3.5 shows characteristic binding curves for the three promoters at 150, 250 and 350 mM potassium acetate (*gln*Ap2 and *nif*H) and 50, 150 and 250 mM potassium acetate (*nif*L). The data were fitted to equation (2.25) to obtain values for the dissociation constant (K_d) and for the anisotropy for free (r_P) and complexed (r_{RP}) DNA. After converting the measured r values according to equation (2.24) into the fractional saturation of the DNA θ, the binding curves can be directly compared (Figure 3.6 I and II). Figure 3.6 displays representative binding curves recorded by titrating *gln*Ap2, *nif*H and *nif*L promoters at an approximately physiological ionic strength (200 mM potassium acetate and 5 mM magensium acetate, $I = 0.229$ M). A good agreement of the measured data according to the 1:1 binding model described by equations (2.24) and (2.25) was obtained yielding K_d values of 0.7 ± 0.1 (*gln*Ap2), 1.2 ±0.1 (*nif*H) and 10.1 ±1.1 nM (*nif*L) for the titrations shown in Figure 3.6. While the *gln*Ap2 and *nif*H promoters displayed a similar affinity at an ionic strength of $I = 0.229$ M, binding to the *nif*L sequence was about an order of magnitude weaker. Average values from multiple measurements are summarized in Table 3.1 with K_d values of 0.94 ±0.55 (*gln*Ap2), 0.85 ±0.30 (*nif*H) and 8.5 ± 1.9 nM at approximately physiological ionic strength

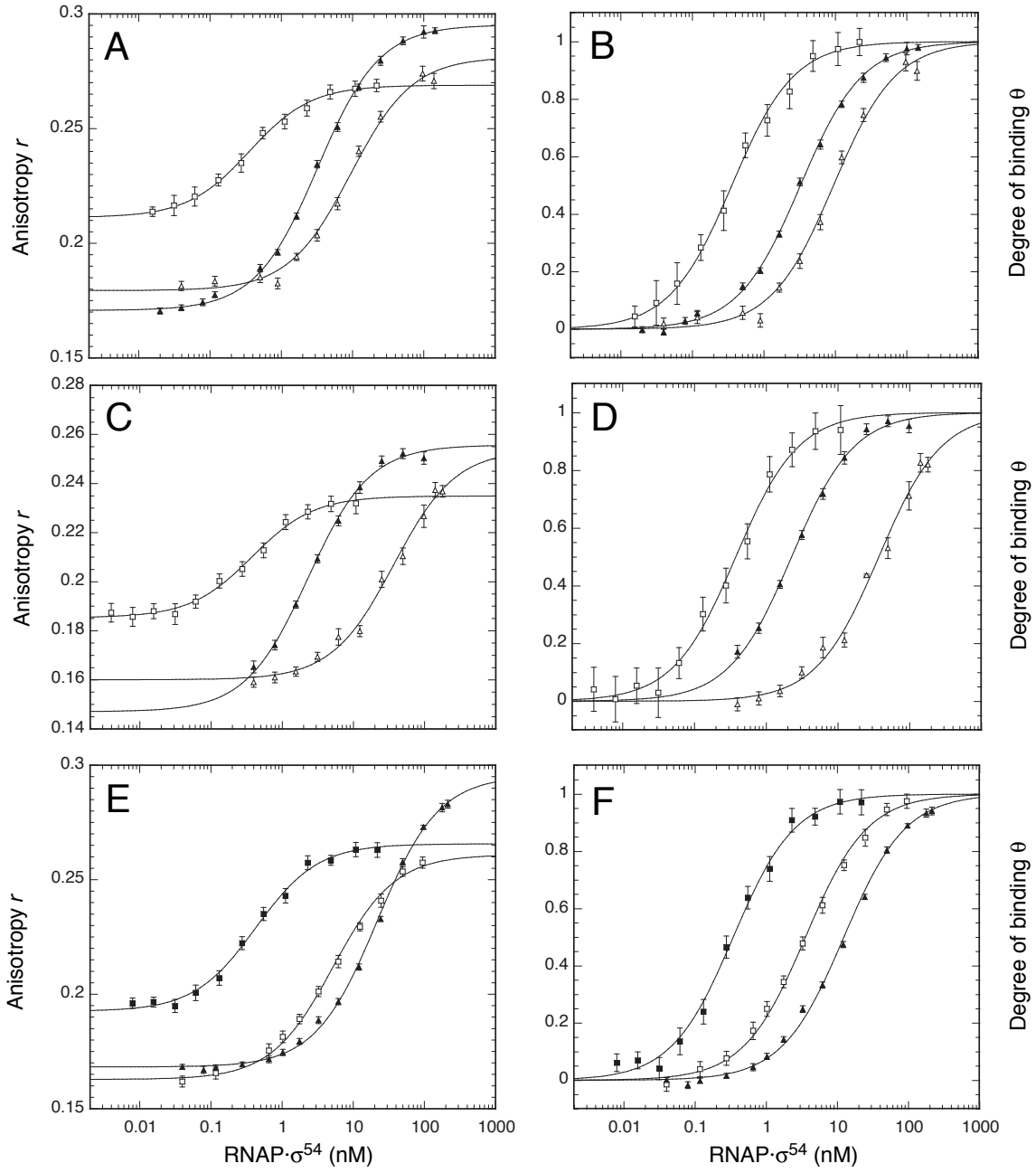

Figure 3.5: Representative binding curves of RNAP·σ^{54} to different promoter sequences at different ionic strength. Fluorescence anisotropy data of *gln*Ap2 (A+B), *nif*H (C+D) and *nif*L (E+F) are shown for 50 mM (filled squares), 150 mM (open squares), 250 mM (filled triangles) and 350 mM (open triangles) potassium acetate buffer. A, C, E. The resulting binding curves of anisotropy r versus the concentration of RNAP·σ^{54} were fitted according to equation (2.25) to determine K_d. B, D, F. In order to account for differences in the values of free (r_P) and complexed (r_{RP}) DNA, the measured anisotropy values can be converted into the fractional saturation of the DNA, Θ, according to equation (2.24) for a direct comparison of the titrations.

($I = 0.229$ M). In addition, it was tested, whether the ROX-fluorophore affected the differences in binding affinities observed in the experiments described above. The binding affinities of ROX-labeled DNA duplexes to RNAP·σ^{54} were tested at the same ionic strength by competition with unlabeled DNA duplexes. A 10 nM solution of preformed RNAP·σ^{54} complex with a given ROX-labeled promoter DNA was titrated with unlabeled *gln*Ap2, *nif*H or *nif*L duplex. The concentration of the unlabeled DNA which was required to displace 50 % of the ROX-DNA from the complex with RNAP·σ^{54} was determined. For titrating *gln*Ap2-ROX with *nif*H and *nif*H-ROX with *gln*Ap2 this concentration of the duplexes were the same within ∼10 %. Thus, the unlabeled *gln*Ap2 and *nif*H promoter fragments displayed essentially the same binding affinities at physiological ionic strength. In contrast, the *nif*L promoter (*nif*L-ROX versus *gln*Ap2, *nif*L-ROX versus *nif*H and *gln*Ap2-ROX versus *nif*L) displayed a significantly weaker association with RNAP·σ^{54}.

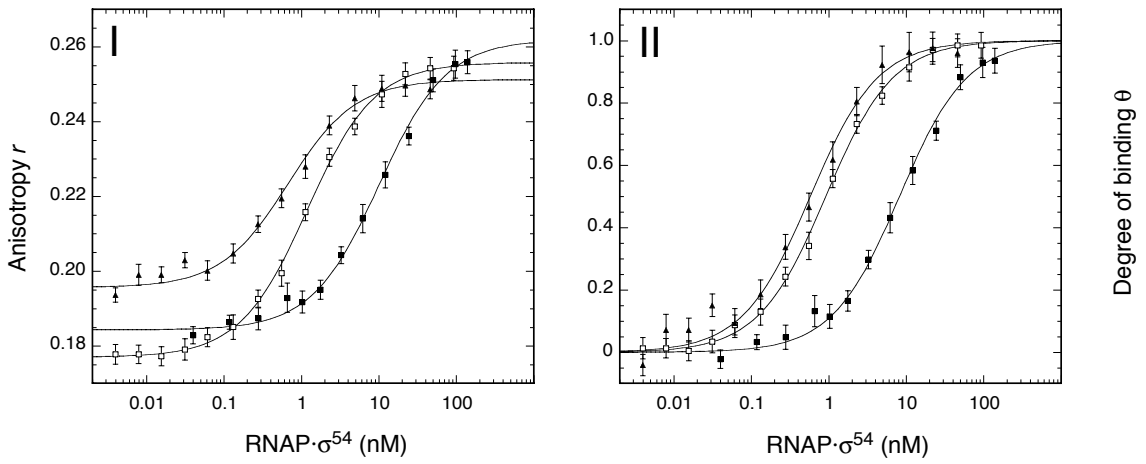

Figure 3.6: A comparison of the binding affinity to three different promoter duplexes at approximately physiological ionic strength is shown. The ROX-labeled DNA at a concentration of 50 pM for *gln*Ap2 (filled triangles) and *nif*H (open squares) and of 100 pM for *nif*L (filled squares) was preincubated in a buffer supplemented with 200 mM potassium acetate and 5 mM magnesium acetate ($I = 0.229$ M). This solution was titrated with the indicated concentrations of RNAP·σ^{54}. **I**. The resulting binding curves of anisotropy r versus the RNAP·σ^{54} concentration were analyzed according to equation (2.25) to determine K_d. Values of 0.7 ± 0.1 (*gln*Ap2), 1.2 ± 0.1 (*nif*H) and 10.1 ± 1.1 nM (*nif*L) were obtained for the experiments shown in this Figure. **II**. To account for differences in the values of free (r_P) and complexed (r_{RP}) DNA between the three promoters the measured anisotropy values can be converted into the fractional saturation of the DNA, Θ, according to equation (2.24) for a direct comparison of the titrations.

Salt dependence of the binding affinity of RNAP·σ^{54} to promoter DNA

When the experiments were performed at different salt concentrations in the range of $I = 0.079-0.379$ M K^+ equivalents the value of K_d increased at higher ionic strength. This is due to a weakening of electrostatic interactions between protein and DNA as reviewed in Record *et al* [119]. Thus, experiments over a large range of ionic strength provide information about the number of salt bridges that form upon binding of RNAP·σ^{54} to the promoter sequence. Examples of this type of experiment are given in Figure 3.5 which shows binding curves of the three different promoters *gln*Ap2, *nif*H and *nif*L, respectively. The measurements of this data set were conducted in a buffer supplemented with potassium acetate at a concentration of 50, 150 and 250 mM (*nif*L) and 150, 250 and 350 mM (*gln*Ap2 and *nif*H). The dissociation constants K_d determined for the displayed binding curves are 0.36 nM, 3.3 nM and 9.5 nM for *gln*Ap2 (at 150, 250 and 350 mM potassium acetate, respectively), 0.38 nM, 2.3 nM and 37 nM for *nif*H (at 150, 250 and 350 mM potassium acetate, respectively) and 0.43 nM, 5.2 nM and 22 nM for *nif*L (at 50, 150 and 250 mM potassium acetate, respectively). A plot of the logarithm of the averaged K_d values determined at a given salt concentration versus the logarithm of the ionic strength displayed an apparently linear relation (Figure 3.7). The slopes of this plots $-\triangle(K_d)/\triangle log(I)$ were 6.1± 0.5 (*gln*Ap2), 5.2 ±1.2 (*nif*H) and 2.1 ±0.1 (*nif*L). This means that the dissociation constant became weaker by a factor of $10^{6.1}$ (*gln*Ap2), $10^{5.2}$ (*nif*H) and $10^{2.1}$ (*nif*L) per decade of higher ionic strength. Again, the *gln*Ap2 and *nif*H promoters were indistinghuishable within the accuracy of the measurements, whereas the *nif*L promoter showed a much weaker salt dependence.

3.1.2 Binding of NtrC to the enhancer

Stoichiometric binding of the activator NtrC to a single strong enhancer site

Unphosphorylated NtrC is a dimer in solution which is able to bind an enhancer sequence. Stoichiometric binding of unphosphorylated NtrC to a single strong NtrC binding site (DNA duplex ES-1) served to determinate the binding activity of the NtrC preparation. The synthetic oligonucleotide ES-1 contains an Lp site, which in the *in vivo* sequence overlaps the promoter for *ntrB* (*gln*L) [64]. A preincubated solution of 10 nM of ROX-labeled DNA duplex was titrated with prediluted NtrC (300 nM of monomer) in low salt binding buffer (50 mM potassium acetate) as previously described. Figure 3.8 shows a stoichiometric binding curve. In contrast to

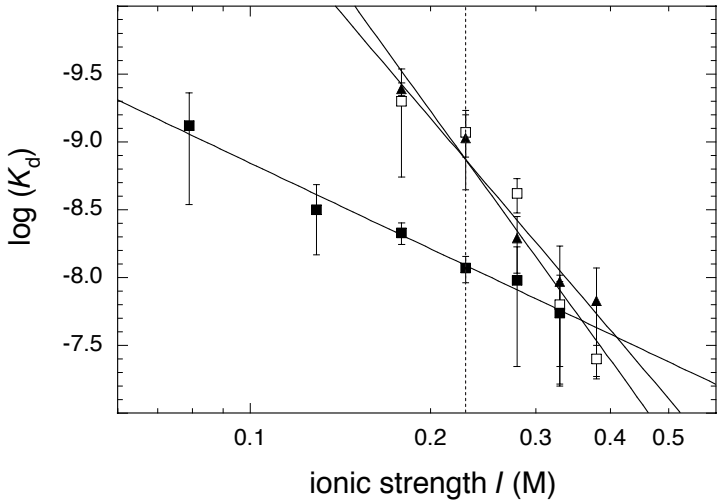

Figure 3.7: Effect of ionic strength on binding affinity. All K_d values for the *gln*Ap2 (filled triangles), *nif*H (open squares) and *nif*L (filled squares) promoters are displayed in a double-logarithmic plot against the ionic strength I (see Table 3.2). The lines correspond to linear regressions according to $\log(K_d) = -5.6 + 5.2 \log I$ (*gln*Ap2), $\log(K_d) = -5.0 + 6.1 \log I$ (*nif*H) and $\log(K_d) = -6.8 + 2.1 \log I$ (*nif*L). The vertical dashed line indicates an approximately physiological ionic strength.

Dissociation constants of RNAP·σ^{54} to different promoters determined by fluorescence anisotropy measurements

Salt conc. K-acetate [mM]	Ionic Strength (I) [M]	*gln*Ap2	*nif*H	*nif*L
50	0.079			0.76 ± 0.56 (5)
100	0.129			3.2 ± 1.7 (4)
150	0.179	0.40 ± 0.04 (4)	0.50 ± 0.36 (3)	4.6 ± 0.9 (2)
200	0.229	0.94 ± 0.55 (6)	0.85 ± 0.30 (3)	8.5 ± 1.9 (3)
250	0.279	5.1 ± 2.3 (13)	2.4 ± 0.7 (4)	10 ± 8 (7)
300	0.329	11 ± 9 (6)	16 ± 10 (3)	18 ± 13 (3)
350	0.379	15 ± 11 (8)	40 ± 11 (3)	

Table 3.2: Dissociation constants K_d for the binding of RNAP·σ^{54} to the *gln*Ap2, *nif*H and *nif*L promoters as determined by fluorecence anisotropy measurements. Average values for K_d and corresponding standard deviations are given in nanomolar concentrations and were determined in binding buffer (20 mM Hepes/KOH pH 8.0, 5 mM magnesium acetate, 1 mM DTT, 0.1 mg/ml BSA, 0.01% NP-40), supplemented with the indicated potassium acetate concentrationss, yielding the ionic strength I. The number in parantheses after the value of the dissociation constant refers to the number of experiments averaged.

binding of RNAP·σ^{54} to promoter DNA (Figure 3.4), binding of NtrC to a single enhancer site showed no plateau in its binding curve. Two linear sections can be distinguished. The first resulted from the strong binding of one NtrC dimer, the second was assigned to additional binding of NtrC dimers to the DNA-protein complex. The intersection of the extrapolated regression lines led to the equivalence point, i.e. the point where the enhancer was saturated by the protein. From the equivalence point and the known DNA concentration, the concentration of active NtrC dimer in the protein stock solution was determined. DNA binding activity of NtrC to the specific enhancer site was calculated to be between 70 and 80 % with respect to the nominal concentration of the NtrC preparation.

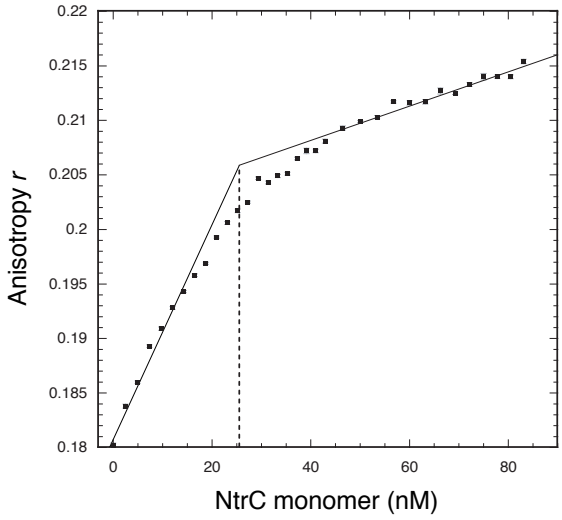

Figure 3.8: Determination of enhancer binding activity of unphosphorylated NtrC determined by stoichiometric titration in low salt binding buffer (50 mM potassium acetate). 10 nM DNA duplex containing a single strong NtrC binding site (ES-1) was titrated with a prediluted solution of NtrC. Measured anisotropy values are plotted versus the actual concentration of added NtrC at a given point of titration. The concentration of NtrC at the equivalence point is indicated by the dotted line.

Oligomerization of the activator protein NtrC to two strong enhancer sites

Previous studies have shown that bacterial enhancer-binding protein NtrC activates transcription only when phosphorylated at aspartate 54 (D54) that is found within a sequence conserved in all members of the family of regulatory proteins [120, 121]. Phosphorylation results in conformational change of the protein allowing NtrC to hydrolyze ATP and activate transcription. Activity of the NtrC stock solution was

quantified from stoichiometric titration described before. *In vivo*, NtrC binds to two adjacent enhancer sites separated by 3 bp as shown in Figure 2.2. In order to determine enhancer-binding activity of NtrC a DNA sequence of 59 bp containing two strong NtrC binding sites was used. These NtrC sites corresponded to the high affinity binding site Lp overlapping the promoter for *ntrB* (*gln*L) (Figure 1.4) [64]. The activator protein NtrC binds to two adjacent enhancer sites in a cooperative way. Unphosphorylated NtrC is supposed to bind as a tetramer (2 dimers) whereas upon phosphorylation of the activator by the chemical phosphodonor carbamylphosphate, NtrC oligomerizes to an octameric complex [122]. Figure 3.9 shows the binding curves of NtrC and its phosphorylated form.

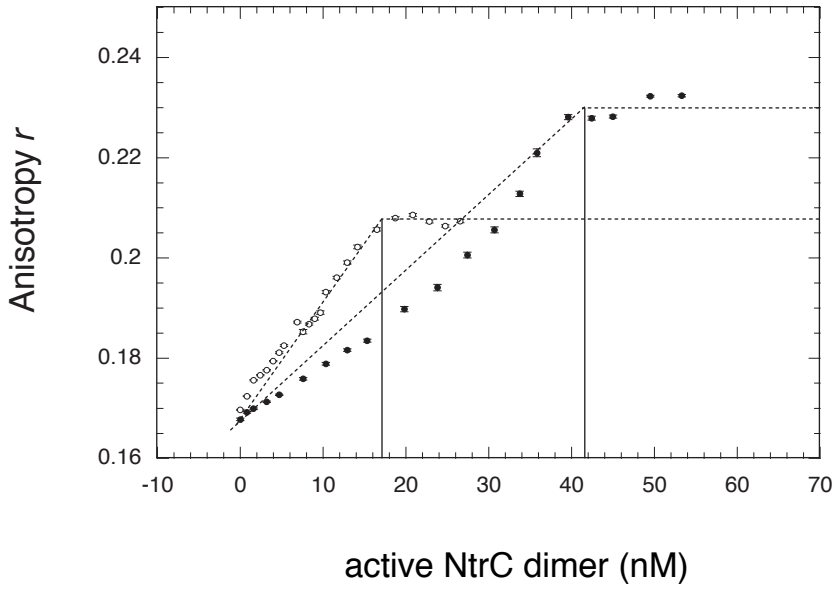

Figure 3.9: Oligomerization of NtrC upon phosphorylation.
NtrC was titrated in absence (open circles) and presence (filled circles) of 25 mM carbamylphosphate in low salt binding buffer (50 mM potassium acetate). 10 nM DNA duplex with two strong NtrC binding sites (ES-2) was titrated with NtrC. The concentration of NtrC was corrected for the active fraction of the preparation as determined from the stoichiometric titrations. The vertical lines indicate the equivalence point of the titrations.

In order to determine the stoichiometry of the formed protein-DNA complexes the equivalent points were determined. The initial increasing fluorescence anisotropy of the titration reflects a continous binding of added NtrC to the DNA until binding sites were saturated, i. e. until anisotropy reached a plateau value. The intersection point of these two lines indicates the equivalence point where the molecules are fully saturated. With known concentrations of DNA and protein at the equivalent point,

the stoichiometry of the complex can be derived if any concurrent reaction can be excluded, e.g. aggregation of the protein or formation of another species of protein-DNA complex. Two different changes are apparent upon phosphorylation of NtrC: First, unphosphorylated NtrC reaches a lower plateau level than the phosphorylated protein. Second, this plateau level is achieved at a lower amount of added NtrC. These two effects both indicate an oligomerization of NtrC upon binding to strong enhancer sites that. Unphosphorylated NtrC binds to two adjacent bindings sites apparently as a tetramer. Determination of the concentrations of DNA and NtrC at the equivalent point gives a 4:1 stoichiometry for unphosphorylated NtrC. The effects of cooperativity and oligomerization is supported by anisotropy measurements under phosphorylating and non-phosphorylating conditions.

3.1.3 Binding of σ^{54} to promoter DNA

Isolated σ^{54} binds to the *nif*H promoter in a 1:1 complex

It has been shown for the *Rhizobium meliloti nif*H promoter that it binds isolated σ^{54} subunit under certain conditions [71]. Heteroduplex molecules were used, in which the DNA is stably opened one and two bases downstream of the consensus GC of the conserved –12/11 region, for σ^{54} binding in the absence of core RNA polymerase subunits [68]. It has been shown that σ^{54} binds tightly to this locally opened promoter DNA and is even able to isomerize independently of core RNA polymerase. This isomerization is associated with an increased DNase I footprint of σ^{54} on DNA [71], extending towards the transcription start site comparable to the protection pattern by RNA·σ^{54} holoenzyme [69, 92].

Four different synthetic oligonucleotides were used to examine binding of σ^{54}: Promoter *nif*H from *R. meliloti* and *gln*Ap2 from *K. pneumoniae* both in a native, homoduplex form and an altered heteroduplex form (Figure 3.10). The binding of σ^{54} to the promoter-DNA duplexes was characterized in an electrophoretic mobility shift assay. σ^{54} was titrated into a 100 nM DNA solution in low salt binding buffer (50 mM potassium acetate). Figure 3.11 displays the formation of a σ^{54}-promoter-DNA-complex with increasing amounts of σ^{54}. Analysis of the gels (Figure 3.11) reveals that σ^{54} binds to *nif*H with its native sequence as well as in a heteroduplex form where 2 base pairs in the conserved –12/11 region are mutated (Figure 3.10). σ^{54} was also able to bind to the *gln*Ap2 homo- or heteroduplex but only at higher concentration of the protein. Thus, the association of σ^{54} without the core enzyme is about one order of magnitude higher to the *nif*H than to the *gln*Ap2 promoter.

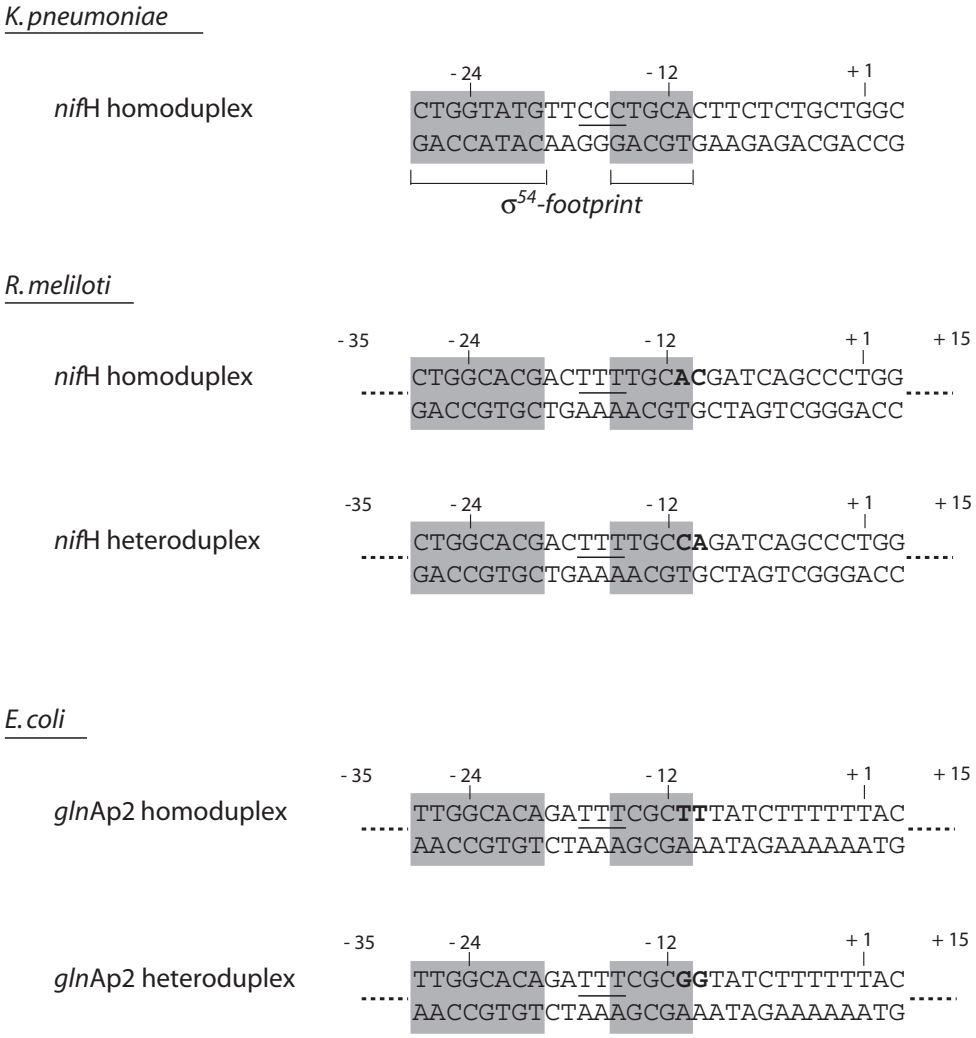

Figure 3.10: Sequences of homo- and heteroduplexes used for σ^{54}-binding
*R. meliloti nif*H homo- and heteroduplexes and *E. coli gln*Ap2 homo- and heteroduplexes were studied in their ability to bind to σ^{54}. The σ^{54}-binding region that fit the –24/–12 consensus sequence is shaded in grey. The original (homoduplexes) and modified base pairs are in bold. Heteroduplexes were formed to mimic the DNA in the Closed Complex in which the DNA is stably opened two bases next to the consensus GC (–13/12). The underlined CCC or TTT (–15 to –17) are supposed to be involved in binding of σ^{54}.

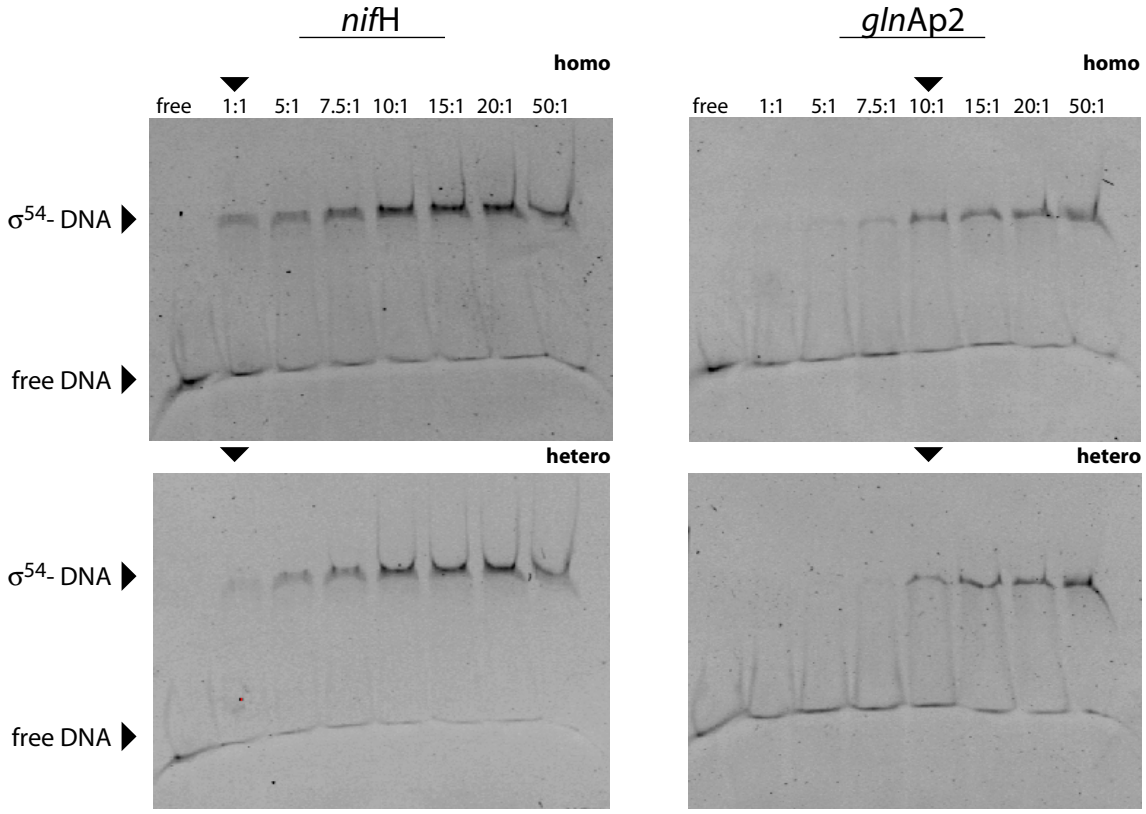

Figure 3.11: Gel shift analysis of σ^{54} bound to promoter DNA
The eight lanes for each promoter sequence display an increasing ratio of σ^{54} to the DNA duplex (100 nM) from 0:1, 1:1 (100 nM), 5:1 (500 nM), 7.5:1 (750 nM), 10:1 (1 μM), 15:1 (1.5 μM), 20:1 (2 μM) and 50:1 (5 μM) in low salt binding buffer (50 mM potassium acetate). The concentration in brackets refer to the concentration of added σ^{54}. The samples were analyzed on a native 6 % polyacrylamide gel.

Assuming a 1:1 binding model, the dissociation constants can be estimated from the gel. The association of σ^{54}-DNA complex is rather weak, i.e. the concentration of promoter DNA is $\leq K_d/10$ and the reduction of the total amount of free σ^{54} due to closed complex formation can be neglected. Under these conditions the concentration of free σ^{54} can be approximated by its total concentration. In this case, K_d is equivalent to the added protein concentration when 50 % of the DNA is bound by this protein. The dissociation constants were estimated to be $\sim$ 1 x 10^{-7}M for *nif*H homo- and heteroduplex and $\sim$ 1 x 10^{-6} M for *gln*Ap2 homo- and heteroduplex. Apparently, σ^{54} binds to both promoter sequences, but binds one order of magnitude stronger to the *nif*H than to the *gln*Ap2 promoter. In order to determine the association state of free sigma factor σ^{54} and σ^{54}-promoter DNA complexes sedimentation

equilibrium ultracentrifugation was used. In sedimentation equilibrium experiments, an initially uniform solution is centrifuged at a lower velocity than is required for total sedimentation. After an appropriate period of time an equilibrium is established between the process of diffusion and the opposed process of sedimentation of the molecule. This equilibrium depends on the molecular weight and the angular velocity. This yields to a concentration gradient of molecules increasing exponentially towards the cell bottom (Figure 3.12).

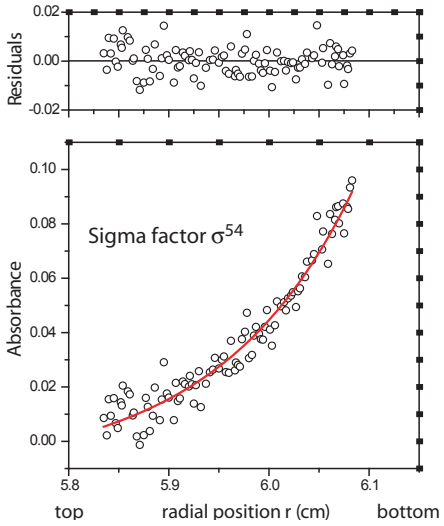

Figure 3.12: Equilibrium sedimentation data of sigma factor σ^{54}
Centrifugation was carried out at 13,000 rpm and 20°C. σ^{54} was used at a concentration of ~ 3 μM. In the bottom part of the Figure the measured absorbance at 260 nm versus the radial position (distance to the center of the rotor) is shown. The continuous line represents the result from a single exponential fit of the data points. The top part of the Figure gives the residuals to the fit expressed as the difference between experimental and fitted values. The molecular weight of sigma factor σ^{54} for this data set was determined to be 59.6 kDa. An averaged value determined for different angular velocities is displayed in Table 3.3.

The distribution of the molecules determined by absorption at 260 nm, can be theoretically described by an exponential curve (equations 2.5 and 2.6). In order to determine the molecular weight of the σ^{54}-promoter DNA complexes, σ^{54} and promoter DNA duplexes were mixed in low salt binding buffer (50 mM potassium acetate) containing 610 nM DNA and 3.05 μM σ^{54}. The results of the analytical ultracentrifugation supports the findings of the DNA binding assays of σ^{54}. Table 3.3 summarizes the molecular weights of free σ^{54} protein and promoter-duplexes and of σ^{54}-promoter complexes. It can be shown that σ^{54} binds to the promoter DNA in a 1:1 binding model. Best results were obtained with a single exponential fit for

Molecular weight (MW) of σ^{54} and σ^{54}-DNA complexes

	MW measured [kDa]	MW calculated [kDa]	Association state
Single molecules			
sigma factor σ^{54}	58,9 ± 1,9	56,8[a]	monomer
*nif*H homoduplex[c]	31,4 ± 0,1	31,5[a]	monomer
*nif*H heteroduplex[c]	31,7 ± 0,1	31,5[a]	monomer
*gln*Ap2 homoduplex[d]	31,5 ± 0,09	31,5[a]	monomer
*gln*Ap2 heteroduplex[d]	33,6 ± 0,1	31,5[a]	monomer
Protein-DNA complexes			
σ^{54}-*nif*H homoduplex[c]	89,3 ± 4,7	88,3[b]	1:1 complex
σ^{54}-*nif*H heteroduplex[c]	89,4 ± 2,8	88,3[b]	1:1 complex
σ^{54}-*gln*Ap2 homoduplex[d]	33,5 ± 0,2	88,3[b]	no binding
σ^{54}-*gln*Ap2 heteroduplex[d]	30,4 ± 0,2	88,3[b]	no binding

Table 3.3: Promoter Binding of isolated σ^{54} subunit to homo- or heteroduplexes of two different promoter DNA sequences. Heteroduplexes differ from homoduplexes in two bases near the consensus GC (–13/12) at position –11/10 respective the transcription start site. The determined molecular weights are averaged values calculated from different angular velocities.
[a] Molecular weights of His-tagged σ^{54} and DNA duplexes were calculated from the amino acid or the nucleic acid composition, respectively.
[b] Molecular weight of the σ^{54}-DNA complex was calculated with the calculated molecular weight of Sigma in a 1: 1 binding model
[c] Molecular weights for free promoters *nif*H-homo and *nif*H-hetero were determined by a single exponential fit (model ideal 1, see Eq. 2.5) and for 1:1 complexes by a two exponential fit (model ideal 2, see Equation 2.6)
[d] Molecular weights for free promoters *gln*Ap2-homo and *gln*Ap2-hetero were determined by a single exponential fit (model ideal 1). Best fits for the protein-DNA mixture were equally achieved with a single exponential fit

binding of σ^{54} to the *gln*Ap2 promoter indicating that σ^{54} binds not or very weakly to this promoter sequence. The molecular weights of σ^{54}-*nif*H complexes were determined with a two exponential fit. Obviously, σ^{54} binds the *nif*H as homo- and heteroduplex but is not able to bind *gln*Ap2, wether as homo- nor as heteroduplex. Figures 3.12 and 3.13 displays typical data sets and the results of of the analysis are summarized in Table 3.3. Experimental data for free and σ^{54}-bound *nif*H and *gln*Ap2 heteroduplex are comparable to the data for the analogous homoduplexes and are not shown.

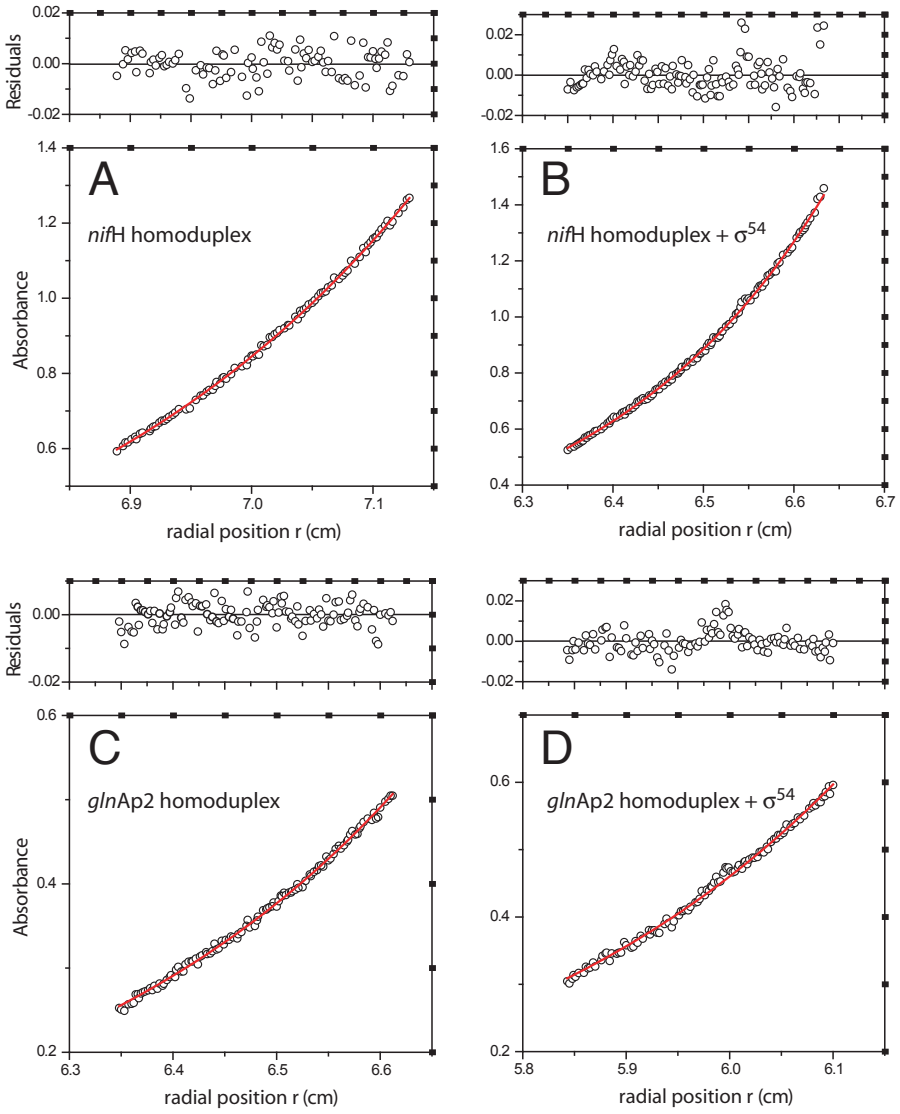

Figure 3.13: Equilibrium sedimentation data for free promoter DNA and σ^{54}-DNA complexes. Centrifugation was carried out at 8,000 rpm and 20°C. In the bottom part of the Figure the measured absorbance at 260 nm *versus* the radial position (distance to the center of the rotor) is shown. The continuous line represents the result from a single or a two exponential fit of the data points. The top part of the Figure gives the residuals to the fit expressed as the difference between experimental and fitted values. A+B. *nif*H homoduplex alone and complexed with σ^{54}, respectively. C+D. *gln*Ap2 homoduplex alone and in a mixture with σ^{54}. For the data represented in A and C, the molecular weights determined from a single exponential fit were 32.7 kDa and 31.6 kDa. For average values determined at different velocities see Table 3.3. B. Data of promoter *nif*H homoduplex complexed with σ^{54} yields best results when fitted with a two exponential fit. In this fit, the molecular weight M of the free DNA component was fixed at the calculated molecular weight ($\sim$ 31 kDa, Table 3.3) and only the M f the DNA-protein complexes was allowed to vary. The molecular weight for the complex determined from the fit of this data set was 88 kDa which corresponds to a 1:1 complex. D. Data of promoter *gln*Ap2 homoduplex mixed with σ^{54} gives best results when fitted with a single exponential fit. The resulting molecular weight was determined to be 33.5 kDa.

3.2 ATPase activity of NtrC

The ATPase activity of NtrC was investigated in response to different cofactors by examining the amount of hydrolysis of the $\beta - \gamma$-bond of ATP. To test the effect of isolated but promoter-bound σ^{54}, the subunit was incubated with *nif*H promotor in which the single DNA strands form a heteroduplex at position –11/10 (Figure 3.10). As shown in the previous section, isolated σ^{54} is able to bind to promoter DNA under the conditions used here. The results of the ATPase assay are shown in Figure 3.14.

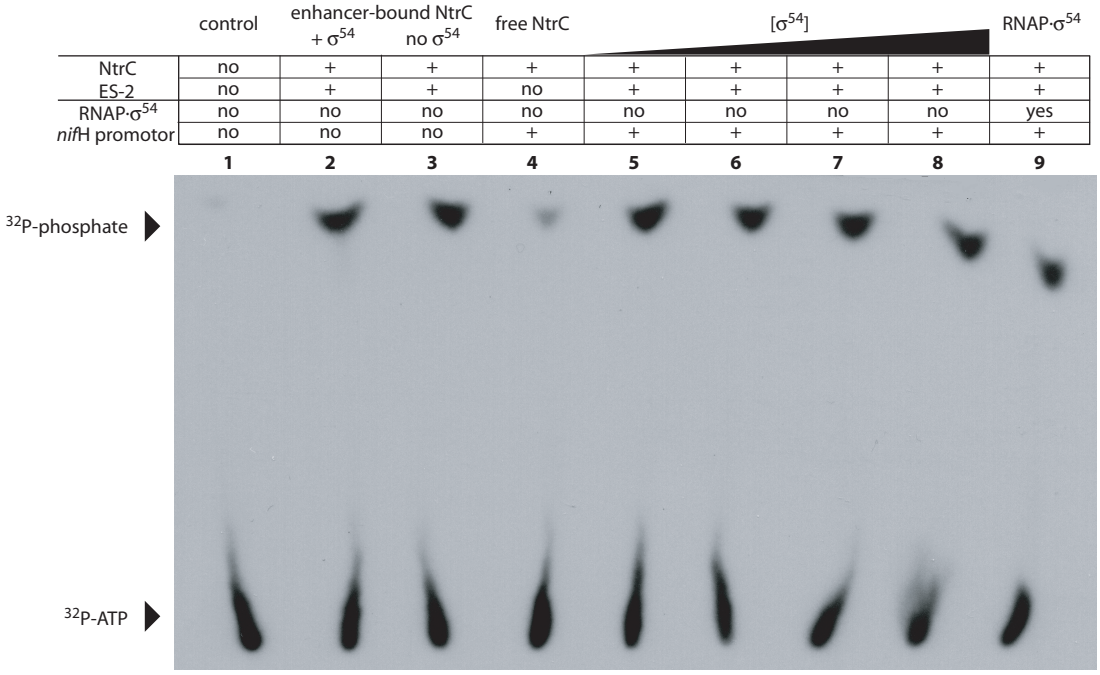

Figure 3.14: ATPase assay of NtrC
ATP (lower spots) and free ortho-phosphate (upper spots) which results from ATP hydrolysis are separated by thin layer chromatography on a silica gel. The amount of free phosphate correlates with ATPase activity. Carbamylphosphate was present in each reaction at a concentration of 25 mM. The amount of total ATP (400 μM) and radioactive ATP was kept constant except for the quality test of the premix of radioactive ATP (**1**) where just the amount of radioactive ATP-Mix was tested to account for degradtion. **1**: Test of quality of radioactive labeled γ-ATP. **2** and **3**: Enhancer-bound NtrC and its stimulation by free σ^{54}. **4**: Activity of free NtrC. **5-8**: Effect of promotor-bound σ^{54}. Incubation occured with increasing amount of σ^{45} (100, 500, 750 and 1000 nM). **9**: Effect of promoter-bound RNAP·σ^{54} holoenzyme

ATPase activity was significantly stimulated by the enhancer sequence ES-2 containing two strong NtrC binding sites (lane 3 versus 4). Addition of isolated σ^{54} or promotor-bound σ^{54} did not stimulate or reduce NtrC ATPase activity (lane 2 versus lane 7 and lanes 5 to 8, respectively) within the accuracy of the measurement. Increasing concentration of σ^{54} did not effect the activity of NtrC.

3.3 Transcription experiments

In vitro transcription experiments were used to elucidate the relation between the short range enhancer position and the activation rate of NtrC protein. A series of plasmids have been constructed with different numbers of binding sites for NtrC that also differ in the affinity for NtrC and the distance to the *gln*Ap2 promoter. A schematic overview over the different classes of transcription templates is given in Figure 3.15.

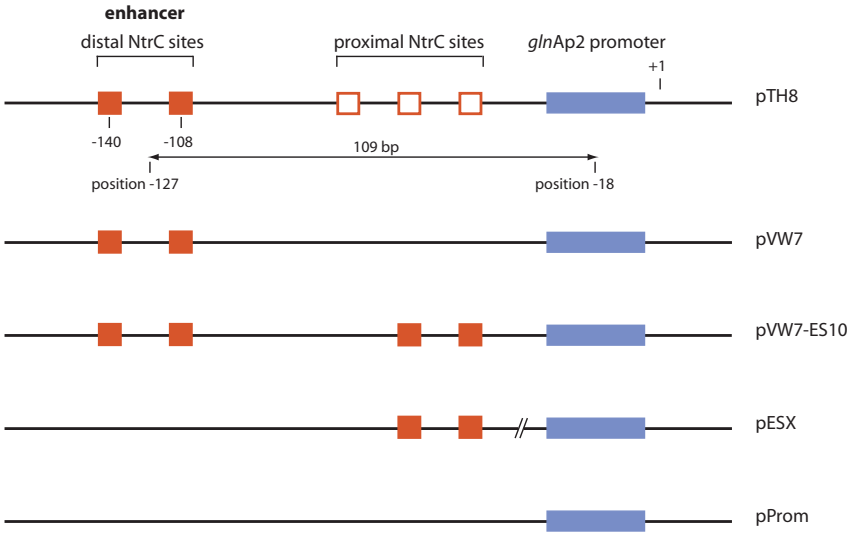

Figure 3.15: Schematic overview of different classes of transcription templates.
The transcription templates contain besides the glnAp2 promoter different numbers of strong enhancer sites (filled rectangles) and weak enhancer sites (open rectangles). Plasmid pTH8 contains the *in vivo* sequence with two strong NtrC sites at a distance of 109 bp with respect to the center of the promoter and three weak NtrC sites near the *gln*Ap2 promoter. pVW7 contains only two distal strong NtrC sites which were shown to be sufficient for transcription activation. pVW7-ES10 contains two distal and two proximal strong binding sites for NtrC. The pESX series of plasmids contain two strong NtrC sites adjacent to the promoter with different distances to the promoter from 2 up to 16 bp. pProm is a reference plasmid which contains no NtrC site.

Plasmid pTH8 contains the *in vivo* sequence of the *gln*Ap2 promoter: Two strong (–148 to –132 and –116 to –100) and three weak (–94 to –81, –73 to –60 and –53 to –37) NtrC binding sites are located upstream of the promoter [53]. The distance between the two strong NtrC binding sites (enhancer) and the center of the promoter is 109 bp. Plasmid pVW7 contains the two strong NtrC binding sites at the same distance as in pTH8 but without the weak binding sites [100]. The templates constructed for the *in vitro* transcription assays were all derived from pVW7 either by inserting two additional strong NtrC binding sites (pVW7-ES10), by deleting all NtrC binding sites (pProm), by removing the enhancer sites near the promoter with a distance of 10 bp (pES10) and by moving these enhancer sites (sites 1 and 2, see Figure 2.2) by one or several base pairs up- or downstream to get enhancer-promoter distances between 2 and 16 base pairs. This series of plasmids was used to investigate the role of the weak enhancer sites near the promoter. Adjacent weak NtrC binding sites such as in plasmid pTH8 were replaced in plasmids pVW7-ES10 or pES10 by strong NtrC sites with the idea that the effect of these sites would be more pronounced. Distances between these enhancer sites adjacent to the *gln*Ap2 promoter were varied by site-directed mutagenesis. The used plasmids which differ in the distance between the proximal enhancer and the promoter are listed in Figure 3.16.

Figure 3.16: The templates of the pESX series are derived from pES10 modified by site-directed mutagenesis. They contain the same *gln*Ap2 promoter of *E.coli* and two strong NtrC binding sites (enhancer) which are located adjacent to the promotor. The different constructs differ in the distance between enhancer and promoter. The numbers on the left refer to the distance between the NtrC2 site and the *gln*Ap2 promoter.

In addition, templates were constructed that differed only in the promoter sequence: pVW7 served again as starting plasmid, in which a *Xho*I restriction site was first

inserted by site-directed mutagenesis, then cut by double restriction (*Pst*I, *Xho*I). The resulting plasmid was then ligated with DNA fragments containing the *nif*H and the *nif*L promoters. The plasmids were amplified by bacterial growth under moderate growth conditions to yield high amounts of monomeric supercoiled DNA plasmids. Figure 3.17 shows the purity of the plasmids and the natural superhelicity of the DNA on a 1 % agarose gel. All plasmids were naturally supercoiled and monomeric with hardly any nicked or multimeric species (Figure 3.17).

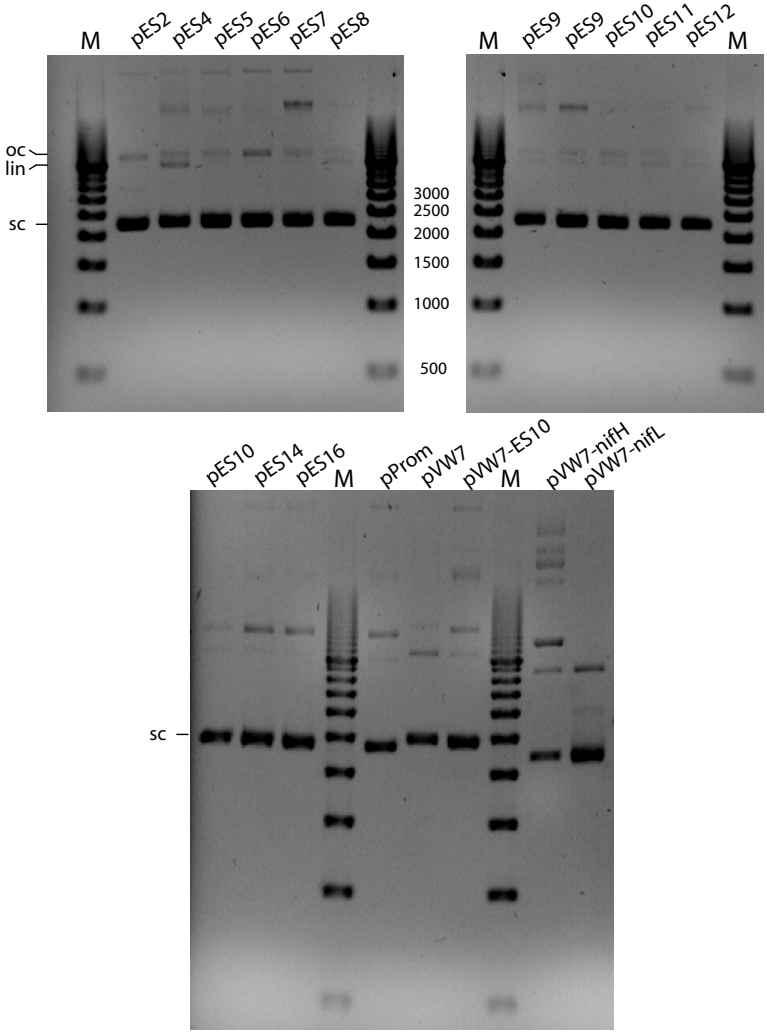

Figure 3.17: Natural superhelicity of transcription templates
oc, open circle DNA, lin, linearized DNA, sc, supercoiled DNA. 100 ng of each DNA preparation was loaded on a 1% agarose gel, M, molecular weight marker EZ load 500 (Bio-Rad). The number refers to The gel shows that all DNA templates used for *in vitro* transcription are naturally supercoiled and monomeric (sc). Supercoiled DNA has a higher electrophoretic mobility than linear DNA. oc, open circle DNA, lin, linearized DNA, sc, supercoiled DNA.

Single-round *in vitro* transcription assays were performed as described in Materials and Methods. The preformed closed complexes of RNAP·σ^{54} on the *gln*Ap2 promoter were incubated with inactive dimeric NtrC prior to activation of NtrC by carbamylphosphate phosphorylation.

3.3.1 Determination of the transcription activity of RNAP·σ^{54}

The optimal concentration of RNAP·σ^{54} to get a maximum of transcription rate was determined as follows: Control plasmid pVW7-158 was incubated with different concentrations of RNAP·σ^{54} holoenzyme between 0 and 80 nM. Figure 3.18 shows the yielded amounts of 158 nt transcript. At a RNAP·σ^{54} concentration of 50 nM, a plateau value of transcription activity is reached. This concentration was used for all transcription experiments.

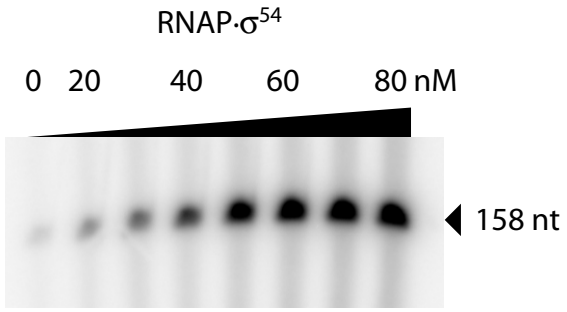

Figure 3.18: Determination of transcription activity of RNAP·σ^{54}. The protein was titrated from 0 to 80 nM into a reaction mixture containing 10 nM plasmid DNA (pVW7-158) and an excess of the activator NtrC.

3.3.2 Data analysis of *in vitro* transcription assays

In vitro transcription assays were performed in a reaction which includes a control plasmid pVW7-158 coding for a shorter transcript of 158 nucleotides. This control serves to correct for small variations in e.g. temperature, added concentrations of protein etc. between different assays.
Figure 3.19 shows the results of an *in vitro* transcription experiment from DNA template pVW7. In this example a template coding for a transcript of 481 nt length (pVW7, Figure 3.15) was tested under increasing concentration of activator protein NtrC from 0 to 200 nM NtrC dimer. The amount of transcript was quantified by

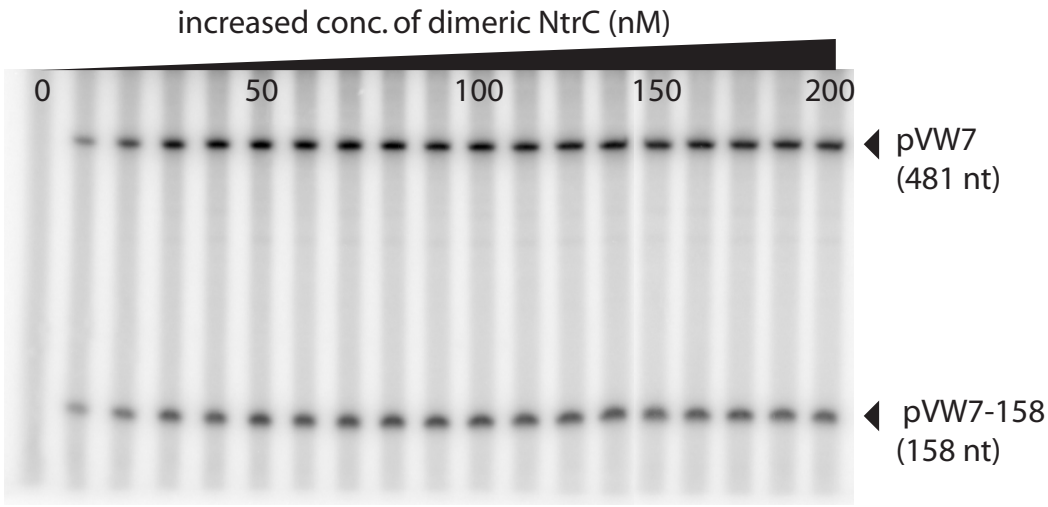

Figure 3.19: Example for *in vitro* transcription experiments. Images of a 6 % denaturing polyacrylamide gel of a reaction containing DNA template pVW7 and pVW7-158 as the control template shows two different length of transcript. The transcript of pVW7 has 481 nt in size whereas control plasmid pVW7-158 encodes for a shorter transcript of 158 nt. The reactions were incubated with increasing amounts of activator protein from 0 to 200 nM NtrC dimer.

measuring intensities for each band. The background intensity was determined at 0 nM NtrC for both transcripts and substracted from the absolute intensity of each lane. After correction for the background, the ratio of the intensities of the given template to the control transcript was determined.

3.3.3 Dependence of transcription activity on promoter-binding

In order to examine transcription activation in dependence of promoter-binding by RNAP·σ^{54}, three DNA templates were constructed that differed only in the promoter region between positions –41 and + 2 (Figure 2.1). These sequences strongly resemble the ROX-labeled DNA duplexes used for binding studies of RNAP·σ^{54} measured by fluorescence anisotropy (Figure 3.2 and [123]). The initial plasmid pVW7 containing the *gln*Ap2 promoter regulated by two enhancer sites located at –109 bp upstream was modified by replacing the promoter for the two other promoter regions from *K. pneumoniae* namely *nif*H and *nif*L. Transcription activation of RNAP·σ^{54} was measured on these three promoters with fully saturated enhancer sites (100 nM NtrC monomer). Figure 3.20 shows transcription from promoters *gln*Ap2, *nif*H and *nif*L under conditions of partially and fully saturated promoter sites.

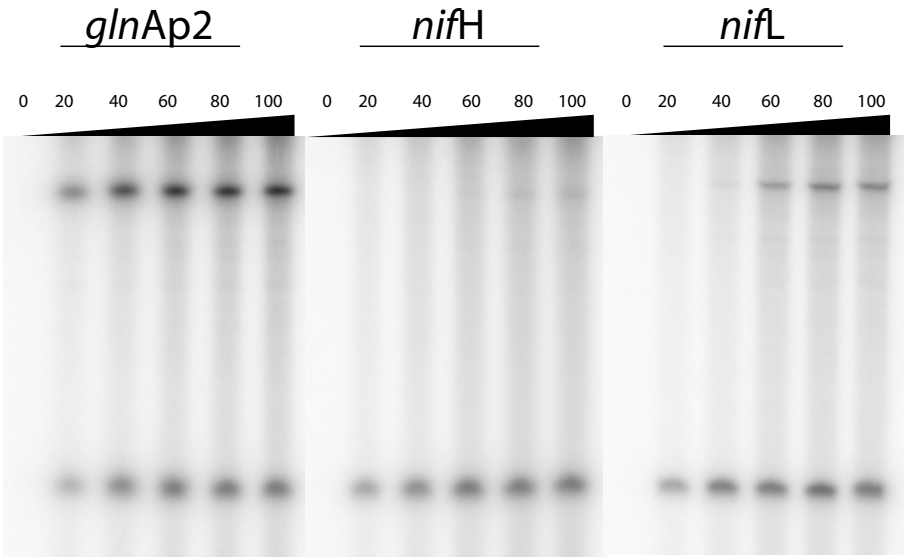

Figure 3.20: Dependence of transcription activity on promoter affinity of RNAP·σ^{54}
The DNA templates differed only in the promoter sequence. Promoters *gln*Ap2 from *E. coli* and *nif*H and *nif*L from *K. pneumoniae* were tested. 10 nM of DNA template (including 5 nM of control plasmid pVW7-158) were titrated from 0 to 100 nM RNAP·σ^{54} in low salt binding buffer (50 mM potassium acetate). The upper bands are specific transcripts from the plasmids of interest, the lower bands are specific transcripts of the control plasmid pVW7-158.

Promoter *gln*Ap2 showed considerable amounts of transcript over the entire range of RNAP·σ^{54} concentration beginning at 20 nM and increasing rapidly to maximal transcription activation. Fluorescence anisotropy measurments of the promoter *nif*H showed comparable binding affinities to RNAP·σ^{54} over a broad range of ionic strength thus similar amounts of transcripts were expected. However, *nif*H showed no transcription activation indicating that transcription activation not only depends on promoter binding. Promoter *nif*L showed only weak transcription activity at higher concentration of RNAP·σ^{54} where the promoter is fully saturated.

3.3.4 Transcriptional control by different arrangements of weak and strong NtrC sites

In the following, the results of the different arrangements of NtrC sites with respect to the promoter are classified in groups depending on their transcription activity. DNA templates can be distinguished bfrom which transcription is only weakly acivated (Group I) or highly activated upon specific binding of NtrC (Group II). One

group of templates produced low amounts of transcript comparable to the reference plasmid pProm (Group III). It has no enhancer site but contains the *gln*Ap2 promoter. Reference plasmids pTH8 and pVW7 are summarized in Group IV together with pVW7-ES10. Figure 3.21 shows the raw data of the gel separated transcripts from four different DNA templates after phosphoimager detection.
Previous studies have shown that NtrC is able to stimulate transcription by RNAP·σ^{54} even when it is not specifically bound to an enhancer site but when these sites were replaced by superhelical inserts that were able to stimulate NtrC oligomerization [124]. Apparently NtrC need not to be bound to a specific site on the DNA to bring about the activation of transcription. Experiments with a mutant form of NtrC that was not able to bind DNA was nontheless able to activate transcription when present in high concentrations [76]. Thus, some transcription activity observed for group III of DNA templates may result from an unspecific binding of NtrC either to the DNA template or directly to RNAP·σ^{54}. This should only be the case when NtrC is added at higher concentrations. pProm serves as an internal reference plasmid that is used to estimate the amount of transcription activation due to 'unspecific' NtrC binding, e. i. for the case, that NtrC binds unspecifically to other DNA sites or even activates transcription from solution by direct interacting with RNAP·σ^{54}. As shown in Figure 3.22, pProm is transcriptionally active, but only at higher NtrC concentrations. The level of transcript does not exceed the level obtained by the control plasmid pVW7-158, indicated by a normalized TXN activity AU (y-axis) of 1 which was calculated by the ratio of transcript intensities of the plasmid of interest to the control plasmid (pVW7-158). Figure 3.23 summarizes the transcription activity of plasmids differing in the distance between the two enhancer sites and the *gln*Ap2 promoter from 2 to 16 bp (Figures 3.15 and 3.16). The *in vivo* distance between proximal NtrC binding sites and promoter is 10 bp. Transcription activation from the pESX plasmids was examined in response to increasing NtrC concentration and was then compared to the plasmid pVW7 containing two enhancer sites at a distance of –109 bp [100].

I. Enhancer sites close to the promoter inhibit transcription

One group of plasmids was identified where NtrC represses transcription: pES2, pES4 and pES5 showed no or very little amounts of transcript (Figure 3.22 A and Figure 3.23). Assumably, enhancer and promoter site are too close to each other. At low ionic strength (50 mM potassium acetate) unphosphorylated NtrC binds with a dissociation constant K_d of $\sim$ 0.21 x 10^{-9} M [111]. It is known that phosphorylation

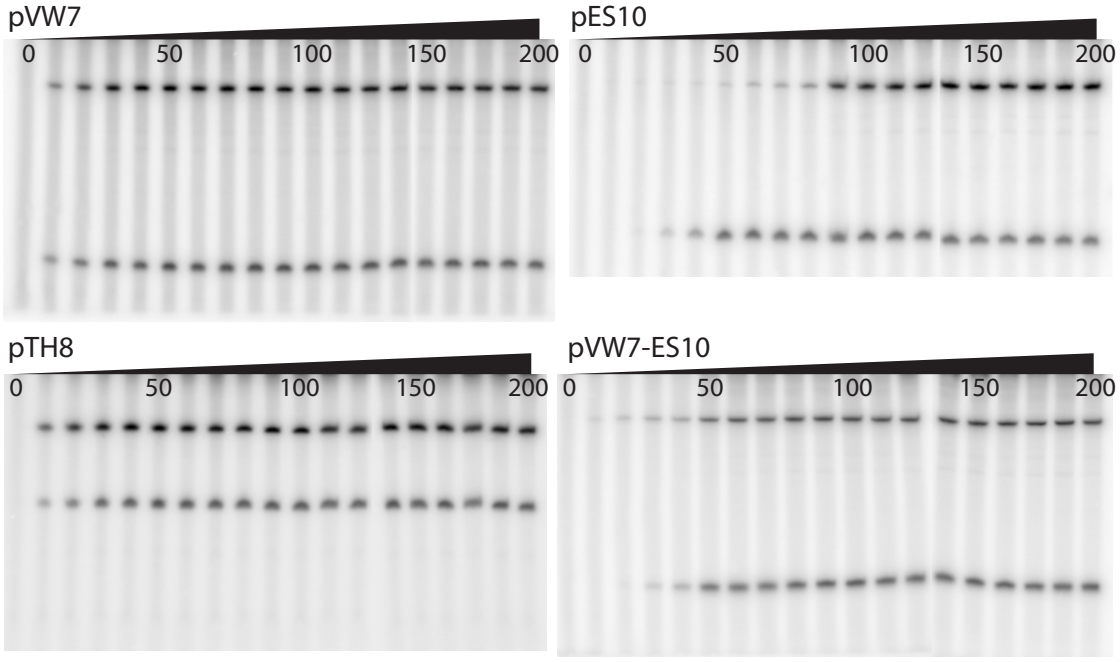

Figure 3.21: Gel analysis of *in vitro* transcription assays
The upper bands are specific transcripts from the plasmids of interest, the lower bands are specific transcripts of the control plasmid pVW7-158 (transcript length of 158 nt). All plasmids used for *in vitro* transcription produce RNA transcripts of 481nt except for pTH8 which produces a shorter transcript of 298 nt. pVW7 and pTH8 show transcription at low and high concentration of NtrC (left side). It has been shown previously that both plasmids only slightly vary in their response to NtrC [32]. In contrast, plasmid pES10 shows transcription only at high concentration of NtrC (right side, above). Compared to pTH8 and pVW7, transcription from plasmid pVW7-ES10 shows to reach a maximal level at higher concentration.

leads to a strong cooperativity of NtrC-P binding [64, 76, 88, 100, 125]. The dissociation constant of phosphorylated NtrC binding to two strong adjacent enhancer sites could not be determined but seems to occur in a cooperative way. Thus, binding of NtrC-P to the enhancer is stronger than binding of RNAP·σ^{54} (K_d of $\sim 10^{-11}$ M) to the promoter site [123] at the same ionic strength. Under conditions of low ionic strength chosen for *in vitro* transcription experiments, tight binding of NtrC to the promoter prevents binding of RNAP·σ^{54} to the promoter. Apparently, NtrC and/or RNAP·σ^{54} cannot bind simultaneously to their binding sites for three-dimensional reasons when these two binding sites are closer than $\sim$ 5 bp. In this case, NtrC seems to act as a repressor.

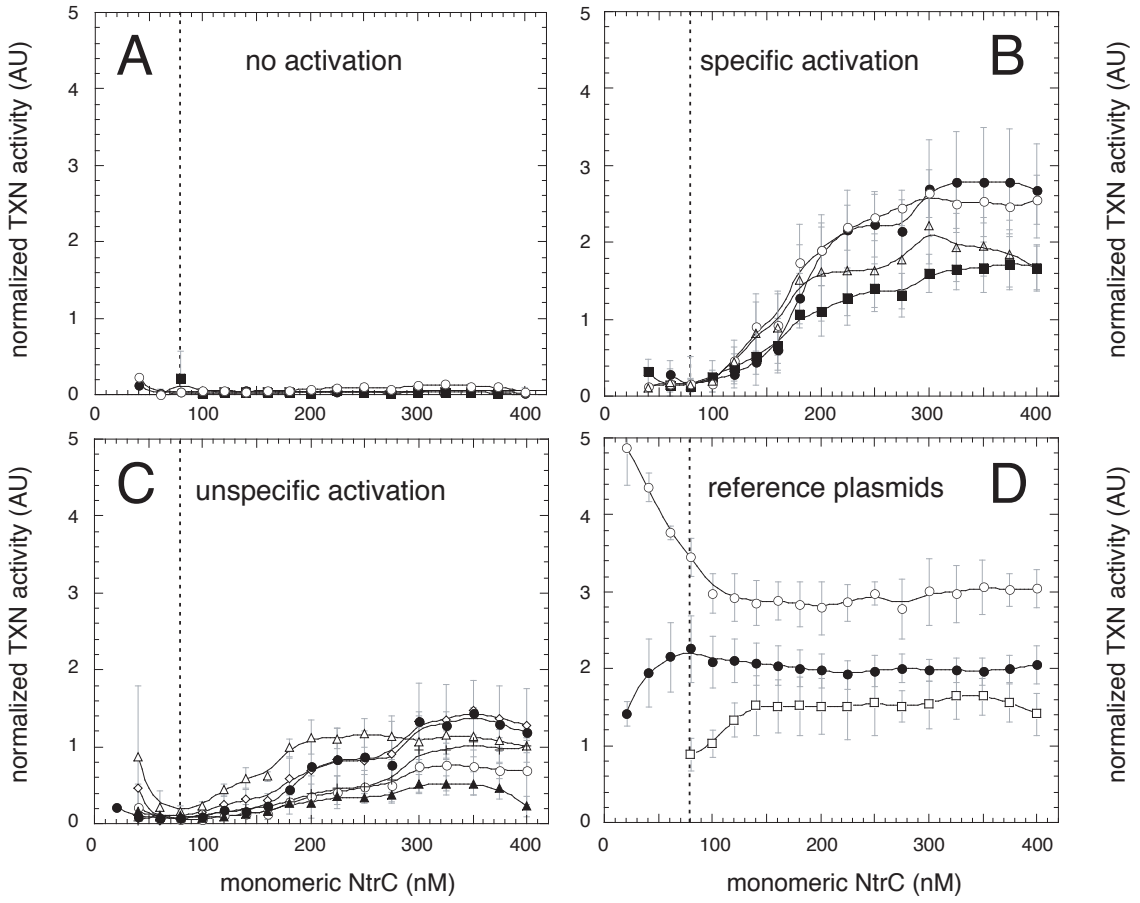

Figure 3.22: *In vitro* transcription of templates containing different arrangements of the enhancer region. Transcription activation was examined over a broad range of NtrC concentration between 0 and 400 nM NtrC. The dotted line is at 80 nM NtrC monomer concentration which corresponds to 100 % occupancy of two strong binding sites under phosphorylating conditions. (A) Transcription from DNA templates pES2 (filled circles), pES4 (filled rectangles) and pES5 (open circles) showed no or little amounts of transcript. (B) Transcription from templates pES8 (filled circles), pES9 (filled rectangles), pES10 (open circles) and pES11(open triangles) showed transcription activation at higher levels of NtrC over 80 nM. (C) Transcription from templates pES6 (open rectangles), pES7 (open triangles), pES12 (open circles), pES14 (filled triangles) and pES16 (crosses) showed transcription at higher NtrC concentrations. The transcription activity from these DNA templates is comparable to that of the enhancerless plasmid pProm (filled circles). (D) Reference plasmids pVW7 (filled circles), pTH8 (open circles) and pVW7-ES10 (open rectangles) are compared.

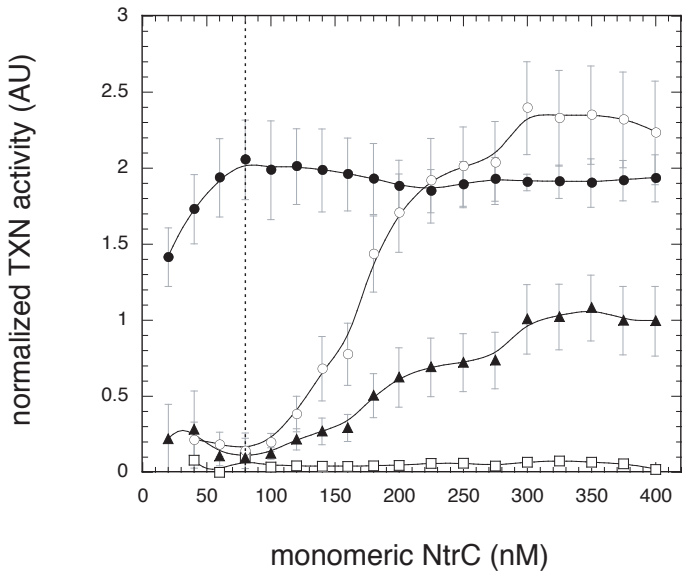

Figure 3.23: Comparison in transcription activity of different classes of DNA templates
The relative transcription activities of the DNA templates used here are plotted versus the nominal concentration of NtrC. The templates were classified into different groups and compared to transcription activity from plasmid pVW7 (filled circles) accordingly to transcription activation. It should be noted that plasmid pVW7 contains two enhancer sites that were shown to be sufficient to activate transcription at a distance [17,18]. Group I (open boxes, see also Figure 3.22 A) were found to repress transcription, whereas group III (filled triangles, see also Figure 3.22 C) yield low levels of transcription activity, but only at higher concentration of NtrC. Group II (open circles, see also Figure 3.22 B) showed considerable amounts of transcription activity comparable to those of plasmid pVW7, albeit at higher concentrations of NtrC around 300 nM. The dotted line refers to a NtrC concentration of 80 nM monomers which corresponds to 100 % occupancy of two strong binding sites under phosphorylating conditions. At this concentration reference plasmid pVW7 shows a maximal transcription activity.

II. Enhancer sites with an enhancer-promoter distance of ∼10 bp show specific transcription

The second group of plasmids (pES8, pES9, pES10 and pES11, Figure 3.22 B and Figure 3.23) show comparable amounts of transcripts beginning at a NtrC concentration of ∼120 nM. The activation of transcription stimulated by NtrC reaches a plateau region comparable to that of plasmid pVW7 only at higher concentration of NtrC of about 300 nM. The fact that fully occupied strong NtrC sites at a NtrC concentration of 80 nM for 10 nM DNA template assuming a stoichiometry of 8:1 respective NtrC:DNA with two strong enhancer sites, Figure 3.23) sites near the *gln*Ap2 promoter at an enhancer-promoter distance around 10 bp are not sufficient to stimulate transcription activity indicates that there must be another condition

that determines activation of transcription.

III. Some enhancer sites do not stimulate transcription

Finally, a third group of plasmids was identified (pES6, pES7, pES12, pES14 and pES16, Figure 3.22 C and Figure 3.23) which showed transcription activation at higher concentration of NtrC. However, the amount of transcript did not differ from that of the enhancer-less plasmid pProm. This indicates that transcription from these DNA templates is due to an unspecific binding of the activator that enables effective interaction with RNAP·σ^{54}.

IV. Competitive effects of different plasmids on NtrC binding

Before analyzing the transcription activity of the different DNA templates, the transcription activity of the control plasmid pVW7-158 with a transcript length of 158 nt was investigated for its reproducibility in amount of transcript in combination with different DNA templates. The presence of different numbers of NtrC sites may effect the total concentration of free NtrC available to bind to the NtrC sites of the control plasmid. Obviously, the different transcription templates have different competitive effects regarding the transcription activity at a given activator concentration on the control plasmid pVW7-158. Since the amount of transcript of pVW7-158 serves as internal control of possible experimental variabilities, it was assumed to be constant for all measurements within the accuracy of measurement. Differences in the amount of transcript have to be taken into account. Figure 3.24 shows the transcription activity of the control plasmid between 0 and 200 nM of NtrC monomer.
During analysis of the data of the transcription experiments, the transcript of the control plasmid pVW7-158 showed different amounts when incubated in transcription reactions with plasmids containing different combinations of weak and strong NtrC binding sites (Figure 3.24). Within this concentration scale three groups of plasmids can be identified which give the same transcription activity of the control plasmid pVW7-158 at different concentration of the activator. In the first class of plasmids containing pTH8, pVW7 and pProm the amount of transcript increases nearly linearily with increasing concentration of NtrC until a plateau level is reached. In the second class, the plasmids of the pESX series, transcription activity gives a sigmoidal shape of the curve shifted to higher amounts of NtrC. The third class consisting of only pVW7-ES10 shows the same sigmoidal shape of the curve, but shifted to even more higher NtrC concentrations.

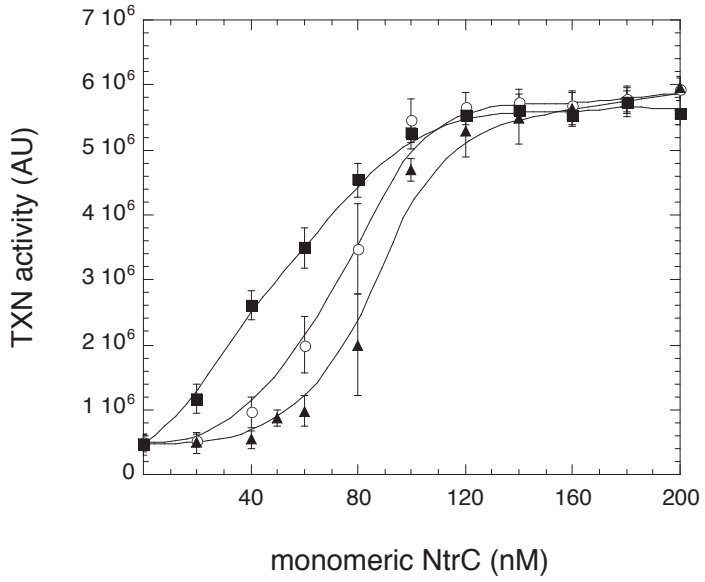

Figure 3.24: Competitive effects between the plasmid of interest and the control plasmid pVW7-158. The figure shows averaged titration curves within a concentration scale from 0 to 200 nM of monomeric NtrC. The effects can be divided into three groups: the enhancer-less pProm, pTH8 with the *in vivo* sequence of two high-affinity and three low-affinity NtrC binding sites and pVW7 with two distant high-affinity binding sites (filled rectangles), the templates of the pESX series (open circles) and pVW7-ES-10 containing the two high-affinity NtrC binding sites positioned at a distance of 109 bp relative to the promoter (center to center) and two high-affinity binding sites adjacent to the promoter (filled triangles).

V. Combination of distal and proximal enhancers

Up to now, all examined plasmids contained 2 strong NtrC binding sites (enhancers) adjacent to the *gln*Ap2 promoter at distances between 2 and 16 bp between the end of the second enhancer site (NtrC 2, see Figure 3.16) and the beginning of the RNAP·σ^{54} footprint region spanning from –26 to –11. Comparison to plasmid pVW7 containing equally two strong NtrC sites at a longer distance of –109 bp revealed that NtrC is able to activate transcription without looping of the intervening DNA, but at higher concentration of NtrC than needed to fully saturate these two strong NtrC sites. Titration of NtrC into a reaction containing pVW7 as DNA template shows an initial linear increasing amount of transcript that reflects the binding of the added activator protein to the DNA until the activation reached a plateau value at 80 nM NtrC monomer for 10 nM DNA (Figure 3.22 D). The intersection point of these to lines indicates the equivalence point where all NtrC sites are fully saturated and yield a maximum transcription activation. This is the case at a NtrC concentration

of 80 nM, from which a stoichiometry of 8 NtrC molecules to two strong NtrC sites can be derived. This is in good agreement with previous studies that proposed that NtrC binds in an octameric complex to two adjacent strong NtrC sites [122]. Transcription from plasmid pTH8 showed a different dependence on NtrC concentration. The amount of transcript from this template was corrected for its shorter length (298 nucleotides) before comparing with the other results. Since pTH8 has not the same termination sequence as pVW7 and pVW7-ES10 an altered termination efficiency cannot be excluded. This may explain the differences in the plateau value of the maximal transcription activity.

In order to extent the knowledge of the role of proximal enhancers in combination with remote enhancers, another DNA template was constructed. The resulting plasmid pVW7-ES10 is a chimeric construct between pVW7 and pES10: It contains the two enhancer sites at –109 bp comparable to those of pVW7 and the two enhancer sites at -10 bp from pES10 (see Figure 3.15). Strong NtrC binding sites are used adjacent to the promoter site instead of weak binding sites as it is the case of the *in vivo* sequence represented by plasmid pTH8. Effects in transcription activity by proximal strong enhancer sites were expected to be stronger than by weak NtrC binding sites at the same position.

Apparently, the presence of 4 strong NtrC sites in pWV7-ES10 has a competitive effect on NtrC binding to the reference plasmid pVW7-158 (see Figure 3.24). In this case the NtrC concentration by which the transcription starts is shifted to higher concentrations. In contrast to the other templates, pVW7-ES10 provides twice as much strong NtrC sites and thus needs higher amounts of activator protein to be fully saturated. To compare the results, the amounts of transcripts have to be corrected for this difference. The correction was made by determination of an averaged and normalized standard titration of control plasmid pVW7-158 from representing transcription experiments. This corrected and normalized titration of the control plasmid was then used to replace the results of the control plasmid for pVW7-ES10. The normalized TXN activity was calculated by the ratio of intensities from the amount of transcript of pVW7-ES10 to the normalized amount of transcript for the control plasmid pVW7-158. Transcription of pVW7-ES10 showed a different dependence on NtrC concentration. Two effects could be distinguished (Figure 3.22 D): First, transcription activation increases with increasing NtrC concentration between 80 and 140 nM NtrC. Compared with pVW7, transcription from pVW7-ES10 needs higher amounts of NtrC to yield same rate of activation. Second, transcription activation reaches a plateau value which is lower than the plateau value of pVW7. Since

pVW7-ES10 was derived from pVW7, both DNA templates are supposed to have the same termination efficiency. Thus, a difference in the plateau value must be due to the additional strong NtrC sites near the *gln*Ap2 promoter in pVW7-ES10.

VI. Dependence of the distance between enhancer and promoter sites on the activation of transcription

The effect of alteration of spacing between the enhancer and the promoter was examined by titrating purified *E. coli* NtrC protein to reactions containing the control plasmid pVW7-158 and the plasmid of the pESX series to be investigated. Plasmids of the pESX series were derived from pVW7 by deletion of X bp between enhancer and *gln*Ap2 promoter resulting in pES10 with an enhancer-promoter distance of 10 bp. The remaining pESX plasmids were derived from pES10 by insertion or deletion of one or several bp resulting in a desired distance from 2 up to 16 bp. Figure 3.25 and Table 3.4 summarizes the results of transcription experiments at a NtrC concentration of 250 nM monomers.

Transcription activation at different enhancer-promoter distances

DNA template	TXN Activity (AU)	DNA template	TXN Activity (AU)
pES2	0.034 ± 0.009	pES10	2.322 ± 0.297
pES4	0.031 ± 0.007	pES11	1.635 ± 0.480
pES5	0.114 ± 0.036	pES12	0.485 ± 0.209
pES6	0.820 ± 0.382	pES14	0.338 ± 0.053
pES7	1.180 ± 0.191	pES16	0.475 ± 0.161
pES8	2.243 ± 0.426	pVW7	1.897 ± 0.152
pES9	1.410 ± 0.307	pProm	0.868 ± 0.699

Table 3.4: Transcription activation at different enhancer-promoter distances.
The averaged values for transcription activity in arbitrary units (AU) at a NtrC concentration of 250 nM within a 95 % confidence interval are listed. All plasmids contained two strong NtrC sites at different distances from the *gln*Ap2 promoter except for pProm which which contained no enhancer and served as a reference plasmid for any 'unspecific' activation by NtrC.

At this concentration, the enhancer sites are fully occupied by NtrC. The amount of transcript is plotted versus the distance between enhancer and glnAp2 promoter. pES2 and pES4 do not show any transcript whereas pES5 shows very little amounts of transcript. The amount of transcript increases dramatically at a distance of 6 bp. The transcription reaches a maximum at the *in vivo* distance of 10 bp and decreases with increased distance to a minimal level of transcription (see a distance of 14 or 16 bp). Experiments with pES9 show reproducingly lower amounts of transcript.

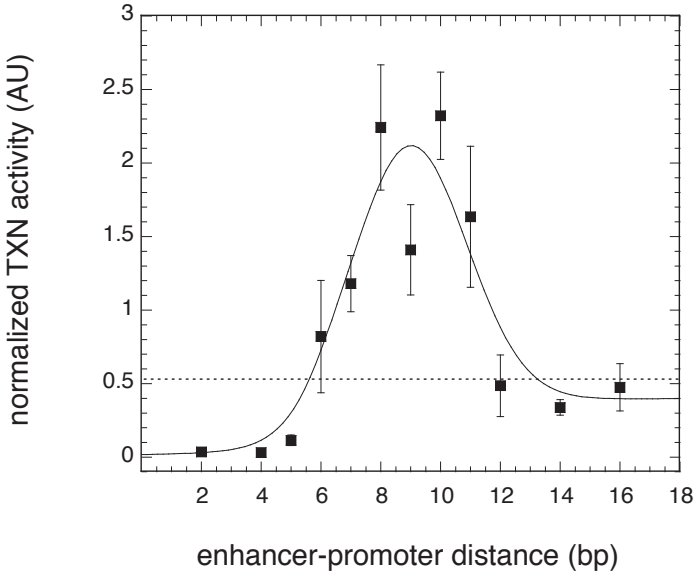

Figure 3.25: Effect of alterations in spacing between enhancer and promoter on transcription activity. The averaged transcription values at 250 nM of monomeric NtrC within the 95 % confidence interval are displayed against the distance between enhancer and promoter. The plot shows a clear maximum of transcription activity around the native enhancer-promoter distance of 10 bp. Transcription is not activated at little distances of 2, 4, and 5 bp. At higher distances of 12, 14, and 16 bp transcription decreases to a lower level of transcription. The dashed line indicates transcription activity from DNA templates that produced amounts of transcript comparable to the enhancer-less template pProm. The data set from this plot is listed in Table 3.4 together with the transcription activities plasmids pVW7 and the enhancer-less pProm.

Transcription without looping depends on the distance between the enhancer and promoter site. The relation between transcription activity and distance between proximal enhancer and promoter can be described with an empirical fit curve:

$$y = 0.2 + 1.75 \cdot exp(-0.14(x-9)^2) - 0.0023 \cdot arctan(5.78 - x) \qquad (3.1)$$

The *in vivo* conformation of DNA is a right-handed double-helical hydrated B-form which is characterized to have 10.4 bp per turn. Two neighboring basepairs are twisted for about 35°C against each other. Although the enhancer–promoter distance can be only altered in minimal steps of one base pair and therefore an empirical fit curve provides no more information about the mechanism an empirical fit seems still useful. Any effect altering the distance between two basepairs by stretching or contracting could be described by this fit.

In the following Table 3.6 the DNA templates used for *in vitro* transcription are described with respect to composition of distal and proximal NtrC binding sites.

Different composition of NtrC binding sites in DNA templates

plasmid	total length (bp)	distance (bp) enhancer–promoter	strong enhancer at –109 bp	weak enhancer at –10 bp	strong enhancer at –10 bp	n
pES2	3229	2	–	–	+	3
pES4	3231	4	–	–	+	3
pES5	3232	5	–	–	+	3
pES6	3233	6	–	–	+	4
pES7	3234	7	–	–	+	4
pES8	3235	8	–	–	+	5
pES9	3236	9	–	–	+	3
pES10	3237	10	–	–	+	6
pES11	3238	11	–	–	+	3
pES12	3239	12	–	–	+	3
pES14	3241	14	–	–	+	3
pES16	3243	16	–	–	+	3
pProm	3177	–	–	–	–	3
pVW7	3311	109	+	–	–	6
pVW7-ES10	3300	109	+	–	+	4
pTH8	3576	109	+	+	–	3

Table 3.5: Description of the DNA templates for *in vitro* transcription activation by NtrC. n is the number of experiments.

3.4 Scanning force microscopy

Visualization of RNAP·σ^{54} complexes with supercoiled DNA containing the promoter site provides information about the topology of the closed RNAP·σ^{54}-DNA complexes. In order to investigate the binding of RNAP·σ^{54} to a specific promoter site on a supercoiled DNA plasmid, closed complexes were preformed in an appropriate buffer that allows the DNA to maintain the superhelicity when deposited on the mica surface. A crucial step for DNA fixation on the negatively charged surface is the addition of bivalent cations such as Mg^{2+}. Figure 3.26 shows four images of closed complexes.

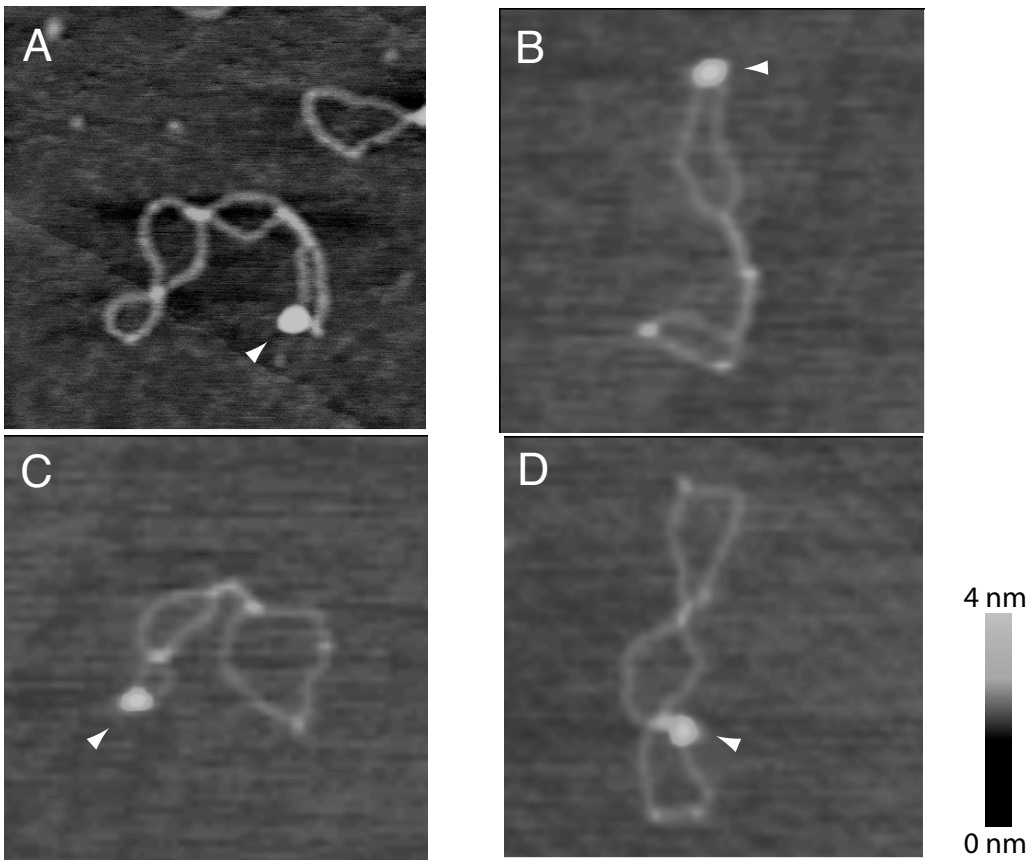

Figure 3.26: Closed complexes visualized by scanning force microscopy. The images size is 500 nm x 500 nm. The supercoiled DNA of 3311 bp length is bound by one RNAP·σ^{54} molecule, indicated by the arrows which is preferentially localized in one of the two end-loops of the DNA (A, B and C).

In order to examine if promoter-bound RNAP·σ^{54} is statistically distributed at any position of the supercoiled DNA or whether a particular localization is preferred,the

data analysis was done as follows. First, supercoiled DNA was 'defined' by the numbers of crossovers between the two strands to be at least three. Second, the plectonemic DNA should have two end-loops. Branched DNA conformations with three end-loops were not analyzed. The third condition was that one DNA molecule should be bound by only one RNAP·σ^{54}. The length of both end-loops and the total length of the DNA were determined as previously described. Table 3.6 summarizes the results of the analysis. Quantification of 15 complexes showed that 80 % of the closed RNAP·σ^{54} complexes were located in one of the two end-loops of the DNA whereas the two end-loops constituted only 45 % of the total contour length. That means, that the RNAP·σ^{54} is preferentially localized in the end-loop.

Number of crossovers	Length of end-loops loop 1 + loop 2 [nm]	End-loop localization ?	Relation of length of end-loops over total contour length [%]
4	82 + 238	yes	0.69
14	0 + 0	no	0.30
9	0 + 0	yes	0.31
3	92 + 265	yes	0.70
9	0 + 0	yes	0.31
9	222 + 229	yes	0.45
11	407 + 0	no	0.41
5	0 + 0	yes	0.84
6	89 + 160	yes	0.49
4	87 + 150	yes	0.40
7	0 + 0	yes	0.61
8	0 + 0	yes	0.31
19	0 + 0	no	0
7	0 + 0	yes	0.62
10	0 + 0	yes	0.30
			Averaged: 0.45

Table 3.6: Analysis of closed RNAP·σ^{54} complexes by scanning force microscopy.

Chapter 4

Discussion

In this thesis, a prokaryotic model system for transcription activation by an enhancer was examined. The core RNA polymerase is associated with an alternative sigma factor, σ^{54}, which initiates transcription from the *gln*Ap2 promoter. RNAP·σ^{54} is specific for a class of promoters which are mostly involved in nitrogen metabolism and share a consensus sequence [52,53,58]. After binding to the promoter, RNAP·σ^{54} is blocked in DNA melting activity until the interaction with the enhancer-bound activator protein NtrC occurs and the block is relieved [56, 71]. The interaction between enhancer-bound activator and promoter-bound RNAP·σ^{54} occurs via looping of the intervening DNA [10,15,18,19,31]. The activator protein NtrC has an inactive dimeric form. Its activation occurs *in vivo* by the histidine kinase NtrB which phosphorylates NtrC [76,100,125]. For *in vitro* transcription experiments enzymatic phosphorylation was replaced by a chemical phosporylation with carbamylphosphate [91]. Hydrolysis of ATP catalyzed by NtrC provides free energy to melt DNA around the transcription start site +1. This system was used to study various aspects of the transcription activation process. Possible rate limiting steps for the total reaction are the binding of the activator and the RNA polymerase to their specific enhancer sites, looping of the intervening DNA, interaction of the DNA-bound proteins and finally local melting of the DNA at the transcription start site.

First, binding of RNAP·σ^{54} to three different isolated promoter sequences was studied by anisotropy measurements over a broad range of ionic strength in order to estimate if this binding step was rate limiting for the overall reaction. Second, the closed RNAP·σ^{54} complexes was examined by scanning force microscopy (SFM) in air to get topographical images of the molecules. It was tested if promoter-bound RNAP·σ^{54} was preferentially localized in the end-loop of the supercoiled DNA, which would result in a higher contact probability to enhancer-bound activator. Third, in

order to investigate the dependence of the enhancer-promoter distance for an enhancer very close to the promoter ($\leq$ 16 bp) on the activation process, *in vitro* transcription experiments were performed. In these experiments, it was also investigated wether activation occurs in the absence of DNA looping, and to elucidate how the transcription activity by NtrC can be modulated.

4.1 Assembly of the transcription machinery at the promoter

4.1.1 Binding affinity of RNAP·σ^{54} for *gln*Ap2, *nif*H and *nif*L promoters

The overall promoter strength as defined by the expression level depends on various steps in the transcription reaction. The promoter binding affinity of RNAP·σ^{54} is given by the dissociation constant K_d. It is an important parameter for analyzing the strength of a promoter. In addition, other steps involved in the activation pathway leading to the melting of the DNA at the transcription start site could also be rate limiting (Figure 1.3). These involve the interaction of the closed complex with the activator protein at the enhancer, the release of the block imposed by σ^{54} to open complex formation as well as the kinetics of the isomerization step itself. For the standard *E. coli* RNAP·σ^{70} it has been demonstrated that binding of the RNA polymerase to the promoter as well as the subsequent isomerization of the closed complex can be rate limiting [126]. For RNAP·σ^{54} no quantitative analysis of the relative contributions of the separate steps such as the promoter binding to the overall reaction has been reported so far.

The binding studies performed by fluorescence anisotropy measurements (also designated as polarization) are based on the fact that a molecule changes its ability to depolarize polarized light depending on its rotational diffusion [108]. Rotational diffusion of a molecule is reduced upon binding of a second molecule resulting in a decreased depolarization according to the Perrin equation. This method benefit from the possibility to choose a wide range of conditions such as temperature, ionic strength, pH etc. In addition, it provides information about the system free in solution at thermodynamic equilibrium. Here, in order to follow changes in anisotropy, the promoter containing DNA duplexes were end labeled with carboxyrhodamine at 5'-end (see Figure 3.1). The fluorescent signal of free and RNAP·σ^{54}-bound DNA was monitored by measuring fluorescence anisotropy which increases upon binding.

Three different promoter DNA duplexes of 43 bp length were analyzed in their ability to bind RNAP·σ^{54} in a closed complex: *gln*Ap2 from *E. coli* and *nif*H and *nif*L from *K. pneumoniae* (Figure 3.1). From DNase I protection experiments (also referred to as *in vitro* footprinting), the *gln*Ap2 promoter showed good protection, and a K_d of $\sim$ 3 nM was estimated at approximately physiological salt concentrations [97]. In contrast, promoters *nif*H [59, 95] and *nif*L [93, 94, 96] showed no or very weak protection under similar conditions. This is consistent with the *in vivo* expression levels from these three promoters. Accordingly, *gln*Ap2 has been referred to as a strong promoter as opposed to the weak *nif*H and *nif*L promoters. Table 4.1 summarizes previous data and the results from the present study.

Promoter	**Expression level**[a] ***in vivo***	**IHF dependence**[b]	**Binding by footprint**[c] [K_d=$\sim$ 3 nM]	**Binding by fluorescence anisotropy**[d]
*gln*Ap2	high	no	Strong	Strong [K_d=0.94 nM]
*nif*H	low/high[e]	yes	Weak	Strong [K_d=0.85 nM]
*nif*L	low	no	Weak	Weak [K_d=8.5 nM]

Table 4.1: Summary of binding studies from RNAP·σ^{54} to specific promoter DNA
Dissociation constants K_d for closed complex formation at physiological ionic strength are given in brackets. IHF, integration host factor
[a] Dixon *et al*,1980 [127], Weiss *et al*, 1992 [128]
[b] Magasanik *et al* 1996 [64]
[c] Popham *et al* 1991 [97], Morret *et al.*, 1989 [59], Buck *et al*, 1992 [95], Wong *et al*, 1987 [93], Minchin *et al*, 1989, [96], Austin *et al*, 1991 [94]
[d] this study, Vogel *et al*, 2002 [123]
[e] *nif*H is a weak promoter as determined from DNase I protection and *in vivo* expression (see Table), but can be fully induced under suitable physiological conditions as reported in Dixon *et al*, 1980 [127] and Weiss *et al*, 1992 [128]

It should be noted that *nif*H can be regarded as a strong promoter in the sense that it can be expressed at high levels under suitable physiological conditions [127, 128]. In contrast, the *nif*L promoter displayed a 5-fold lower expression level than the *nif*H promoter [127]. Promoters for RNAP·σ^{54} are characterized by a common consensus sequence containing two highly conserved regions: A –25/24 domain with the sequence 5'-(T/C)TGGCACG-3' and a domain around –12/11 with the sequence 5'-TTGC(A/T)-3' [58]. These highly conserved motifs allow recognition of the DNA in double-stranded form [58]. All three promoters have conserved –25/24 and –13/12 residues, changes of which have been shown to strongly reduce binding of RNAP·σ^{54} (Figure 3.1) [68, 77]. The *gln*Ap2 promoter most closely resembles the consensus

sequence (two deviations at positions –20 and at –14 with respect to the transcription start site +1) whereas *nif*H (positions –23, –21 and –15) and *nif*L (positions –26, –22 and –20) have differences in three positions. A change of the G·C base pair at position –22 in the *nif*L sequence into the consensus sequence A·T increased the expression level more than 2-fold [129]. However, the simple assumption that the consensus sequence with the conserved residues from –27 to –20 and –15 to –11 provides the highest rate of transcription appears not to be correct, as deduced from *in vivo* comparison of 17 promoter sequences [77]. In this context it is noteworthy that the *gln*Ap2 promoter has a consecutive tract of seven A·T base pairs from –5 to +2 whereas in the *nif*H and *nif*L promoters only two or three A·T base pairs are found in this region (Figure 3.1). This might lead to differences in the kinetics of strand separation during open complex formation.

It has been shown for RNAP·σ^{70} that the promoter affinity is strongly dependent on the ionic strength [130, 131]. Accordingly, the K_d for RNAP·σ^{54} was quantified at different salt concentrations. The ionic strength in *E. coli* varies between 0.17 and 0.3 K^+ equivalents [132, 133] and an *in vivo* activity of divalent cations such as Mg^{2+} between 1 and 10 mM has been estimated [134]. Since Mg^{2+} is also essential for the synthesis activity of RNA polymerase it was included at a concentration of 5 mM in all fluorescence anisotropy binding measurements. Typical physiological conditions should correspond to an ionic strength around I= 0.23 M. At this ionic strength average K_d values of 0.94 ± 0.55 and 0.85 ± 0.3 nM for the *nif*H and *gln*Ap2 promoters and 8.5 ± 1.9 nM for the *nif*L promoter were measured (Table 3.2). Thus, the *nif*L promoter displayed an about 10-fold lower binding affinity as compared to the two other promoters. The results of the *gln*Ap2 and *nif*L promoters are in good agreement with previous footprinting experiments [93, 94, 96, 97]. However, the *nif*H promoter showed an unexpectedly high affinity under these conditions very similar to that of *gln*Ap2 (Table 3.2 and Figure 3.7). This is in contrast to the data from *in vivo* footprinting using potassium permanganate or *in vitro* footprinting using dimethyl sulphate, which revealed a much lower occupancy of the *nif*H promoter as compared to the *gln*Ap2 promoter [59, 95]. Nevertheless, the binding affinity corresponds to *in vivo* expression studies where the promoters *gln*Ap2 and *nif*H with comparable strong binding affinities to RNAP·σ^{54} displayed high and low expression levels, respectively. Furthermore, a mutation of the CCC residues in the *nif*H promoter from –15 to –17 to TTT as in the *gln*Ap2 sequence (Figure 3.1) increased the footprinting protection [59]. Mutations of C to T at –15 and –16 enhanced integration host factor (IHF)-independent gene expression in an *in vitro*

transcription/translation assay [135] indicating that the binding affinity is also related to the promoter strength. In the fluorescence anisotropy binding experiments the *gln*Ap2 and *nif*H promoters showed comparable K_d values over the whole range of salt concentrations whereas the *nif*L promoter displayed a much weaker salt dependence (Figure 3.7). This excludes the possibility that the apparently very similar binding affinities of the *gln*Ap2 and *nif*H promoters are restricted to a certain ionic strength. It remains unclear how the differences between the results reported here and those of the footprinting experiments described in Morret *et al* [59] and Buck *et al* [95] can be explained. The determination of binding affinities by monitoring changes in the fluorescence anisotropy of dye-labeled DNA duplexes as it has been used here is a true equilibrium method. It is applicable for accurate determinations of K_d values over a large range of solution conditions [111–117]. A potential source of errors could be an effect of the fluorescent dye on the binding affinity as compared to the unlabeled DNA. For the present set of duplexes a spacer sequence of 5 bp (∼17 Å length) separates the dye attached to flexible alkyl linker of ∼9 Å length from the RNAP·σ^{54} binding region as determined by footprinting [69, 92]. Accordingly, a direct interaction between dye and polymerase appears unlikely but cannot be excluded, since the high resolution structure of the closed RNAP·σ^{54} complex is presently unknown. However, when preformed complexes of the ROX-labeled promoters with RNAP·σ^{54} were titrated with unlabeled *gln*Ap2 and *nif*H duplexes no significant differences in their affinities were observed. Thus, it can be inferred that the dye label had no effect on the relative binding affinities. It is also conceivable that residues outside the region protected in the footprinting experiments affect the binding affinity. In addition, the apparent contradiction between the fluorescence anisotropy and footprinting analysis of binding to the *nif*H promoter could be explained by a different mode of binding to *nif*H as opposed to *gln*Ap2, which could lead to a change in the protection pattern.

4.1.2 Salt dependence of closed RNAP·σ^{54} complex formation

A characteristic feature of protein-nucleic acid interactions is the strong dependence of K_d on the ion concentration. The slope of the regression line $-\Delta\log(K_d)/\Delta\log(I)$ in the double logarithmic plot with $\log(K_d)$ versus the log of the salt concentration (Figure 3.7) can be used to calculate the number of salt bridges between a protein and its DNA binding site in the absence of divalent ions [106, 107, 119, 130, 131]. For RNAP·σ^{70} closed complex at 0°C a value of 10.5 ± 1.5 has been determined with

the T7 A1 promoter, which corresponds to about 12 salt bridges formed between polymerase and DNA [131]. If Mg^{2+} is present in addition to monovalent ions, it acts as a competitor with negatively charged phosphate groups of the DNA backbone. This leads to a reduction in the apparent slope and some curvature in the log-log plot, especially at higher Mg^{2+} concentrations [130, 131]. This effect is relevant for binding studies described here, which were conducted in the presence of 5 mM $MgCl_2$. Since the present data set did not display a significant curvature in the range of salt concentration studied the data were fitted with a linear regression line. Values of the slope of 6.1 ± 0.5 (*gln*Ap2) and 5.2 ± 1.2 (*nif*H) were obtained. From the data reported in Strauss *et al.* [131] and Shaner *et al.* [130] a value of $-\Delta\log(K_d)/\Delta\log(I) \approx 6$ in the range 0.1 to 0.4 M NaCl is estimated for RNAP·σ^{70} for a concentration of 5 mM Mg^{2+}. This suggests that similar numbers of salt bridges are formed in the closed complex of RNAP·σ^{54} with the *gln*Ap2 and *nif*H promoters as compared to RNAP·σ^{70} with the T7 A1 promoter. In contrast, the slope of the salt dependence of the *nif*L was clearly reduced and a value of 2.1 ± 0.1 was measured. This demonstrates that the number of ion pairs between RNAP·σ^{54} and the *nif*L sequence is significantly smaller as compared to the two other promoters. Thus, the reduced strength of the *nif*L promoter can be explained by its weak binding affinity due to a reduced number of electrostatic interactions with this promoter DNA.

Apart from overall strength, the three promoters for RNAP·σ^{54} are also different in their response to intrinsic DNA curvature and bending induced by binding of IHF (see Table 4.1). On the basis of the available data it appears that transcription activation of a 'strong' promoter like *gln*Ap2 by NtrC or NifA on superhelical templates is not facilitated by DNA curvature [32]. In contrast, the *nif*H and *nif*L promoters showed a 3- to 20-fold increase in the equilibrium amount of open complexes in single round transcription experiments if a curved sequence or IHF-induced bending was present between enhancer and promoter [34, 135–137]. This observation can be explained by a model in which the strong *gln*Ap2 has a higher affinity than the *nif*H and *nif*L promoters [32], which is supported by footprinting experiments [59, 93–97]. The K_d measurements reported here clearly demonstrate that the *gln*Ap2 promoter has a significantly higher binding affinity than the *nif*L promoter. However, the differences in promoter occupation reported previously between the *gln*Ap2 and *nif*H promoters were not detected in the fluorescence anisotropy experiments, as discussed above. The about 20-fold stimulation of open complex formation by IHF or by intrinsically curved DNA sequence at the *nif*H promoter on supercoiled DNA was not observed with the *gln*Ap2 promoter [32, 34, 135, 137]. If the two promoters indeed have very

similar binding affinities for RNAP·σ^{54}, other steps in the activation reaction that leads to open complex formation must be responsible for the observed differences with respect to promoter strength and in the effect of DNA bending.

4.1.3 Identifying the rate limiting step for NtrC activated transcription from the *gln*Ap2, *nif*H and *nif*L promoters

After determination of the binding affinities of RNAP·σ^{54} to three different promoters *gln*Ap2 from *E. coli* and *nif*H and *nif*L from *Klebsiella pneumoniae*, it was tested if promoter-binding by RNAP·σ^{54} was rate limiting for transcription initiation. Briefly, the DNA templates were incubated with an excess of activator protein NtrC, ATP and carbamylphosphate and increasing amounts of RNAP·σ^{54} from 0 to 100 nM. After establishing of an equilibrium between closed and open complexes (13 min at 37°C) the remaining nucleotides were added and the open complexes could evolve to stable elongation complexes that synthesize the transcript. Addition of heparin destroys the closed complexes and inhibits the formation of new open complexes ('single-round transcription'). The extent of the transcriptional activation process can be quantified by the amount of radioactive-labeled transcript. Since the DNA templates differed only in promoter sequence, transcription activity from these promoters should reflect the binding degree of the promoter bound by RNA polymerase if the binding step is rate limiting.

The three templates with different promoter sequences and two strong enhancer sites at position –109 bp were tested under conditions of partially and fully occupied promoter sites (see Section 3.3.3) according to the dissociation constants K_d determined before by fluorescence anisotropy measurements (see Section 3.1.1 and 4.1.1). The *gln*Ap2 promoter showed transcriptional activity at low and high concentration of RNAP·σ^{54}, in contrast to the *nif*L promoter which was only activated at a high concentration of RNAP·σ^{54} (Figure 3.20). The inability of the *nif*L promoter to support the initiation of transcription at lower concentrations of RNAP·σ^{54} is presumably due to its lower affinity to RNAP·σ^{54} as compared to *gln*Ap2. This is in good agreement with the results of the binding affinity studies performed by fluorescence anisotropy measurements. Transcription from the *nif*H promoter showed a very weak signal only at higher concentration of added RNAP·σ^{54} (Figure 3.20).

Promoter *nif*H was shown to perform high gene expression levels *in vivo* [127, 128] and it remains unclear why *in vitro* transcription is very low (a summary of the

data is given in Table 4.1). The *in vivo* upstream sequence of the *nif*H promoter contains an IHF binding site in contrast to the *gln*Ap2 and *nif*L promoters [64]. Binding of IHF at a specific site between the enhancer and the *nif*H promoter is obviously required for full expression [137]. In addition, single round transcription experiments with *nif*H promoter showed an increase in the equilibrium amount of open RNAP·σ^{54} complexes, when IHF was present [34, 135].

The function of IHF has been controversely discussed. Based on the position of its binding site and the known function in other systems the predominant role of IHF appears to be to introduce a bend of about 160° in the DNA stretch separating enhancer from promoter [138–140]. Examination of the DNA sequences of all known σ^{54} dependent promoters that are activated by the activator proteins NtrC or related factors such as NifA revealed that those promoters that were lacking a IHF binding site had an intrinsic single bend in the DNA separating enhancer from promoter which supports the architectural role of IHF [33, 93, 141–143]. Most of the reports concluded that IHF does not stimulate initial binding of RNAP·σ^{54} or the NtrC protein [34,142]. The IHF-mediated DNA bending increases the probability of a successful interaction of the activator bound to the enhancer and the RNAP·σ^{54} bound to the promoter by facilitating the formation of the loop-complex and thus increasing the local concentration j_M [33,34,135,137,142]. Apart from structural effects, a second role of IHF has been suggested: Carmona *et al* report that binding of IHF to the Pu promoter of *Pseudomonas putida* facilitates binding of RNAP·σ^{54} to its target [144, 145]. This function should only be effective for low-affinity promoter sites since high-affinity sites such as the *gln*Ap2 promoter are already saturated even at low concentration of RNAP·σ^{54}. The DNA bending effect as well as the presumable RNAP·σ^{54} recruitment by specific IHF binding would lead to an increased contact probability between enhancer and promoter.

It has been previously shown by *in vitro* transcription experiments that both DNA superhelicity as well as DNA bending effects increases the contact probability between enhancer and promoter that leads to a higher transcription activation [32]. However, DNA bending had only little effect on NtrC activated transcription initiation from supercoiled DNA templates with high-affinity promoters such as *gln*Ap2 since the promoter is already fully occupied and the contact probability is already very high (j_M of 10^{-6} mol/l) [32].

Transcription activation from DNA templates containing the *gln*Ap2 promoter showed activation even at low concentration of RNAP·σ^{54} whereas *nif*L showed activation at higher concentration of the enzyme. This perfectly fits to the binding affinities

measured by fluorescence anisotropy and indicates that for these two promoters, transcription initiation depends on the binding occupancy of the promoter site. However, the promoters *nif*H and *gln*Ap2 are bound by RNAP·σ^{54} with comparable binding affinities over a large range of ionic strength, but strongly differ in their ability to activate transcription from the same enhancer. The results obtained here indicate that a fully occupied *nif*H promoter is not sufficient to initiate transcription from a supercoiled template as it seems to be the case for the promoters *gln*Ap2 and *nif*L. The recruitment function of IHF can be also excluded in this case since at the used concentration of RNAP·σ^{54} the promoter site is already saturated and IHF would have little effect. Thus, the two different functions of IHF cannot explain the observed reduced activation from the *nif*H promoter. In this case the isomerization is obviously the rate limiting step in the transcription initiation pathway since both DNA bending or RNAP·σ^{54} recruitment to the promoter site would have very little effect on the contact probability. Thus, IHF might have a third function: It might act by facilitating the isomerization step probably in conjunction with the enhancer-bound NtrC protein and thus increases the isomerization rate of RNAP·σ^{54} at the *nif*H promoter.

4.1.4 Determinants of σ^{54}-promoter DNA binding

Interaction between the activator and the RNAP·σ^{54} causes a conformational change within RNAP·σ^{54}, a reaction which requires the hydrolysis of ATP and which leads to isomerization from the closed to the open complex [70, 146, 147]. The transcriptional barrier of the closed RNAP·σ^{54} complex appears to be due to the RNA polymerase conformation rather than to DNA melting *per se* [70, 146]. It has been reported by Cannon *et al* that σ^{54} alone is able to bind the *nif*H promoter DNA under certain conditions [68, 71]. In these experiments, a short *nif*H promoter fragment from *Rhizobium meliloti* in which the DNA was stably opened two base pairs next to the consensus GC at position –12/11 with respect to the transcription start site at +1 was used to bind isolated σ^{54} (Figure 3.11). From footprint experiments, it has been shown that σ^{54} is not only able to tightly bind locally opened promoter DNA [71, 99] but may be even able to isomerize independently of the core RNA polymerase in a reaction that has all the remaining requirements for open complex formation [71]. In the presence of this heteroduplex DNA, the activator and hydrolyzable nucleotide (GTP or dGTP), a new complex called 'supershifted species' formed which moved slowly in a native gel [71]. This possibly indicates a conformational change within

σ^{54} [71]. However, this intermediate form of σ^{54} was not observed in gel shift experiments conducted here.

It has been previously shown, that σ^{54} binding is not restricted to the *nif*H promoter of *Rhizobium meliloti* and to a mutant variant, *nif*H049 [68, 71]. In these sequences an 'T'-tract from –15 to –17 distinguishes them from the *nif*H promoter of *Klebsiella pneumoniae*. Templates in which the 'T'-tract was replaced by an 'U'-tract were not able to bind σ^{54} by itself but as a holoenzyme with RNAP. In comparable experiments in which the dC residues at the same position of the *Klebsiella pneumoniae* *nif*H promoter (at position –15 to –17) were replaced by dm^5C (Cytosin methylated at position 5'), was also able to bind σ^{54} [68]. The sequence from –15 to –17 were therefore found to be critical for σ^{54}-binding. In particular, the methyl groups in the DNA major groove are supposed to be important for binding of σ^{54}. Comparable studies in which the DNA sequence was mutated at positions –26 (G $\mapsto$ T), –15 or –17 (C $\mapsto$ T) or –13 (T $\mapsto$ G) have shown that these positions are crucial determinants in high-affinity binding of RNAP·σ^{54} holoenzyme [142, 148–150]. Another experiment used heteroduplexes of the *nif*H from *R. meliloti* in which the DNA is stably opened one or two bases downstream of the concensus GC promoter sequence (position –13/12 relative to transcription start site +1) [71]. These heteroduplexes mimic the state of the DNA in the closed complex.

To extend this analysis of σ^{54} binding, nonnative heteroduplexes of the two different promoters *nif*H (*R. meliloti*) and *gln*Ap2 (*E. coli*) were used and compared to their homoduplexes. DNA fragments of 50 bp length spanning the region from –35 to +15 bp with respect to the transcription start site were synthesized. The heteroduplexes contained two mismatches each immediately downstream of the consensus GC (–13/12 region) with CA replacing AC for *nif*H and GG replacing TT for *gln*Ap2 at positions –11/10. Studies by analytical ultracentrifugation showed that σ^{54} alone binds to both the *nif*H heteroduplex and the *nif*H homoduplex in a 1:1 complex. At concentrations of 400 nM promoter DNA and 3.05 μM σ^{54} protein, binding of σ^{54} to the *gln*Ap2 promoter was apparently to weak with both the native homoduplex and the heteroduplex form. However, gel mobility analysis with slightly different concentrations of 100 nM promoter DNA and 1 μM σ^{54} protein showed closed complexes for both the *nif*H and the *gln*Ap2 promoters. This difference may be due to a characteristic of the analytical ultracentrifugation where complexes are stabilized during the run (known as the effect of 'molecular cageing'). As estimated from gel mobility analysis, binding of σ^{54} to the *nif*H promoter occurred with an estimated K_d of ~ 1 x 10^{-7} M to the heteroduplex as well as to the homoduplex form. Thus, the partial

opening at position –13/12 did not increase the binding affinity of σ^{54}. In contrast, binding to *gln*Ap2 was one order of magnitude weaker. The sequence of *gln*Ap2 has a 'T'-tract at position –15 to –17 to which an interaction with σ^{54} has been ascribed. The known positions that were investigated previously and that favour binding of σ^{54} and RNAP·σ^{54} are located at template positions –26, –15/16/17 and –13). These positions cannot explain the differences in binding affinity observed in this study since the investigated promoter DNA duplexes contained the same specific nucleotides at the mentioned positions. Another position may be responsible for this: position –11/10 seemed also to assist in binding of σ^{54}. As proposed by Cannon *et al* [71], mismatches at position –11/10 of the *R. meliloti nif*H promoter fragment mimic the state of the early melted DNA in the closed complex. However, this cannot explain the very similar binding affinities between the homo- and heteroduplex form of *R. meliloti nif*H promoter nor the considerably weaker binding affinities to the *gln*Ap2 promoter. The binding studies measured by fluorescence anisotropy (see Sections 3.1.1 and 4.1.1) showed very similar binding affinities of RNAP·σ^{54} to the *gln*Ap2 and the *nif*H promoters. Obviously, the RNAP·σ^{54} holoenzyme provides the main part of the binding energy since it binds about three orders of magnitude stronger than the σ^{54} factor alone. In addition, the RNAP·σ^{54} binds with comparable affinity to the *gln*Ap2 and *nif*H promoters indicating that σ^{54} is rather responsible for promoter specificity than for promoter affinity.

The measured differences in binding affinity between *gln*Ap2 and *nif*H indicate that there may be even more sequence determinants that direct the binding of RNAP·σ^{54} than the conserved –24/23 and –12/11 boxes of the promoter sequence. Promoters *gln*Ap2 and *nif*H that share these common motifs however showed differences in the affinity to σ^{54} by at least one order of magnitude as estimated by gel retardation assay. The triple T at positions –17 to –15 that was also supposed to be required for σ^{54}-binding is alone not sufficient for σ^{54}-binding [71].

4.1.5 Binding of RNAP·σ^{54} on a superhelical DNA template

Closed complexes of RNAP·σ^{54} bound at the *gln*Ap2 promoter on naturally supercoiled DNA plasmids were examined by scanning force microscopy in order to investigate the localization of the protein (Figure 3.26). The pVW7 plasmid that contains this RNAP·σ^{54}-specific promoter has a total length of 3.3 kb which corresponds to a contour length of about 1.1 μm with an averaged length of 0.34 nm per basepair. The experiments were performed under conditions that maintained the interwound

supercoiled conformation of the DNA. Figure 4.1 shows a schematic model of the possible localization of RNAP·σ^{54}.

In many cases of transcription regulation, two or more specific DNA sites are brought into close contact [11]. It has been shown that DNA supercoiling facilitates enhancer-promoter interaction over a large distance [151, 152]. This observation can be explained by DNA 'slithering', a bidirectional movement along the two strands of supercoiled DNA [153]. This movement has been shown to increase the contact probability by two orders of magnitude, but is reduced when an intrinsic curvature between the two sites is present with the two sites located symmetrically to the curved region [32, 154, 155]. In this case, the two sites are in close proximity. An asymmetric position of curvature was shown to even decrease the contact probability by more than one order of magnitude [32]. For DNA containing intrinsic curvatures a preferred end-loop localization is expected for energetic reasons [154]. The region of promoter *gln*Ap2 of plasmid pVW7 contains no intrinsic curvature. Thus, end-loop localization must be due to DNA bending by RNAP·σ^{54}.

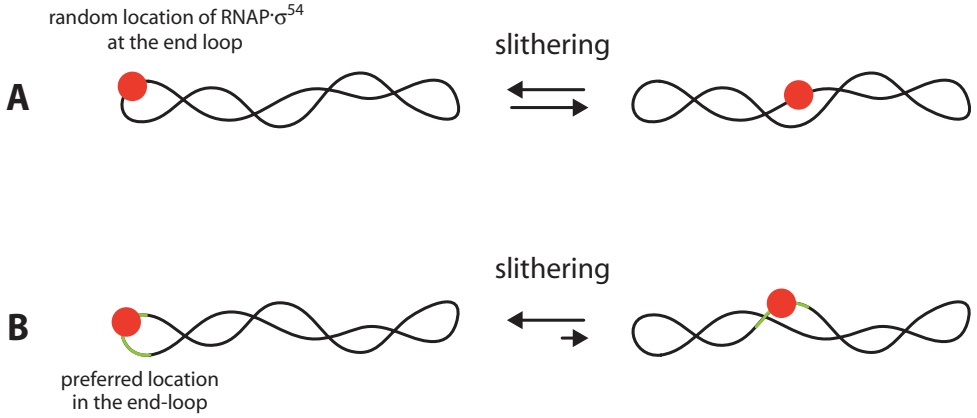

Figure 4.1: Model of RNAP·σ^{54}-induced DNA bending

Closed RNAP·σ^{54} complex, displayed as a circle, binds specifically to the *gln*Ap2 promoter (not emphasized). All conformations of superhelical DNA without intrinsic curvature are equally probable by 'slithering' of the two DNA strands in a fast exchange (equilibirum). **A** Supposing that RNAP·σ^{54} binds the DNA without influencing the structure of the DNA, it will be located anywhere on the supercoiled DNA and only randomly found at the end loop. **B** In a plasmid where a stretch of DNA is curved by the binding of RNAP·σ^{54}, it will be preferentially localized in one of the two end-loops of the supercoiled plasmid where it has to be more strongly curved (on the left side). This end-loop localization is favoured for energetic reasons over a localization at other less curved DNA sites (on the right side).

Schulz *et al* have shown that DNA curvature and superhelicity are features of the DNA conformation that both independently increase the local concentration j_M of enhancer-bound NtrC in the proximity of promoter-bound RNAP·σ^{54} [32]. Since an effective interaction requires the intervening DNA to be looped, it would be expected, that a preferred localization of NtrC and/or RNAP·σ^{54} within the strongly curved DNA, the end-loop would favour the interaction between these two sites. Revet *et al* provide indirect evidence that NtrC bends the DNA sequence it binds to [156]. This was concluded from the observation that curved DNA is localized in end-loops of a supercoiled plasmid and that NtrC was also found in these end-loops [156]. Schulz *et al* have also shown by SFM that RNAP·σ^{54} sligthly bends linear DNA upon promoter-binding by about $26 \pm 34°$ [32]. In the end-loop, the DNA is more strongly bent and for this reason, RNAP·σ^{54}-induced DNA bending will be preferably localized within these end-loops. This also accounts for the observation that the effect of superhelicity on the activation rate from a DNA that contains no curvature between enhancer and promoter is more prominent than from a template which already contains a curvature. Here it was tested whether the promoter-bound RNAP·σ^{54} is statistically distributed at any position of the plectonemic DNA structure or whether a particular localization is preferred due to DNA bending. It was found that RNAP·σ^{54} is preferrably localized in the end-loop of a superhelical DNA plasmid which indirectly supports the idea that RNAP·σ^{54} bends the DNA at the promoter site. Together with the observation that NtrC equally bends the DNA at the enhancer site which would lead also to an end-loop localization, the following model is proposed: DNA bending of RNAP·σ^{54} and NtrC directs the proteins to be preferrably localized in the end-loop of a supercoiled DNA. Due to the relatively small distance between enhancer and promoter, the two proteins are co-localized in the same end-loop and the proteins are in very close proximity which facilitates the formation of a so called 'enhancesome' constituted by the two proteins each bound to its specific binding site. This explains the relatively small *in vivo* distance between NtrC and RNAP·σ^{54} of 109 bp which is comparable to the persistence length of 150 bp for double-stranded DNA. At this characteristic length the DNA direction 'persists' and the polymer is difficult to bent. The higher the value of the persistence length is, the stiffer is the polymer. The ideal distance between two sites on double-stranded DNA that allows highest contact probability is 500 bp if no DNA bending would occur [11].

Moreover, this model may explain the effect of eukaryotic enhancers that are separated at even higher distances from the promoter they regulate. Eukaryotic DNA is supposed to be organized in higher-order chromatin-loops that could be comparable

to DNA-loops of prokaryotic plasmid DNA [157, 158]. Localization of enhancer and promoter within this loop may also lead to a higher local concentration of enhancer and promoter sites.

4.2 Mechanism of transcription activation

The *in vitro* transcription experiments conducted here, make use of purified components in order to investigate the mechanism of transcription activation regulated by the activator protein NtrC-P. In these experiments it was investigated how transcription activation can be modulated by different combinations of weak and strong NtrC sites in response to the activator concentration.

Transcription experiments were performed as shown in the schematic diagram (Figure 4.2). After preincubation of DNA template, RNAP·σ^{54} and NtrC in the presence of the phosphorylating agent carbamylphosphate, the formation of the open complexes was started by the addition of ATP. The incubation time of open complex formation was not limiting so that an equlibrium of closed and open complexes was established [32]. Addition of remaining nucleotides to the reaction started the elongation by the open complexes formed. Simultaneous addition of heparin destroyed RNAP·σ^{54} closed complexes whereas open complexes are heparin-resistent (Figure 4.2). Heparin is a polyanion, which competes with DNA by binding RNA polymerase. Addition of heparin before addition of the remaining nucleotides causes the RNA polymerase open complexes to transcribe one single round. After the first transcription round, RNAP·σ^{54} falls off the template and is not able anymore to bind the DNA again. Thus, the amount of transcript produced is proportional to the amount of open complex formation. In the transcription experiments presented here, the incubation time for open complex formation was chosen to be 13 min. At this time, an equilibrium between closed and open complexes is established [32].

The upstream sequence of the *gln*Ap2 promoter was modified to create different combinations of high- and low-affinity NtrC binding sites. A schematic overview over the different classes of transcription templates is given in Figure 3.15. Plasmid pTH8 contains the *in vivo* sequence of the *gln*Ap2 promoter with two strong distal sites (enhancer) and three weak proximal NtrC sites upstream [53]. These two strong NtrC sites behave like a eukaryotic transcriptional enhancer in that they function efficiently even when they are moved at distances of kilobases from the promoter [17, 18]. Activation of plasmid pTH8 occurs by looping of the intervening DNA that allows the enhancer-bound NtrC-P directly to interact with RNAP·σ^{54}

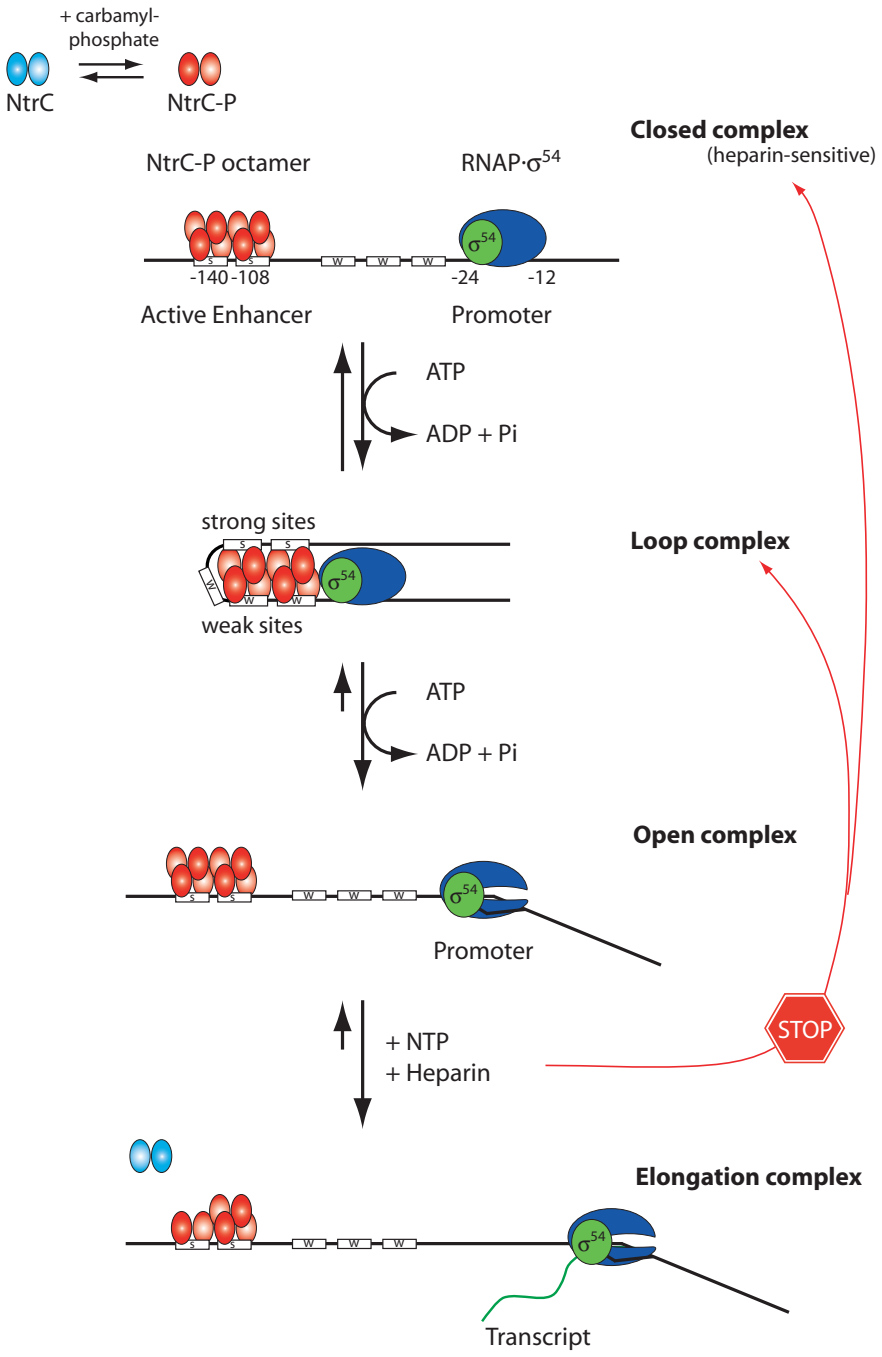

Figure 4.2: Scheme of *in vitro* transcription assay.
Phosphorylated NtrC binds as an octamer to the enhancer (S, strong NtrC sites). However, the exact stoichiometry of the NtrC complex is currently under discussion. RNAP·σ^{54} binds to the *gln*Ap2 promoter in a closed complex, in which the DNA remains double-stranded. Phosphorylated NtrC must form an oligomer at the enhancer to be able to activate RNAP·σ^{54} by direct protein-protein interaction. Activated NtrC contacts RNAP·σ^{54} by means of DNA looping. The interaction between NtrC-P and the RNAP·σ^{54} in the loop complex is still not known and may be stabilized by the weak NtrC sites (W). Isomerization to the open complex is driven by NtrC-dependent ATP hydrolysis. Addition of the remaining nucleotides leads to the formation of the elongation complex and thus starts the synthesis of the transcript. Simultaneous addition of heparin destroys closed complexes whereas open complexes are heparin-resistent.

at the promoter [10, 19]. It has been demonstrated that these two strong NtrC sites alone are required for the activation of the *gln*Ap2 promoter at low NtrC-P concentration (Figure 3.15) [18]. This was demonstrated with plasmid pVW7 that contains only these two strong NtrC sites and shows excellent activation of the *gln*Ap2 promoter [17, 18, 30, 64, 88]. In plasmid pVW7-ES10 the three weak binding sites close to the promoter have been replaced by two strong sites. This construct was used to investigate the role of these NtrC sites very next to the promoter. To account for transcriptional activation by unspecifically bound NtrC, plasmid pProm that has no specific NtrC site but the *gln*Ap2 promoter served as a reference plasmid. For a last project, plasmids containing only two strong NtrC sites but with different enhancer-promoter distances (pESX series, Figure 3.16) from 2 up to 16 bp were created in order to investigate the relation between enhancer position and transcription activation. In addition, it should be tested if NtrC activates transcription without DNA looping.

4.2.1 Relation between enhancer position and transcription activation: Activation without DNA looping

Two different models were proposed each supporting the formation of the loop complex to explain the function of the three weak enhancer sites near the *gln*Ap2 promoter: In the first model, Rippe proposed a conformation of the loop intermediate in which the enhancer-bound NtrC oligomer could interact with the weak NtrC sites at the promoter as outlined in Figure 4.3 [122, 159].

According to this model, the additional weak binding adjacent to the promoter may stabilizes the interaction between activator and RNAP·σ^{54} (Figure 4.3, left side). This model is supported by the observation from fluorescence cross-correlation spectroscopy studies (FCCS) in which the octamer complex of phosphorylated NtrC can simultaneously bind two DNA duplexes each containing two strong binding sites [159]. It has been additionally shown that the weak binding sites lead to a higher amount of open complexes [32]. In contrast, Atkinson and coworkers proposed that the weak enhancer sites acts by limiting somehow the maximal transcription activity without suggesting a specific mechanism [161]. The elucidation of a more detailed mechanism was addressed here by examining the role of the NtrC sites near the *gln*Ap2 promoter. A series of plasmids with different enhancer-promoter distances of 2 up to 16 bp was constructed (pESX series, Figure 3.16). The constructs contained the same *gln*Ap2 promoter and were derived from pES10. According to

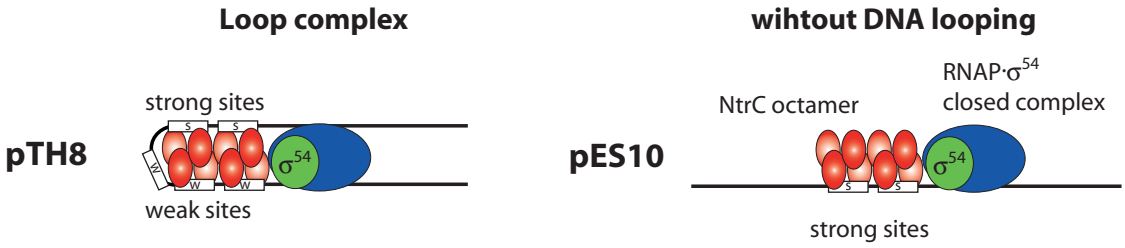

Figure 4.3: Proposed models of transcription activation from Rippe [159]
The schematic model demonstrates the direct interaction of NtrC with the RNAP·σ^{54} that takes place during transcription activation from different DNA templates pES10 and pTH8. The size of the NtrC octamer was estimated from SFM images [160] and the arrangement of the constituting monomers was taken from a hydrodynamic model proposed from Rippe [122,159]. The protein sizes were approximately adjusted with the length of the DNA they bind to as well as the linker DNA between the binding sites in order to predict as accurately as possible. Model of transcriptional activation from plasmid pTH8 which carries the *in vivo* sequence: Binding of an NtrC octamer simultaneously occur to the enhancer (two distant strong sites) and to two of the three weak NtrC sites and thus an intermediate loop complex is formed. According to this model, transcriptional activation would be also expected when the two enhancer sites at a distance of 10 bp (DNA template pES10) that replace the weak NtrC sites from pTH8 at the same position are occupied by an NtrC octamer.

the proposed model, transcriptional activation from plasmid pES10 would be also expected when the two strong NtrC sites are occupied by an NtrC octamer (Figure 4.3). The three weak NtrC sites of the *in vivo* sequence were replaced by two strong NtrC sites and the two enhancer sites at a distance of –109 bp were deleted.
From *in vitro* transcription experiments three different groups of DNA templates can be distinguished which yield different amounts of transcript and thus differed in activation by NtrC (Figures 3.22 and 3.23). (1) A first group of plasmids produced no or very small amounts of transcripts. This was the case for enhancer-promoter distances of 2, 4 and 5 bp (DNA templates pES2, pES4 and pES5). In these plasmids, NtrC sites and promoter site are too close to each other. In this case, activator NtrC and RNAP·σ^{54} cannot bind simultaneously and NtrC acts as a repressor. (2) A second group of plasmids (DNA templates pES6, pES7 and pES12, pES14, pES16) showed transcription activation comparable to the reference plasmid pProm which contained no specific NtrC site. However, NtrC activated transcription from the enhancer-less plasmid pProm was also possible strongly indicating that NtrC is able to act by binding unspecifically elsewhere on the template. It has been shown by electron microscopy studies that NtrC has a high affinity to supercoiled DNA that contains no homology to the NtrC consensus sequence [156]. Thus, sequence specificity together

with the three-dimensional structure of the DNA determine the affinity to NtrC. The superhelical sites were shown to be as effective as the sequence-coded NtrC sites in NtrC binding and its oligomerization [124]. Consequently, NtrC may be distributed statistically on a supercoiled plasmid with favorable and unfavorable distances to the promoter (see pProm in Figure 4.4). This explains why transcription from plasmid pProm needs a higher NtrC concentration as compared to a plasmid containing specific NtrC sites. Binding of NtrC does not seem to activate transcription in a specific way as the results are indistinguishable from pProm. The reasons for this may be different: First, for plasmids pES12, pES14 and pES16 the enhancer sites are presumably too far away from the promoter so that the bound NtrC oligomer cannot directly interact with the polymerase and too close to form a loop since the short DNA stretch is too stiff. Second, DNA 'phasing' could effect the optimal distance between enhancer-bound NtrC and promoter-bound RNAP·σ^{54}. Third, it is also possible that NtrC binds directly to RNAP·σ^{54} as it has been shown previously: *In vivo* and *in vitro* transcription revealed that NtrC is able to activate transcription from the *gln*Ap2 and the *nif*L promoters where all upstream NtrC sites were deleted [18, 93, 162]. These observations suggest that NtrC acts by binding DNA in an unspecific manner. A mutant form of the activator that was not able to bind DNA activated transcription when added at much higher concentration in the μM range [76]. The concentration of NtrC that was needed for the same level of transcription was about fourfold higher than from a template that contained specific strong NtrC sites [76]. However, at lower NtrC concentration ($< \mu$M), this interaction has not been demonstrated. Thus, the apparent role of enhancer binding by NtrC is to increase the local concentration of NtrC-P in the vicinity of RNAP·σ^{54} and to facilitate the formation of an NtrC oligomer. Obviously, enhancer sites at these positions in pES behave 'neutral' with respect to specific transcription activation and the observed transcription activation can be ascribed to unspecifically bound NtrC on the supercoiled DNA template. (3) A third group of plasmids produced considerable amounts of transcript (DNA templates pES8, pES9, pES10 and pES11). The enhancer-promoter distances of these templates were from 8 to 11 bp, e.i around the *in vivo* distance of 10 bp. Transcription activation from this group of plasmids showed amounts of transcript compared to plasmid pVW7. However, a NtrC concentration that is assumed to fully occupy the two enhancer sites from plasmid pES10 e.g. was not sufficient to activate transcription (Figure 3.22). Transcription from pES10 required much higher NtrC concentration ($>$ 200 nM monomer) to show maximal amounts of transcript, contrarily as it would be expected from the

proposed model (Figure 4.3). Thus, the difference between pVW7 and the plasmids of the pESX series is the response to different concentrations of the activator (Figure 3.23). Figure 4.4 shows a model of the NtrC arrangements that explain these observations: At NtrC concentrations > 200 nM a higher-oligomeric NtrC species consisting of two octamers is formed that is able to contact σ^{54} and to activate RNAP·σ^{54}. Apparently, the first NtrC octamer recruits a second octamer that properly interacts with the enzyme.
Taken together, strong NtrC sites have different functions in dependence on their localization with respect to the promoter:

- **Repressor**
  NtrC sites very close to the promoter so that protein binding sites overlap (pES2, pES4 and pES5)

- **Neutral Positions**
  NtrC sites with unfavourable distance and/or three-dimensional orientation towards RNAP·σ^{54} at which the enhancer has no stimulating effect compared to the enhancer-less DNA template pProm (pES6, pES7 and pES12, pES14, pES16)

- **Activator**
  NtrC sites with a distance to the promoter around 10 bp (pES8, pES9, pES10 and pES11)

In order to understand the results of the *in vitro* transcription studies, the different NtrC arrangements are outlined in Figure 4.4. In the model proposed by Rippe, NtrC-P binds first to two strong enhancer sites centered at position –109 bp [159]. Formation of the DNA loop between enhancer and promoter is then facilitated by the additional weak NtrC sites near the promoter. The experiments above now show that transcription activation without looping of the intervening DNA is in fact possible by binding of NtrC to two strong sites proximal to the promoter site (Figure 3.23). However, the NtrC-P concentration required to reach the same level of transcript from plasmid pES10 was about fourfold higher than needed to occupy the two strong NtrC binding sites by an octameric complex (Figure 3.23). Thus, a new model for the mechanism of transcription activation had to be derived to explain the data.

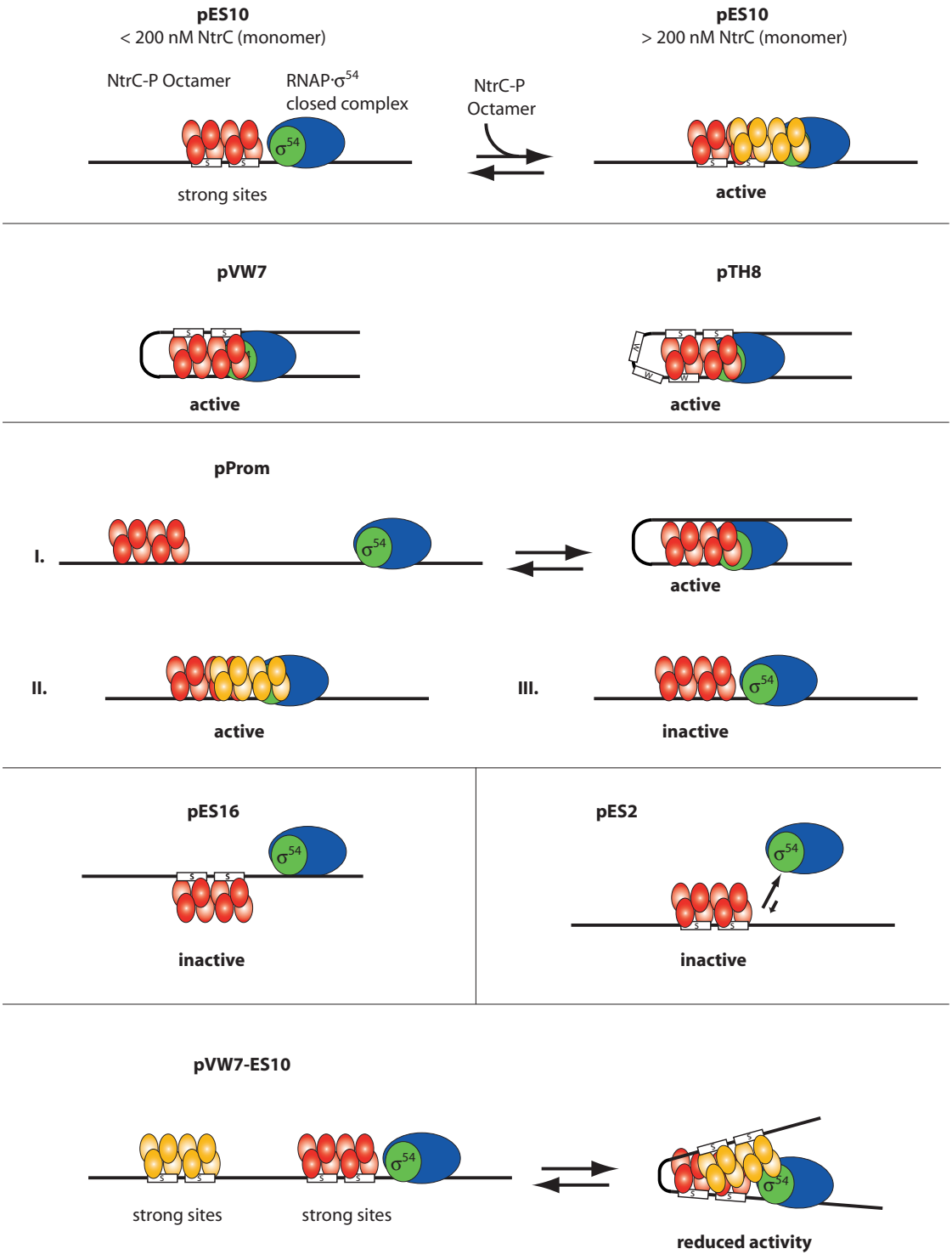
pES10
< 200 nM NtrC (monomer)
NtrC-P Octamer
RNAP·σ54
closed complex
strong sites
NtrC-P
Octamer
pES10
> 200 nM NtrC (monomer)
active
pVW7
active
pTH8
active
pProm
I.
active
II.
active
III.
inactive
pES16
inactive
pES2
inactive
pVW7-ES10
strong sites
strong sites
reduced activity

Figure 4.4: (previous page) Model of NtrC complex formation on different arrangements of enhancer and promoter derived from the data from *in vitro* transcription. In order to distinguish the different NtrC octamers they are in red and yellow. S and W indicate strong and weak NtrC binding sites. pES10. At lower concentration of NtrC ($<$ 200 nM monomer) the enhancer is fully saturated, but transcription is not activated. At higher concentration $>$ 200 nM a higher-oligomeric NtrC species consisting of two octamers is formed which is able to contact σ^{54} and to activate the RNAP·σ^{54}. Apparently, the first NtrC octamer recruits a second octamer that properly interacts with the enzyme. pVW7. The two distal enhancer sites bind NtrC and activation occurs through the interaction between the NtrC octamer and σ^{54}. The octamer is sufficient to activate transcription. pTH8. Interaction with one or more weak NtrC sites seem to stabilize the interaction between NtrC octamer and RNAP·σ^{54}. pProm. NtrC has been shown to have a high-affinity to supercoiled DNA. Binding of NtrC is equally probable at any DNA site. This model depicts three of them: Binding at a distant site with subsequent DNA looping and thus activation (I), binding at e.g. 10 bp at higher (II) and lower (III) NtrC concentration. pES16. NtrC sites are too far away from the promoter and DNA phasing lead to an unfavorable orientation between activator and RNAP·σ^{54}. pES2. NtrC sites are to close to the promoter and simoultaneous binding of activator and RNAP·σ^{54} is not possible. pVW7-ES10. NtrC binds equally well to the strong distal and proximal NtrC sites. The higher-oligomeric NtrC species forms by DNA looping but not in an ideal arrangement.

4.2.2 Modulating transcription activation by strong and weak NtrC sites

As demonstrated by transcription experiments described above, the position of the NtrC sites determines if NtrC acts as a repressor, has a neutral position or acts as an activator. The coexistence of low- and high-affinity binding sites for NtrC at different positions allows the fine regulation of expression from this promoter by modulating the concentration of NtrC. Three parameters that affected transcription activation were investigated in this work:

- **Number and affinity of NtrC sites**
  strong sites/ weak sites/ no sites
- **Arrangement of the sites with respect to the promoter**
  proximal/ distal/ overlapped with the promoter
- **Concentration of NtrC-P**
  from 0 to 400 nM of NtrC monomer which
  corresponds to the physiological range

Phosphorylation and dephosphorylation of NtrC is regulated by a complex signal transduction system in response to changes in the extracellular nitrogen status [72, 87, 163]. Since phosphorylation of NtrC is upregulated in ammonia starved

cells, the concentration of NtrC-P is a signal to modulate transcription activity at the σ^{54} dependent *gln*Ap2 promoter. The intracellular concentration of NtrC-P rises dramatically and sequentially acitvates different operons involved in nitrogen metabolism [33, 79, 82]. In order to respond adequately to the changes in NtrC concentration, the different nitrogen-regulated promoters contain distinct arrangements of NtrC binding sites: Some promoters consist of high- and low-affinity binding sites such as *gln*Ap2 whereas others consist of only high affinity binding sites such as *gln*Hp2. Table 4.2 summarizes promoters with different combinations of NtrC sites and their qualitative response to the activator concentration in an *in vitro* transcription experiment.

Promoter	**Arrangement of NtrC sites *in vivo***	**[NtrC-P]** low	**[NtrC-P]** high
*gln*Ap2[a]	two adjacent strong NtrC binding sites at –109 bp and three weak sites at –10 bp	+	+
*gln*Hp2[b]	two overlapping strong NtrC binding sites at a distance	+	+
*gln*Kp[c]	not described	–	+
*nif*LA[d]	adjacent low-affinity NtrC binding sites at –152 bp	–	+
nac[e]	combination of one high-affinity and one low-affinity binding site for NtrC	–	+
*gln*Lp[f]	one NtrC site overlapping the promoter (acts as a repressor)	–	–

Table 4.2: Comparison of different arrangements of strong and weak NtrC binding sites with their position relative to the indicated promoter and the response to different concentrations of NtrC-P.
[a] Ninfa *et al*, 1987 and Reitzer *et al*, 1985 [17, 81]
[b] Carmona *et al*, 1997 and Claverie-Martin *et al*, 1991 [141, 164]
[c] Atkinson *et al*, 2002 [165]
[d] Atkinson *et al.*, 2002 and Austin *et al*, 1987 and Wong *et al*, 1987 [93, 143, 165]
[e] Feng *et al*, 1995 [79]
[f] Reitzer *et al*, 1996 [78]

Previous studies have revealed different aspects of NtrC function: A mutant form of the activator is unable to bind to DNA but is able to activate transcription *in vitro* when provided in sufficient concentration [76]. Thus, DNA binding of the activator itself is apparently not required for transcriptional activation when present at very high concentration. DNA binding probably increases the local concentration of the activator in the vicinity of promoter-bound RNAP·σ^{54}. In addition, examination of the ATPase activity of NtrC has shown that enzymatic activity of NtrC is strongly stimulated by binding to two strong enhancer sites (Figure 3.14). Enhancer-bound activator and promoter-RNAP·σ^{54} do not have to be located on the same DNA strand

but can be located on separate, concatenated circular DNA molecules without losing enhancer-dependent transcription activation [19]. This experiment suggests that the activator interacts directly with the RNA polymerase and excludes 'tracking' mechanisms or mechanisms where the activator sends its signal by somehow altering the structure of the DNA between enhancer and promoter. However, the results indicate that enhancer-binding and DNA connection between enhancer and promoter strongly stimulate activation of transcription (Figure 3.14).

Until now, only few studies have tried to elucidate the role of the different low- and high-affinity binding sites for the activator NtrC upstream the promoter site: Comparison of different nitrogen regulated promoters showed a dependence of transcriptional activation on the concentration of NtrC-P resulting in a sequential activation. The different promoters contain distinct arrangements of NtrC sites. Promoters with potent enhancers (e.g. *gln*Ap2 and *gln*Hp2, Table 4.2) are activated first followed by promoters where the NtrC sites are less efficient (e.g. *nif*LA, *gln*Kp and *nac*). The strong *gln*Ap2 promoter showed that high- and low-affinity NtrC sites stimulate transcription but are not essential and at very high activator concentrations, the enhancer were not required for promoter activity [17]. The *gln*Hp2 promoter, consisting of two overlapping high-affinity NtrC binding sites is slightly less efficient than *gln*Ap2 where the NtrC sites do not overlap [141, 164]. Promoters *gln*Kp and *nac* required much higher concentration of NtrC-P [89, 165]. The nitrogen regulated promoter, *nac* from *Klebsiella aerogenes* contains an upstream enhancer consisting of a single high-affinity NtrC binding site and an adjacent low-affinity NtrC binding site [89]. This combination has a lower affinity to NtrC as the enhancer at the *gln*Ap2 promoter [89, 165] and is only effective at higher concentrations of NtrC-P *in vitro*. This is consistent with the fact that phosphorylated NtrC results in an oligomerization of NtrC accompanied with highly cooperative binding to two adjacent enhancer sites [100, 122]. Finally, one strong NtrC sites overlaps the *gln*L promoter and NtrC-P acts as a repressor [78]. These examples give a good insight in the different possibilities to regulate transcription with activator concentration in combination with different arrangements of activator binding sites.

The next interesting question that was addressed in this context was the role of the weak NtrC sites next to the *gln*Ap2 promoter that was previously discussed to have opposed functions [159, 161]. For this study, the *gln*Ap2 promoter was combined with two distal enhancer sites (–109 bp) and two proximal enhancer sites (promoter-enhancer distance of 10 bp) resulting in the DNA-template pVW7-pES10. The idea was that the proximal enhancer sites now substituting for the three weak NtrC sites

of the *in vivo* sequence (represented in pTH8), pronounce the effect of these sites. *In vitro* transcription from pTH8 showed higher levels of transcript compared to pVW7 (Figures 3.15 and 3.22). This is probably due to the lack of intrinsically curved DNA compared to the wild type sequence pTH8 [33, 141]. However, these results are questionable, since gel retardation experiments showed only very weak intrinsic curvature of pTH8 [32]. Assuming similar termination efficiencies of these two constructs, the observed higher amount of open complexes from template pTH8 should be due to the additional three weak NtrC sites near the promoter [32]. This is consistent with the view that the weak NtrC sites increase the transcriptional activation probably by facilitating the formation of the loop intermediate (Figure 4.3). This stimulates the open complex formation over the dissociation of the enzyme from the promoter sequence which yields a higher amount of open complexes in the equilibrium state.

Plasmid pVW7-ES10 contains two enhancer sites at –109 bp and two enhancer sites with a distance of 10 bp to the *gln*Ap2 promoter (Figure 3.15). It was used to investigate the role of the NtrC sites very next to the promoter. The *in vivo* weak NtrC sites were here replaced by two strong sites with the idea that the effect of these sites would be pronounced. Two effects can be distinguished: First, the maximum level of transcription activation from pVW7-ES10 is only reached at higher NtrC concentrations than needed for pVW7 or pTH8 (Figure 3.22) although it contains more strong NtrC binding sites and therefore a lower requirement in NtrC concentration would be expected. In detail, the plateau region is reached at a NtrC-P concentration of >120 nM NtrC monomer where all NtrC sites were 100 % occupied. This indicates, that NtrC-P probably acts a species that contains two octamers. A model that demonstrates NtrC binding at the sites of plasmid pVW7-ES10 is shown in Figure 4.4. Second, the maximum amount of transcript is lower as compared to that from plasmids pVW7 or pES10. At high NtrC concentration, the two octamers of the NtrC complex do not optimally interact with each other which leads to a reduced formation of open complexes (Figure 4.4). This observation is in good agreement with the idea that the weak NtrC sites near the promoter also designated as 'governor sites' limit promoter activity at high NtrC-P concentration as previously proposed [161]. These sites act either by preventing the formation of the DNA loop that brings activator and RNA polymerase into direct contact or by preventing a productive interaction between these two sites. Atkinson and coworkers have given a first hint to the limiting function of NtrC even though it was observed only at very high and thus non-physiological concentrations of NtrC (> 500 nM monomer) [161]. However,

the range of NtrC concentration used in this study (0 to 400 nM NtrC monomer) is physiological and hence these results indicate the importance of a concentration effect within this range for regulation of transcription. The combination of enhancer low-affinity NtrC sites adjacent to the promoter provides efficient transcription activation when the activator concentration is low, while limiting the maximum level of promoter activity when the activator concentration is high. Thus, the modulated NtrC concentration in combination with strong and weak NtrC sites at different positions seem to be a very versatile tool to respond within a defined time frame.
In contrast, Rippe proposed that the weak NtrC sites near the promoter could facilitate the formation of the loop complex with promoter-bound RNAP·σ^{54} by simultaneous binding of the NtrC-P octamer with the two strong and one or more of the three weak binding sites. As a consequence, the formation of the open complex would be stimulated [159]. This model is supported by the observation from plasmid pVW7-ES10 that at lower NtrC concentration, the function of NtrC is to activate transcription comparable to plasmids pTH8 and pVW7.
In summary, the two strong NtrC binding sites that are located between 100 and 150 bp upstream of the promoter, serve as enhancer for the activation of transcription initiation. The presence of NtrC binding sites immediately upstream of the promoter has different functions dependent on the exact position with respect to the promoter as well as on the affinity to the activator protein. In this thesis, these proximal sites were shown to enhance the interaction between NtrC and RNAP·σ^{54} to some extent, but also to limit maxmial level of activation or in some cases even to repress the transcriptional process. The affinity and number of these proximal activator binding sites may determine the temporal order in which transcription at the corresponding promoters is initiated as a function of the intracellular concentration of the activator. It shows that different parameters such as activator concentration, affinity and arrangement of their binding sites act together to obtain fine-regulated cellular response.

4.2.3 A model for transcriptional activation by NtrC

Previous studies have shown that NtrC is able to activate transcription when bound to the strong distal NtrC binding sites (enhancer) even if they were moved far away from the promoter they regulate [16–19]. Transcription activation occurs by means of looping of the intervening DNA to bring enhancer-bound NtrC and promoter-bound RNAP·σ^{54} into direct contact [159]. The role of the three additional weak NtrC sites

near the promoter is currently under discussion and was addressed in the following experiments.

The current model of transcription activation by a prokaryotic enhancer is the formation of a loop intermediate that forms at the transition from closed to open complex [159]. This is supported by the observation that phosphorylated NtrC is able to bind to two DNA duplexes each containing two enhancer sites [122]. In addition, it has been shown in *in vitro* transcription experiments, that the amount of open complexes at DNA template pTH8 (*in vivo* enhancer and promoter sequence) is 2- to 3-fold higher than at the template pVW7 that lacks the NtrC binding sites near the promoter [32]. As a consequence, the interaction between NtrC and RNAP·σ^{54} can be assumed to be stabilized by these proximal weak NtrC sites.

In order to test whether transcription activation occurs without DNA looping, a plasmid (pES10) was derived from pVW7 by reducing the enhancer-promoter distance to 10 bp. Thus, as compared to the *in vivo* sequence (plasmid pTH8) the weak NtrC binding sites were replaced by two strong NtrC sites (enhancer) (Figure 3.15). In addition, this construct lacks the distal enhancer sites. According to the model of a loop complex as intermediate state between closed and open complex, these sites should be sufficient for an effective interaction when replaced by stronger ones since in the loop complex, the interaction between activator and RNAP·σ^{54} is stabilized by additional weak NtrC binding sites near the promoter (Figure 4.3, DNA template pTH8). *In vitro* transcription from DNA templates pVW7 and pES10 that differ only in the position of the two enhancer sites, revealed that transcription from pVW7 and from pES10 are both activated by NtrC but at different concentrations of the activator. Transcription from pVW7 is activated at NtrC concentrations where the two enhancer sites are fully saturated whereas transcription from pES10 is only activated at higher NtrC concentrations (Figure 3.23). Thus, the model in which the enhancer-bound NtrC octamer additionally binds to two weak NtrC sites near the promoter (Figure 4.3, right side) does not explain the observed results from *in vitro* transcription experiments performed in this thesis. Instead, another NtrC-P species containing more monomers and/or which is associated in a different way could explain the transcriptional response occuring at higher concentrations of NtrC-P (Figure 4.4, pVW7-ES10). Figure 4.5 schematically displays the supposed NtrC complex formation and orientation with respect to the promoter-bound RNAP·σ^{54} according to the actual observations.

Studies with analytical ultracentrifugation performed by Rippe *et al* strongly support the existence of a higher-oligomeric complex of NtrC [122]. As shown previ-

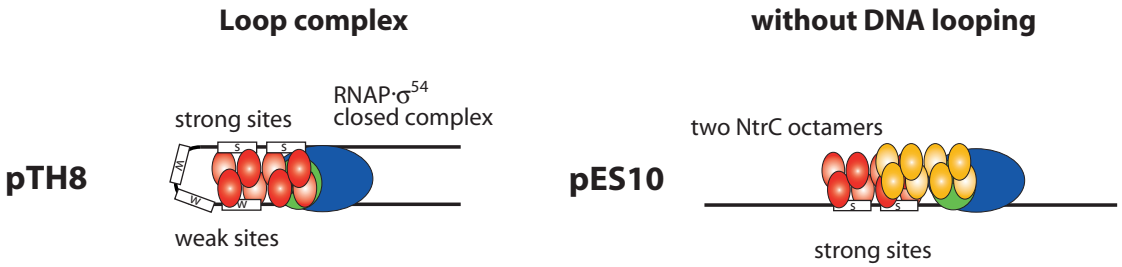

Figure 4.5: Improved model of NtrC-P complex formation for transcriptional activation with and without DNA looping. The schematic model was derived from the results obtained by *in vitro* transcription. In order to distinguish the different NtrC octamers they are in red and yellow. Strong (S) and weak (W) NtrC sites. For pES10 it was shown, that fully occupied enhancers juxtaposed to the promoter with an *in vivo* distance of 10 bp are not sufficient to activate transcription. There is strong evidence that a species constituting of two NtrC-P octamers forms by protein-protein association. This oligomer interacts optimal with σ^{54} which explains the requirement for higher NtrC-P concentration. In contrast, transcription from plasmid pTH8 needs the NtrC concentration that is required to fully occupy the strong NtrC sites. The arrangement of the NtrC-P octamer is therefore proposed as indicated in this scheme which directly contacts the σ^{54} subunit. The NtrC-P complex is additionally stabilized by a weak NtrC site.

ously, NtrC-P probably forms an octameric complex at two adjacent NtrC sites. Sedimentation velocity experiments of NtrC-P complexes formed with a DNA fragment containing two strong enhancer sites (ES-2) showed that different species are formed at different concentrations of NtrC-P [122]. At an excess of DNA one species of NtrC-P/DNA complex with a sedimentation coefficient of s=7.5 ± 0.2 S was observed which would correspond to one NtrC octamer binding two DNA duplexes. At increasing protein concentrations another species appeared (s=6.3 ±0.2) corresponding to the octamer only binding one DNA duplex. These data are in good agreement with fluorescence cross-correlation spectroscopy (FCCS) experiments [159]. At very high protein concentrations an additional species with a sedimentation coefficient of s≈10 S appeared. This species was assumed to be a complex of two octamers. These data are in very good agreement with the data from *in vitro* transcription experiments discussed above.

In summary, the improved model based on the actual data is consistent with the observations from previous studies from which different NtrC species could be assumed: It could be shown that the NtrC binding sites very next to the promoter have different functions: (1) An activating function when these sites just assist in stabilizing the interaction between NtrC and RNAP·σ^{54} by providing two additional NtrC binding sites which results in a higher local concentration (Figure 4.5, plasmid pTH8). (2) The repressive function of these sites is given at high concentration of

NtrC or (3) the presence of high-affinity NtrC sites adjacent to the promoter: binding of a first NtrC octamer is not sufficient for transcriptional activation. Probably, the NtrC octamer binds in an unfavorable distance and/or orientation to RNAP·σ^{54}. Binding of an additional octamer by protein-protein interaction leads to a good spatial conformation of the activator and thus to the activation of RNAP·σ^{54} (Figure 4.5, plasmid pES10).

4.2.4 Conclusions

Previous studies have indicated that activation of transcription by an enhancer-bound activator provides the cell with a broad range of possibilities to respond to an environmental change such as nitrogen limiting growth conditions. The binding affinities of RNAP·σ^{54} and of the activator to their cognate sites are crucial steps as well as their interaction with each other. The interaction between enhancer-bound activator and promoter-bound RNA polymerase is realized *in vivo* either by an intrinsically curved DNA that separates enhancer and promoter or by a protein-induced DNA bending e.g. by the integration host factor. This leads to an increased contact probability between NtrC and RNAP·σ^{54}. A productive interaction results in the formation of an open RNAP·σ^{54} complex.

Similar to control regions in eukaryotic transcription, procaryotic transcriptional control elements are composed in a modular manner of specific sequence elements which may respond to an increased concentration of the regulator in a synergistic way. The modular arrangement of different control elements of transcription enables an organism to respond to an incoming signal in a specific and fine-regulated way.

In vivo, increasing NtrC-P concentration occurs during nitrogen starvation and allows the cell to change the expression pattern. Some promoters are activated only at high concentrations of the activator whereas others respond to a broad range of NtrC concentration and some are even repressed. In this thesis, it could be shown that systematic combination of weak and strong NtrC sites upstream the *gln*Ap2 promoter respond to an increasing NtrC-P concentration. In addition, NtrC sites have very different effects on transcriptional activation depending on their position with respect to the promoter. Thus, a distinct arrangement of strong and weak NtrC sites activates the promoter over a well-defined range of NtrC concentration which reflects activation within a defined time frame. This allows the cell to respond to different environmental requirements.

Appendix A

Vectors

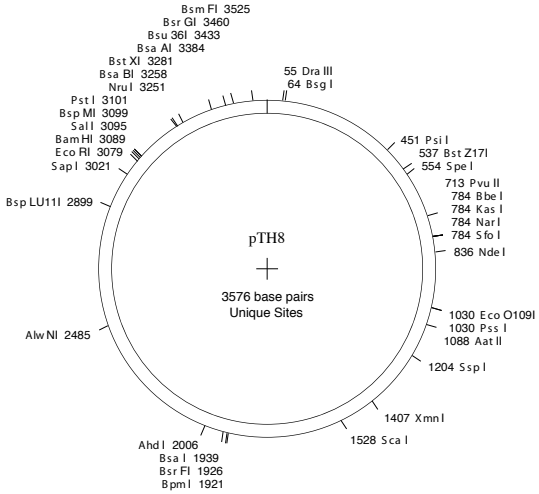
Bsm FI 3525
Bsr GI 3460
Bsu 36I 3433
Bsa AI 3384
Bst XI 3281
Bsa BI 3258
Nru I 3251
Pst I 3101
Bsp MI 3099
Sal I 3095
BamHI 3089
Eco RI 3079
Sap I 3021
Bsp LU11I 2899
AlwNI 2485
Ahd I 2006
Bsa I 1939
Bsr FI 1926
Bpm I 1921
55 Dra III
64 Bsg I
451 Psi I
537 Bst Z17I
554 Spe I
713 Pvu II
784 Bbe I
784 Kas I
784 Nar I
784 Sfo I
836 Nde I
1030 Eco O109I
1030 Pss I
1088 Aat II
1204 Ssp I
1407 Xmn I
1528 Sca I
pTH8
3576 base pairs
Unique Sites

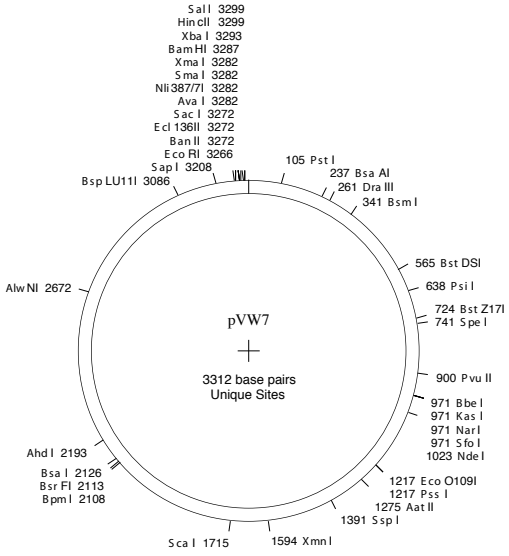
Sal I 3299
Hin cII 3299
Xba I 3293
BamHI 3287
Xma I 3282
Sma I 3282
Nli 387/7I 3282
Ava I 3282
Sac I 3272
Ecl 136II 3272
Ban II 3272
Eco RI 3266
Sap I 3208
Bsp LU11I 3086
AlwNI 2672
Ahd I 2193
Bsa I 2126
Bsr FI 2113
Bpm I 2108
Sca I 1715
105 Pst I
237 Bsa AI
261 Dra III
341 Bsm I
565 Bst DSI
638 Psi I
724 Bst Z17I
741 Spe I
900 Pvu II
971 Bbe I
971 Kas I
971 Nar I
971 Sfo I
1023 Nde I
1217 Eco O109I
1217 Pss I
1275 Aat II
1391 Ssp I
1594 Xmn I
pVW7
3312 base pairs
Unique Sites

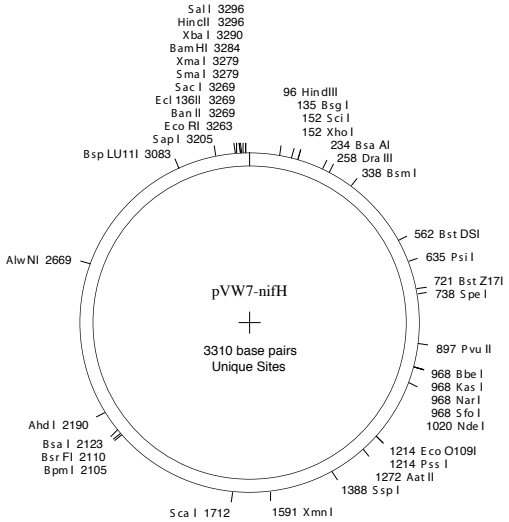
Sal I 3296
Hin cII 3296
Xba I 3290
BamHI 3284
Xma I 3279
Sma I 3279
Sac I 3269
Ecl 136II 3269
Ban II 3269
Eco RI 3263
Sap I 3205
Bsp LU11I 3083
96 HindIII
135 Bsg I
152 Sci I
152 Xho I
234 Bsa AI
258 Dra III
338 Bsm I
562 Bst DSI
635 Psi I
721 Bst Z17I
738 Spe I
897 Pvu II
968 Bbe I
968 Kas I
968 Nar I
968 Sfo I
1020 Nde I
1214 Eco O109I
1214 Pss I
1272 Aat II
1388 Ssp I
1591 Xmn I
Sca I 1712
Ahd I 2190
Bsa I 2123
Bsr FI 2110
Bpm I 2105
AlwNI 2669
pVW7-nifH
3310 base pairs
Unique Sites

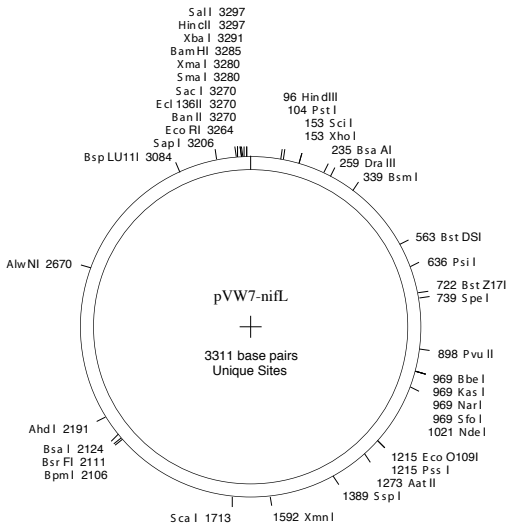
Sal I 3297
Hin cII 3297
Xba I 3291
BamHI 3285
Xma I 3280
Sma I 3280
Sac I 3270
Ecl 136II 3270
Ban II 3270
Eco RI 3264
Sap I 3206
Bsp LU11I 3084
96 HindIII
104 Pst I
153 Sci I
153 Xho I
235 Bsa AI
259 Dra III
339 Bsm I
563 Bst DSI
636 Psi I
722 Bst Z17I
739 Spe I
898 Pvu II
969 Bbe I
969 Kas I
969 Nar I
969 Sfo I
1021 Nde I
1215 Eco O109I
1215 Pss I
1273 Aat II
1389 Ssp I
1592 Xmn I
Sca I 1713
Ahd I 2191
Bsa I 2124
Bsr FI 2111
Bpm I 2106
AlwNI 2670
pVW7-nifL
3311 base pairs
Unique Sites

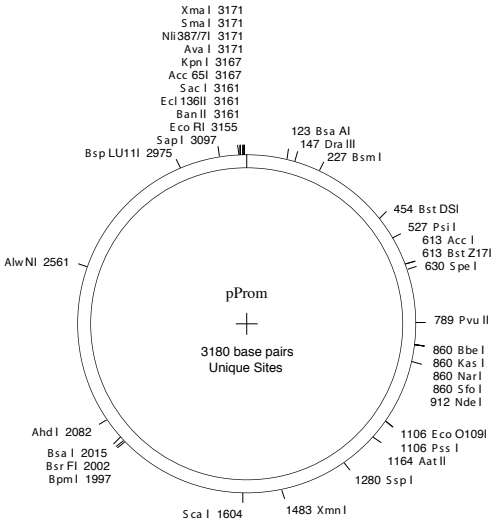
Xma I 3171
Sma I 3171
Nli 387/7I 3171
Ava I 3171
Kpn I 3167
Acc 65I 3167
Sac I 3161
Ecl 136II 3161
Ban II 3161
Eco RI 3155
Sap I 3097
Bsp LU11I 2975
123 Bsa AI
147 Dra III
227 Bsm I
454 Bst DSI
527 Psi I
613 Acc I
613 Bst Z17I
630 Spe I
789 Pvu II
860 Bbe I
860 Kas I
860 Nar I
860 Sfo I
912 Nde I
1106 Eco O109I
1106 Pss I
1164 Aat II
1280 Ssp I
1483 Xmn I
Sca I 1604
Ahd I 2082
Bsa I 2015
Bsr FI 2002
Bpm I 1997
AlwNI 2561
pProm
3180 base pairs
Unique Sites

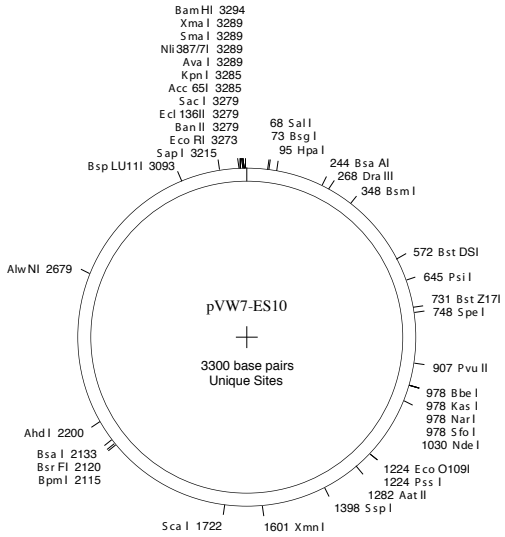
BamHI 3294
Xma I 3289
Sma I 3289
Nli 387/7I 3289
Ava I 3289
Kpn I 3285
Acc 65I 3285
Sac I 3279
Ecl 136II 3279
Ban II 3279
Eco RI 3273
Sap I 3215
Bsp LU11I 3093
68 Sal I
73 Bsg I
95 Hpa I
244 Bsa AI
268 Dra III
348 Bsm I
572 Bst DSI
645 Psi I
731 Bst Z17I
748 Spe I
907 Pvu II
978 Bbe I
978 Kas I
978 Nar I
978 Sfo I
1030 Nde I
1224 Eco O109I
1224 Pss I
1282 Aat II
1398 Ssp I
1601 Xmn I
Sca I 1722
Ahd I 2200
Bsa I 2133
Bsr FI 2120
Bpm I 2115
AlwNI 2679
pVW7-ES10
3300 base pairs
Unique Sites

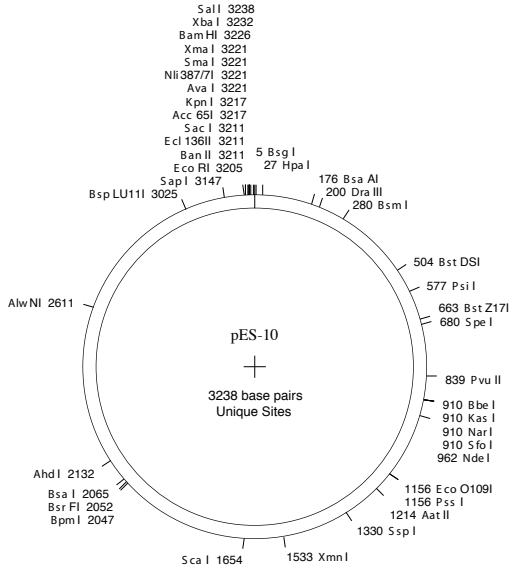
Sal I 3238
Xba I 3232
BamHI 3226
Xma I 3221
Sma I 3221
Nli387/7I 3221
Ava I 3221
Kpn I 3217
Acc 65I 3217
Sac I 3211
Ecl 136II 3211
Ban II 3211
Eco RI 3205
Sap I 3147
Bsp LU11I 3025
5 Bsg I
27 Hpa I
176 Bsa AI
200 Dra III
280 Bsm I
504 Bst DSI
577 Psi I
663 Bst Z17I
680 Spe I
839 Pvu II
910 Bbe I
910 Kas I
910 Nar I
910 Sfo I
962 Nde I
1156 Eco O109I
1156 Pss I
1214 Aat II
1330 Ssp I
1533 Xmn I
Sca I 1654
Ahd I 2132
Bsa I 2065
Bsr FI 2052
Bpm I 2047
AlwNI 2611
pES-10
3238 base pairs
Unique Sites

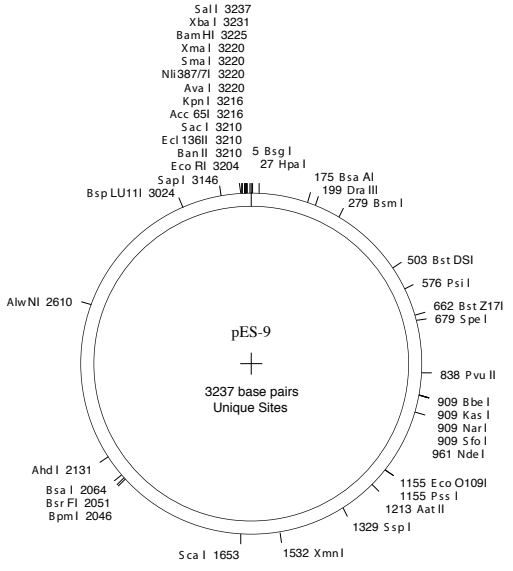
Sal I 3237
Xba I 3231
BamHI 3225
Xma I 3220
Sma I 3220
Nli387/7I 3220
Ava I 3220
Kpn I 3216
Acc 65I 3216
Sac I 3210
Ecl 136II 3210
Ban II 3210
Eco RI 3204
Sap I 3146
Bsp LU11I 3024
5 Bsg I
27 Hpa I
175 Bsa AI
199 Dra III
279 Bsm I
503 Bst DSI
576 Psi I
662 Bst Z17I
679 Spe I
838 Pvu II
909 Bbe I
909 Kas I
909 Nar I
909 Sfo I
961 Nde I
1155 Eco O109I
1155 Pss I
1213 Aat II
1329 Ssp I
1532 Xmn I
Sca I 1653
Ahd I 2131
Bsa I 2064
Bsr FI 2051
Bpm I 2046
AlwNI 2610
pES-9
3237 base pairs
Unique Sites

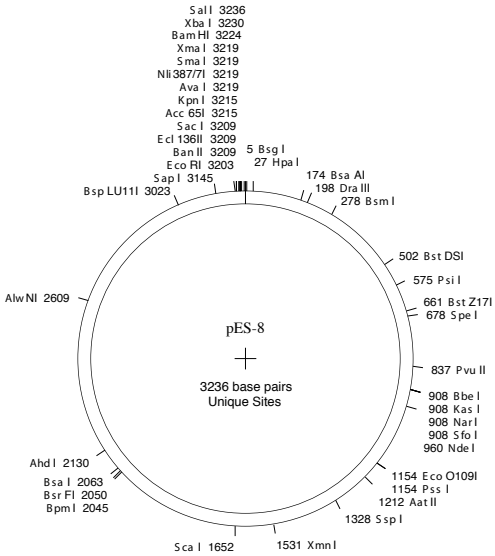
Sal I 3236
Xba I 3230
BamHI 3224
Xma I 3219
Sma I 3219
Nli387/7I 3219
Ava I 3219
Kpn I 3215
Acc 65I 3215
Sac I 3209
Ecl 136II 3209
Ban II 3209
Eco RI 3203
5 Bsg I
27 Hpa I
Sap I 3145
Bsp LU11I 3023
174 Bsa AI
198 Dra III
278 Bsm I
502 Bst DSI
575 Psi I
661 Bst Z17I
678 Spe I
AlwNI 2609
pES-8
3236 base pairs
Unique Sites
837 Pvu II
908 Bbe I
908 Kas I
908 Nar I
908 Sfo I
960 Nde I
Ahd I 2130
Bsa I 2063
Bsr FI 2050
Bpm I 2045
1154 Eco O109I
1154 Pss I
1212 Aat II
1328 Ssp I
Sca I 1652
1531 Xmn I

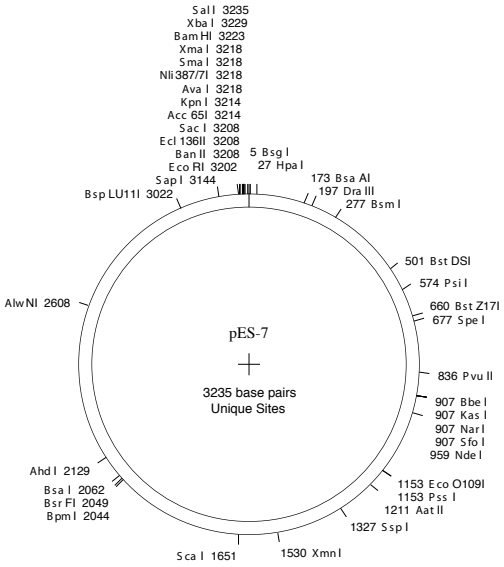
Sal I 3235
Xba I 3229
BamHI 3223
Xma I 3218
Sma I 3218
Nli387/7I 3218
Ava I 3218
Kpn I 3214
Acc 65I 3214
Sac I 3208
Ecl 136II 3208
Ban II 3208
Eco RI 3202
5 Bsg I
27 Hpa I
Sap I 3144
Bsp LU11I 3022
173 Bsa AI
197 Dra III
277 Bsm I
501 Bst DSI
574 Psi I
660 Bst Z17I
677 Spe I
AlwNI 2608
pES-7
3235 base pairs
Unique Sites
836 Pvu II
907 Bbe I
907 Kas I
907 Nar I
907 Sfo I
959 Nde I
Ahd I 2129
Bsa I 2062
Bsr FI 2049
Bpm I 2044
1153 Eco O109I
1153 Pss I
1211 Aat II
1327 Ssp I
Sca I 1651
1530 Xmn I

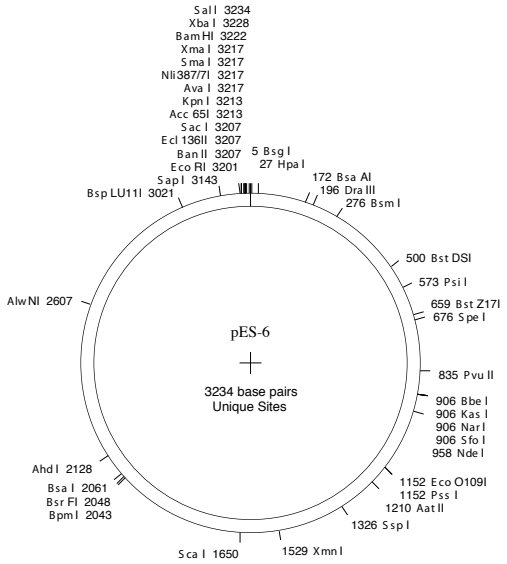
Sal I 3234
Xba I 3228
BamHI 3222
Xma I 3217
Sma I 3217
Nli387/7I 3217
Ava I 3217
Kpn I 3213
Acc 65I 3213
Sac I 3207
Ecl 136II 3207
Ban II 3207
Eco RI 3201
Sap I 3143
Bsp LU11I 3021
AlwNI 2607
Ahd I 2128
Bsa I 2061
Bsr FI 2048
Bpm I 2043
Sca I 1650
1529 Xmn I
1326 Ssp I
1210 Aat II
1152 Eco O109I
1152 Pss I
906 Bbe I
906 Kas I
906 Nar I
906 Sfo I
958 Nde I
835 Pvu II
659 Bst Z17I
676 Spe I
500 Bst DSI
573 Psi I
5 Bsg I
27 Hpa I
172 Bsa AI
196 Dra III
276 Bsm I
pES-6
3234 base pairs
Unique Sites

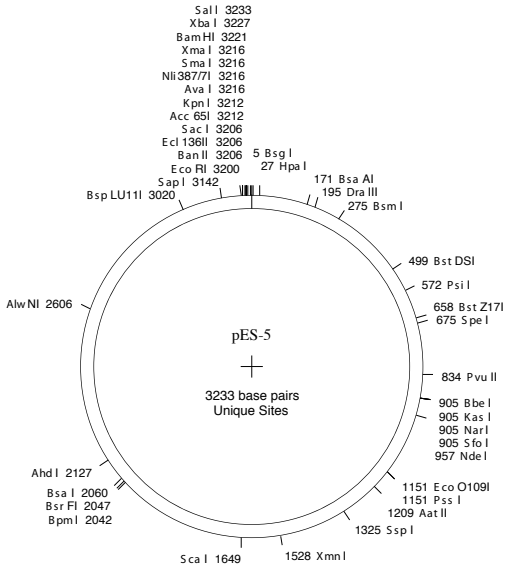
Sal I 3233
Xba I 3227
BamHI 3221
Xma I 3216
Sma I 3216
Nli387/7I 3216
Ava I 3216
Kpn I 3212
Acc 65I 3212
Sac I 3206
Ecl 136II 3206
Ban II 3206
Eco RI 3200
Sap I 3142
Bsp LU11I 3020
AlwNI 2606
Ahd I 2127
Bsa I 2060
Bsr FI 2047
Bpm I 2042
Sca I 1649
1528 Xmn I
1325 Ssp I
1209 Aat II
1151 Eco O109I
1151 Pss I
905 Bbe I
905 Kas I
905 Nar I
905 Sfo I
957 Nde I
834 Pvu II
658 Bst Z17I
675 Spe I
499 Bst DSI
572 Psi I
5 Bsg I
27 Hpa I
171 Bsa AI
195 Dra III
275 Bsm I
pES-5
3233 base pairs
Unique Sites

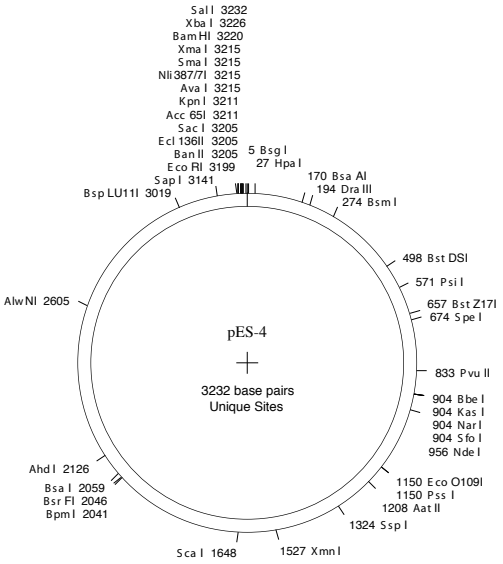
Sal I 3232
Xba I 3226
BamHI 3220
Xma I 3215
Sma I 3215
Nli387/7I 3215
Ava I 3215
Kpn I 3211
Acc 65I 3211
Sac I 3205
Ecl136II 3205
Ban II 3205
Eco RI 3199
Sap I 3141
Bsp LU11I 3019
AlwNI 2605
Ahd I 2126
Bsa I 2059
Bsr FI 2046
Bpm I 2041
Sca I 1648
1527 Xmn I
1324 Ssp I
1208 Aat II
1150 Eco O109I
1150 Pss I
956 Nde I
904 Bbe I
904 Kas I
904 Nar I
904 Sfo I
833 Pvu II
657 Bst Z17I
674 Spe I
498 Bst DSI
571 Psi I
274 Bsm I
170 Bsa AI
194 Dra III
5 Bsg I
27 Hpa I
pES-4
3232 base pairs
Unique Sites

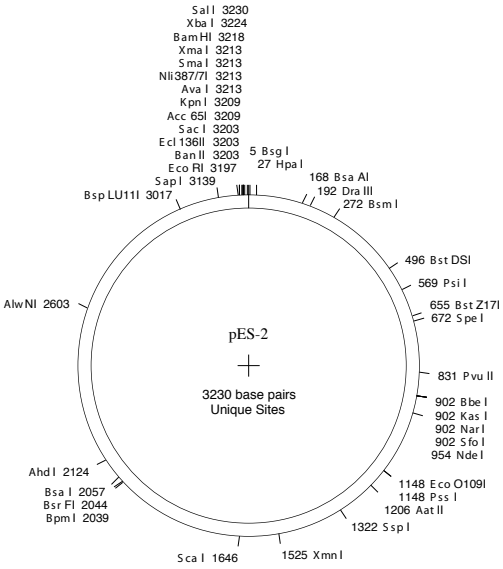
Sal I 3230
Xba I 3224
BamHI 3218
Xma I 3213
Sma I 3213
Nli387/7I 3213
Ava I 3213
Kpn I 3209
Acc 65I 3209
Sac I 3203
Ecl136II 3203
Ban II 3203
Eco RI 3197
Sap I 3139
Bsp LU11I 3017
AlwNI 2603
Ahd I 2124
Bsa I 2057
Bsr FI 2044
Bpm I 2039
Sca I 1646
1525 Xmn I
1322 Ssp I
1206 Aat II
1148 Eco O109I
1148 Pss I
954 Nde I
902 Bbe I
902 Kas I
902 Nar I
902 Sfo I
831 Pvu II
655 Bst Z17I
672 Spe I
496 Bst DSI
569 Psi I
272 Bsm I
168 Bsa AI
192 Dra III
5 Bsg I
27 Hpa I
pES-2
3230 base pairs
Unique Sites

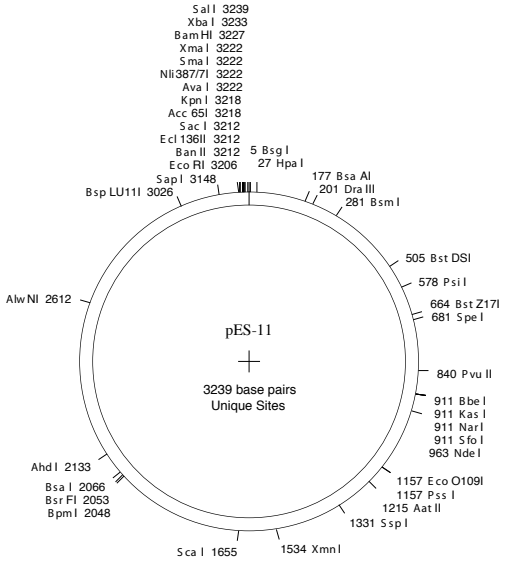
Sal I 3239
Xba I 3233
BamHI 3227
Xma I 3222
Sma I 3222
Nli387/7I 3222
Ava I 3222
Kpn I 3218
Acc 65I 3218
Sac I 3212
Ecl 136II 3212
Ban II 3212
Eco RI 3206
5 Bsg I
27 Hpa I
177 Bsa AI
201 Dra III
281 Bsm I
505 Bst DSI
578 Psi I
664 Bst Z17I
681 Spe I
840 Pvu II
911 Bbe I
911 Kas I
911 Nar I
911 Sfo I
963 Nde I
1157 Eco O109I
1157 Pss I
1215 Aat II
1331 Ssp I
1534 Xmn I
Sca I 1655
Ahd I 2133
Bsa I 2066
Bsr FI 2053
Bpm I 2048
AlwNI 2612
Bsp LU11I 3026
Sap I 3148
pES-11
3239 base pairs
Unique Sites

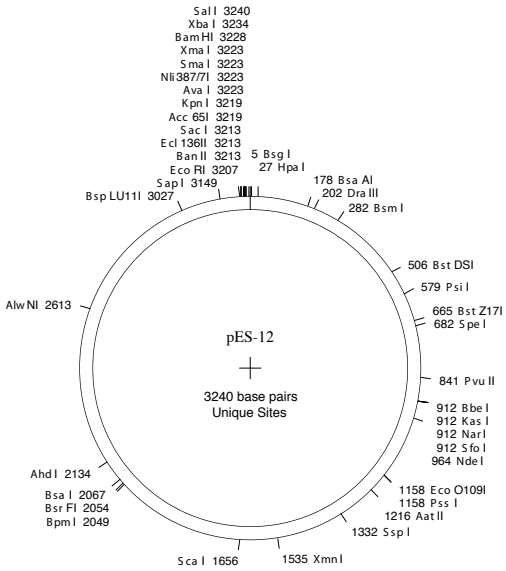
Sal I 3240
Xba I 3234
BamHI 3228
Xma I 3223
Sma I 3223
Nli387/7I 3223
Ava I 3223
Kpn I 3219
Acc 65I 3219
Sac I 3213
Ecl 136II 3213
Ban II 3213
Eco RI 3207
5 Bsg I
27 Hpa I
178 Bsa AI
202 Dra III
282 Bsm I
506 Bst DSI
579 Psi I
665 Bst Z17I
682 Spe I
841 Pvu II
912 Bbe I
912 Kas I
912 Nar I
912 Sfo I
964 Nde I
1158 Eco O109I
1158 Pss I
1216 Aat II
1332 Ssp I
1535 Xmn I
Sca I 1656
Ahd I 2134
Bsa I 2067
Bsr FI 2054
Bpm I 2049
AlwNI 2613
Bsp LU11I 3027
Sap I 3149
pES-12
3240 base pairs
Unique Sites

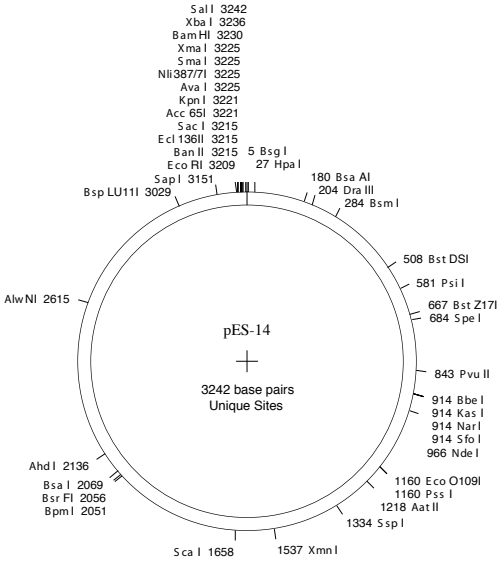
Sal I 3242
Xba I 3236
BamHI 3230
Xma I 3225
Sma I 3225
Nli387/7I 3225
Ava I 3225
Kpn I 3221
Acc 65I 3221
Sac I 3215
Ecl 136II 3215
Ban II 3215
Eco RI 3209
5 Bsg I
27 Hpa I
Sap I 3151
Bsp LU11I 3029
180 Bsa AI
204 Dra III
284 Bsm I
508 Bst DSI
581 Psi I
667 Bst Z17I
684 Spe I
AlwNI 2615
pES-14
3242 base pairs
Unique Sites
843 Pvu II
914 Bbe I
914 Kas I
914 Nar I
914 Sfo I
966 Nde I
Ahd I 2136
Bsa I 2069
Bsr FI 2056
Bpm I 2051
1160 Eco O109I
1160 Pss I
1218 Aat II
1334 Ssp I
Sca I 1658
1537 Xmn I

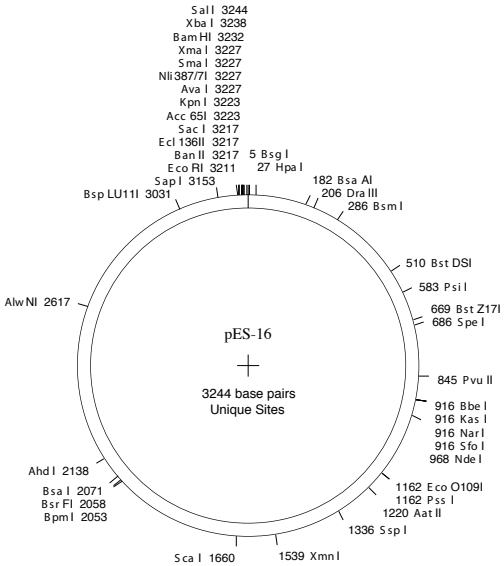
Sal I 3244
Xba I 3238
BamHI 3232
Xma I 3227
Sma I 3227
Nli387/7I 3227
Ava I 3227
Kpn I 3223
Acc 65I 3223
Sac I 3217
Ecl 136II 3217
Ban II 3217
Eco RI 3211
5 Bsg I
27 Hpa I
Sap I 3153
Bsp LU11I 3031
182 Bsa AI
206 Dra III
286 Bsm I
510 Bst DSI
583 Psi I
669 Bst Z17I
686 Spe I
AlwNI 2617
pES-16
3244 base pairs
Unique Sites
845 Pvu II
916 Bbe I
916 Kas I
916 Nar I
916 Sfo I
968 Nde I
Ahd I 2138
Bsa I 2071
Bsr FI 2058
Bpm I 2053
1162 Eco O109I
1162 Pss I
1220 Aat II
1336 Ssp I
Sca I 1660
1539 Xmn I

Appendix B

Abbreviations

Abbreviations

A	absorption or adenin
Å	angstrom
AFM	atomic force microscopy (= scanning force microscopy, SFM)
APS	ammoniumperoxidisulfate
ATP	adenosintriphoshpate
AU	arbitrary units
BSA	bovine serum albumin
bp	base pair(s)
C	cytosin
DNA	desoxyribonucleic acid
DNase	desoxyribonuclease
DTT	di-thio-threitol
dNTP	desoxyribonucleictriphosphate (N=adenin, guanin, cytosin and thymidin)
ε	extinction coefficient
E	extinction or energy
EDTA	ethylendiammintetracetate
EMSA	electrophoretic mobility shift assay
FA	fluorescence anisotropy
g	gramm
G	guanin
IHF	integration host factor
I	ionic strength
I	intensity
Hepes	4-(2-Hydroxyethyl)-piparazin-1-ethansulfonic acid
HPLC	high performance liquid chromatography
NTP	ribonucleotidetriphosphate (N= adenin, guanin, cytison and thymidin)
kB	kilobase(s)
kD	kilodalton
K_d	dissociation constant
M	molar
mA	milliampere
ml	milliliter
MW	molecular weight
nif	gene involved in nitrogen fixation
ng	nanogramm

nm	nanometer
nM	nanomolar
nt	nucleotides
NP-40	detergent Nonidet P40 (ethylphenolpolyethylenglycolether)
NTP	nucleotide triphosphate
NtrB	nitrogen regulatory protein B
NtrC	nitrogen regulatory protein C
NtrC-P	phosphorylated NtrC (= active form of NtrC)
oc	open cirlce
OD_x	optical densitiy at wavelenght x in nm
PAGE	polacrylamide gelelectrophoresis
pH	*potentia hydrogenii* = negative logarithm of H^+ concentration
pmol	picomole
q	quenching factor
r	anisotropy
Rho	fluorescent dye for DNA labeling
RNA	ribonucleic acid
RNAP	RNA polymerase
RNAP·σ^{54}	RNA polymerase associated with sigma54
rNTP	ribonucleictriphosphate (N=adenin, guanin, cytosin and thymidin)
RP_c	closed RNAP complex
ROX	fluorescent dye 6-carboxy-X-rhodamine
σ	sigma factor of RNAP or expression for degree of superhelicity of a DNA
sc	supercoiled
SFM	scanning force microscopy (= atomic force microscopy, AFM)
Θ	(Theta) fractional saturation/ occupancy
T	thymidin
TBE	Tris/borate/EDTA-buffer
TE	Tris/EDTA-buffer
TEMED	N,N,N',N'-tetramethylethylendiamin
TXN	transcription
Tris	Tris-(hydroxymethyl)-aminomethan
UV	ultraviolett
% (v/v)	volume per volume in percent
% (w/v)	weight per volume in percent

Appendix C

Bibliography

Bibliography

[1] A. Sentenac. Eukaryotic RNA polymerases. *CRC Crit Rev Biochem*, 18(1):31–90, 1985.

[2] M. Dundr, U. Hoffmann-Rohrer, Q. Hu, I. Grummt, L. I. Rothblum, R. D. Phair, and T. Misteli. A kinetic framework for a mammalian RNA polymerase *in vivo*. *Science*, 298(5598):1623–6, 2002.

[3] H. Kimura, K. Sugaya, and P. R. Cook. The transcription cycle of RNA polymerase II in living cells. *J Cell Biol*, 159(5):777–82, 2002.

[4] M. Ptashne and A. Gann. Transcriptional activation by recruitment. *Nature*, 386(6625):569–77, 1997.

[5] W. Wang, M. Carey, and J. D. Gralla. Polymerase II promoter activation: closed complex formation and ATP-driven start site opening. *Science*, 255(5043):450–3, 1992.

[6] J. D. Parvin and P. A. Sharp. DNA topology and a minimal set of basal factors for transcription by RNA polymerase II. *Cell*, 73(3):533–40, 1993.

[7] D. S. Luse and G. A. Jacob. Abortive initiation by RNA polymerase II in vitro at the adenovirus 2 major late promoter. *J Biol Chem*, 262(31):14990–7, 1987.

[8] D. S. Luse, T. Kochel, E. D. Kuempel, J. A. Coppola, and H. Cai. Transcription initiation by RNA polymerase II in vitro. At least two nucleotides must be added to form a stable ternary complex. *J Biol Chem*, 262(1):289–97, 1987.

[9] E. M. Blackwood and J. T. Kadonaga. Going the distance: a current view of enhancer action. *Science*, 281(5373):61–3, 1998.

[10] W. Su, S. Porter, S. Kustu, and H. Echols. DNA-looping and enhancer activity: association between DNA-bound NtrC activator and RNA polymerase at the bacterial *gln*A promoter. *Proc Natl Acad Sci U S A*, 87(14):5504–8, 1990.

[11] K. Rippe, P. H. von Hippel, and J. Langowski. Action at a distance: DNA-looping and initiation of transcription. *Trends Biochem Sci*, 20(12):500–6, 1995.

[12] S. T. Smale and J. T. Kadonaga. The RNA polymerase II core promoter. *Annu Rev Biochem*, 72:449–79, 2003.

[13] H. Xu and T. R. Hoover. Transcriptional regulation at a distance in bacteria. *Curr Opin Microbiol*, 4(2):138–44, 2001.

[14] R. H. Ebright. RNA polymerase: structural similarities between bacterial RNA polymerase and and eukaryotic rna polymerase II. *J Mol Biol*, 304:687–98, 2000.

[15] J. D. Gralla and J. Collado-Vides. Organization and function of transcription regulatory elements. In F. C. Neidhardt, editor, *Escherichia coli and Salmonella*, volume 1, pages 1232–1245. ASM Press, Washington, D. C., 1996.

[16] Martin Buck, Stephen Miller, Martin Drummond, and Ray Dixon. Upstream activator sequences are present in the promoters of nitrogen fixation genes. *Nature*, 320(6060):374–378, 1986.

[17] A. J. Ninfa, L. J. Reitzer, and B. Magasanik. Initiation of transcription at the bacterial *gln*Ap2 promoter by purified *E. coli* components is facilitated by enhancers. *Cell*, 50(7):1039–46, 1987.

[18] L. J. Reitzer and B. Magasanik. Transcription of *gln*A in *E. coli* is stimulated by activator bound to sites far from the promoter. *Cell*, 45(6):785–92, 1986.

[19] A. Wedel, D. S. Weiss, D. Popham, P. Droge, and S. Kustu. A bacterial enhancer functions to tether a transcriptional activator near a promoter. *Science*, 248(4954):486–90, 1990.

[20] S. Kustu, A. K. North, and D. S. Weiss. Prokaryotic transcriptional enhancers and enhancer-binding proteins. *Trends Biochem Sci*, 16(11):397–402, 1991.

[21] B. Magasanik. The regulation of nitrogen utilization in enteric bacteria. *J Cell Biochem*, 51(1):34–40, 1993.

[22] L. F. Liu and J. C. Wang. Supercoiling of the DNA template during transcription. *Proc Natl Acad Sci U S A*, 84(20):7024–7, 1987.

[23] D. M. Lilley, D. Chen, and R. P. Bowater. DNA supercoiling and transcription: topological coupling of promoters. *Q Rev Biophys*, 29(3):203–25, 1996.

[24] R. L. Tinker, K. P. Williams, G. A. Kassavetis, and E. P. Geiduschek. Transcriptional activation by a DNA-tracking protein: structural consequences of enhancement at the T4 late promoter. *Cell*, 77(2):225–37, 1994.

[25] K. Rippe. Making contacts on a nucleic acid polymer. *Trends Biochem Sci*, 26(12):733–40, 2001.

[26] J. D. Gralla. Transcriptional control–lessons from an *E. coli* promoter data base. *Cell*, 66(3):415–8, 1991.

[27] R. Schleif. DNA looping. *Annual Review of Biochemistry*, 61:199–223, 1992.

[28] M. Dunaway and P. Droge. Transactivation of the *Xenopus* rRNA gene promoter by its enhancer. *Nature*, 341(6243):657–9, 1989.

[29] H. P. Mueller-Storm, J. M. Sogo, and W. Schaffner. An enhancer stimulates transcription in trans when attached to the promoter via a protein bridge. *Cell*, 58(4):767–77, 1989.

[30] L. J. Reitzer, B. Movsas, and B. Magasanik. Activation of *gln*A transcription by nitrogen regulator I (NRI)-phosphate in *Escherichia coli*: evidence for a long-range physical interaction between NRI-phosphate and RNA polymerase. *J Bacteriol*, 171(10):5512–22, 1989.

[31] K. Rippe, M. Guthold, P. H. von Hippel, and C. Bustamante. Transcriptional activation via DNA-looping: visualization of intermediates in the activation pathway of *E. coli* RNA polymerase x sigma 54 holoenzyme by scanning force microscopy. *J Mol Biol*, 270(2):125–38, 1997.

[32] A. Schulz, J. Langowski, and K. Rippe. The effect of the DNA conformation on the rate of NtrC activated transcription of *Escherichia coli* RNA polymerase.sigma(54) holoenzyme. *J Mol Biol*, 300(4):709–25, 2000.

[33] M. Carmona and B. Magasanik. Activation of transcription at sigma 54-dependent promoters on linear templates requires intrinsic or induced bending of the DNA. *J Mol Biol*, 261(3):348–56, 1996.

[34] E. Santero, T. R. Hoover, A. K. North, D. K. Berger, S. C. Porter, and S. Kustu. Role of integration host factor in stimulating transcription from the sigma 54-dependent *nif*H promoter. *J Mol Biol*, 227(3):602–20, 1992.

[35] K. Rippe. Regulation der Transkription durch Enhancer. Habilitationsschrift, Universität Heidelberg, 1998.

[36] H. Merlitz, K. Rippe, K. V. Klenin, and J. Langowski. Looping dynamics of linear DNA molecules and the effect of DNA curvature: a study by Brownian dynamics simulation. *Biophysical Journal*, 74(2 Pt 1):773–779, 1998.

[37] M. J. Haykinson and R. C. Johnson. DNA looping and the helical repeat *in vitro* and *in vivo*: effect of HU protein and enhancer location on Hin invertasome assembly. *The EMBO Journal*, 12:2503–2512, 1993.

[38] S. M. Law, G. R. Bellomy, P. J. Schlax, and Jr. Record, M. T. In vivo thermodynamic analysis of repression with and without looping in lac constructs. Estimates of free and local lac repressor concentrations and of physical properties of a region of supercoiled DNA *in vivo*. *Journal of Molecular Biology*, 230:161–173, 1993.

[39] J. Shimada and H. Yamakawa. Ring-closure probabilities of twisted wormlike chains. Application to DNA. *Macromolecules*, 17:689–698, 1984.

[40] D Shore and R. L. Baldwin. Energetics of DNA twisting. I. Relation between twist and cyclization probability. *Journal of Molecular Biology*, 179:957–981, 1983.

[41] R. R. Burgess, A. A. Travers, J. J. Dunn, and E. K. Bautz. Factor stimulating transcription by RNA polymerase. *Nature*, 221(175):43–6, 1969.

[42] R. Gross, N. H. Carbonetti, R. Rossi, and R. Rappuoli. Functional analysis of the pertussis toxin promoter. *Res Microbiol*, 143(7):671–81, 1992.

[43] D. N. Arnosti and M. J. Chamberlin. Secondary sigma factor controls transcription of flagellar and chemotaxis genes in *Escherichia coli*. *Proc Natl Acad Sci U S A*, 86(3):830–4, 1989.

[44] A. D. Grossman, J. W. Erickson, and C. A. Gross. The *htp*r gene product of *E. coli* is a sigma factor for heat-shock promoters. *Cell*, 38(2):383–90, 1984.

[45] J. D. Helmann. Alternative sigma factors and the regulation of flagellar gene expression. *Mol Microbiol*, 5(12):2875–82, 1991.

[46] M. Lonetto, M. Gribskov, and C. A. Gross. The sigma 70 family: sequence conservation and evolutionary relationships. *J Bacteriol*, 174(12):3843–9, 1992.

[47] M. A. Lonetto, K. L. Brown, K. E. Rudd, and M. J. Buttner. Analysis of the *Streptomyces coelicolor sig*e gene reveals the existence of a subfamily of eubacterial RNA polymerase sigma factors involved in the regulation of extracytoplasmic functions. *Proc Natl Acad Sci U S A*, 91(16):7573–7, 1994.

[48] P. C. Loewen and R. Hengge-Aronis. The role of the sigma factor sigma s (KatF) in bacterial global regulation. *Annu Rev Microbiol*, 48:53–80, 1994.

[49] B. Magasanik. Genetic control of nitrogen assimilation in bacteria. *Annu Rev Genet*, 16:135–68, 1982.

[50] M. J. Merrick. In a class of its own–the RNA polymerase sigma factor sigma 54 (sigma N). *Mol Microbiol*, 10(5):903–9, 1993.

[51] D. B. Straus, W. A. Walter, and C. A. Gross. The heat shock response of *E. coli* is regulated by changes in the concentration of sigma 32. *Nature*, 329(6137):348–51, 1987.

[52] J. Hirschman, P. K. Wong, K. Sei, J. Keener, and S. Kustu. Products of nitrogen regulatory genes *ntr*A and *ntr*C of enteric bacteria activate *gln*A transcription *in vitro*: evidence that the *ntr*A product is a sigma factor. *Proc Natl Acad Sci U S A*, 82(22):7525–9, 1985.

[53] T. P. Hunt and B. Magasanik. Transcription of *gln*A by purified *Escherichia coli* components: core RNA polymerase and the products of *gln*F, *gln*G, and *gln*L. *Proc Natl Acad Sci U S A*, 82(24):8453–7, 1985.

[54] M. Buck, M. T. Gallegos, D. J. Studholme, Y. Guo, and J. D. Gralla. The bacterial enhancer-dependent sigma(54) (sigma(N)) transcription factor. *J Bacteriol*, 182(15):4129–36, 2000.

[55] S. Kustu, E. Santero, J. Keener, D. Popham, and D. Weiss. Expression of sigma 54 (*ntr*a)-dependent genes is probably united by a common mechanism. *Microbiol Rev*, 53(3):367–76, 1989.

[56] S. Sasse-Dwight and J. D. Gralla. Role of eukaryotic-type functional domains found in the prokaryotic enhancer receptor factor sigma 54. *Cell*, 62(5):945–54, 1990.

[57] J. T. Wang, A. Syed, M. Hsieh, and J. D. Gralla. Converting *Escherichia coli* (RNA) polymerase into an enhancer-responsive enzyme: role of an NH2-terminal leucine patch in sigma 54. *Science*, 270(5238):992–4, 1995.

[58] H. Barrios, B. Valderrama, and E. Morett. Compilation and analysis of sigma(54)-dependent promoter sequences. *Nucleic Acids Res*, 27(22):4305–13, 1999.

[59] E. Morett and M. Buck. *In vivo* studies on the interaction of RNA polymerase-sigma 54 with the *Klebsiella pneumoniae* and *Rhizobium meliloti nif*H promoters. The role of NifA in the formation of an open promoter complex. *J Mol Biol*, 210(1):65–77, 1989.

[60] D. S. Weiss, J. Batut, K. E. Klose, J. Keener, and S. Kustu. The phosphorylated form of the enhancer-binding protein NTRC has an ATPase activity that is essential for activation of transcription. *Cell*, 67(1):155–67, 1991.

[61] L. Morris, W. Cannon, F. Claverie-Martin, S. Austin, and M. Buck. DNA distortion and nucleation of local DNA unwinding within sigma-54 (sigma N) holoenzyme closed promoter complexes. *J Biol Chem*, 269(15):11563–71, 1994.

[62] S. Sasse-Dwight and J. D. Gralla. Probing the *Escherichia coli gln*ALG upstream activation mechanism *in vivo*. *Proc Natl Acad Sci U S A*, 85(23):8934–8, 1988.

[63] J. Greenblatt. RNA polymerase-associated transcription factors. *Trends Biochem Sci*, 16(11):408–11, 1991.

[64] B. Magasanik. Regulation of nitrogen utilization. In F. C. Neidhardt, editor, *Escherichia coli and Salmonella*, volume 1, pages 1344–1356. ASM Press, Washington, D. C., 1996.

[65] D. Bunick, R. Zandomeni, S. Ackerman, and R. Weinmann. Mechanism of RNA polymerase II–specific initiation of transcription in vitro: ATP requirement and uncapped runoff transcripts. *Cell*, 29(3):877–86, 1982.

[66] R. Hori and M. Carey. The role of activators in assembly of RNA polymerase II transcription complexes. *Current Opinion in Genetics and Development*, 4:236–244, 1994.

[67] A. J. Koleske and R. A. Young. The RNA polymerase II holoenzyme and its implications for gene regulation. *Trends in Biochemical Sciences*, 20:113–116, 1995.

[68] M. Buck and W. Cannon. Specific binding of the transcription factor sigma-54 to promoter DNA. *Nature*, 358(6385):422–4, 1992.

[69] D. L. Popham, D. Szeto, J. Keener, and S. Kustu. Function of a bacterial activator protein that binds to transcriptional enhancers. *Science*, 243(4891):629–35, 1989.

[70] A. Wedel and S. Kustu. The bacterial enhancer-binding protein NTRC is a molecular machine: ATP hydrolysis is coupled to transcriptional activation. *Genes Dev*, 9(16):2042–52, 1995.

[71] W. V. Cannon, M. T. Gallegos, and M. Buck. Isomerization of a binary sigma-promoter DNA complex by transcription activators. *Nat Struct Biol*, 7(7):594–601, 2000.

[72] J. Keener and S. Kustu. Protein kinase and phosphoprotein phosphatase activities of nitrogen regulatory proteins NTRB and NTRC of enteric bacteria: roles of the conserved amino-terminal domain of NTRC. *Proc Natl Acad Sci U S A*, 85(14):4976–80, 1988.

[73] J. Collado-Vides, B. Magasanik, and J. D. Gralla. Control site location and transcriptional regulation in *Escherichia coli*. *Microbiol Rev*, 55(3):371–94, 1991.

[74] J. Collado-Vides. Towards a unified grammatical model of sigma 70 and sigma 54 bacterial promoters. *Biochimie*, 78(5):351–63, 1996.

[75] A. K. North, K. E. Klose, K. M. Stedman, and S. Kustu. Prokaryotic enhancer-binding proteins reflect eukaryote-like modularity: the puzzle of nitrogen regulatory protein C. *J Bacteriol*, 175(14):4267–73, 1993.

[76] S. C. Porter, A. K. North, A. B. Wedel, and S. Kustu. Oligomerization of NTRC at the *gln*A enhancer is required for transcriptional activation. *Genes Dev*, 7(11):2258–73, 1993.

[77] L. Wang and J. D. Gralla. Multiple *in vivo* roles for the -12-region elements of sigma 54 promoters. *J Bacteriol*, 180(21):5626–31, 1998.

[78] L. J. Reitzer. Ammonia Assimilation and the Biosynthesis of Glutamine, Glutamate, Aspartate, Asparagine, L-Alanine, and D-Alanine. In F. C. Neidhardt, editor, *Escherichia coli and Salmonella*, volume 1, pages 391–407. ASM Press, Washington, D. C., 1996.

[79] J. Feng, T. J. Goss, R. A. Bender, and A. J. Ninfa. Repression of the *Klebsiella aerogenes nac* promoter. *J Bacteriol*, 177(19):5535–8, 1995.

[80] Boris Magasanik. Reversible phosphorylation of an enhancer binding protein regulates the transcription of bacterial nitrogen utilization genes. *Trends Biochem. Sci.*, 13(12):475–479, 1988.

[81] L. J. Reitzer and B. Magasanik. Expression of *gln*A in *Escherichia coli* is regulated at tandem promoters. *Proc Natl Acad Sci U S A*, 82(7):1979–83, 1985.

[82] L. J. Reitzer and B. Magasanik. Isolation of the nitrogen assimilation regulator, NRI, the product of the *gln*G gene of *Escherichia coli*. *Proc Natl Acad Sci U S A*, 80:5554–5558, 1983.

[83] N. McFarland, L. McCarter, S. Artz, and S. Kustu. Nitrogen regulatory locus *gln*r of enteric bacteria is composed of cistrons *ntr*b and *ntr*c: identification of their protein products. *Proc Natl Acad Sci U S A*, 78(4):2135–9, 1981.

[84] Y. M. Chen, K. Backman, and B. Magasanik. Characterization of a gene, *gln*L, the product of which is involved in the regulation of nitrogen utilization in *Escherichia coli*. *J Bacteriol*, 150(1):214–20, 1982.

[85] K. C. Backman, Y. M. Chen, S. Ueno-Nishio, and B. Magasanik. The product of *gln*L is not essential for regulation of bacterial nitrogen assimilation. *J Bacteriol*, 154(1):516–9, 1983.

[86] G. Pahel, D. M. Rothstein, and B. Magasanik. Complex *gln*A-*gln*L-*gln*G operon of *Escherichia coli*. *J Bacteriol*, 150(1):202–13, 1982.

[87] A. J. Ninfa and B. Magasanik. Covalent modification of the *gln*G product, NRI, by the *gln*L product, NRII, regulates the transcription of the *gln*ALG operon in *Escherichia coli*. *Proc Natl Acad Sci U S A*, 83(16):5909–13, 1986.

[88] S. C. Porter, A. K. North, and S. Kustu. Mechanism of transcriptional activation by NTRC. In J. A. Hoch and T. J. Silhavy, editors, *Two-Component Signal Transduction*, pages 147–158. ASM Press, Washington, D. C., 1995.

[89] J. Feng, T. J. Goss, R. A. Bender, and A. J. Ninfa. Activation of transcription initiation from the *nac* promoter of *Klebsiella aerogenes*. *J Bacteriol*, 177(19):5523–34, 1995.

[90] S. P. Shiau, B. L. Schneider, W. Gu, and L. J. Reitzer. Role of nitrogen regulator I (NtrC), the transcriptional activator of *gln*A in enteric bacteria, in reducing expression of *gln*A during nitrogen-limited growth. *J Bacteriol*, 174(1):179–85, 1992.

[91] J. Feng, M. R. Atkinson, W. McCleary, J. B. Stock, B. L. Wanner, and A. J. Ninfa. Role of phosphorylated metabolic intermediates in the regulation of glutamine synthetase synthesis in *Escherichia coli*. *J Bacteriol*, 174(19):6061–70, 1992.

[92] Y. Tintut, C. Wong, Y. Jiang, M. Hsieh, and J. D. Gralla. RNA polymerase binding using a strongly acidic hydrophobic-repeat region of sigma 54. *Proc Natl Acad Sci U S A*, 91(6):2120–4, 1994.

[93] P. K. Wong, D. Popham, J. Keener, and S. Kustu. *In vitro* transcription of the nitrogen fixation regulatory operon *nif*LA of *Klebsiella pneumoniae*. *J Bacteriol*, 169(6):2876–80, 1987.

[94] S. Austin, C. Kundrot, and R. Dixon. Influence of a mutation in the putative nucleotide binding site of the nitrogen regulatory protein NTRC on its positive control function. *Nucleic Acids Res*, 19(9):2281–7, 1991.

[95] M. Buck and W. Cannon. Activator-independent formation of a closed complex between sigma 54-holoenzyme and *nif*H and *nif*U promoters of *Klebsiella pneumoniae*. *Mol Microbiol*, 6(12):1625–30, 1992.

[96] S. D. Minchin, S. Austin, and R. A. Dixon. Transcriptional activation of the *Klebsiella pneumoniae nif*LA promoter by NTRC is face-of-the-helix dependent and the activator stabilizes the interaction of sigma 54-RNA polymerase with the promoter. *Embo J*, 8(11):3491–9, 1989.

[97] D. Popham, J. Keener, and S. Kustu. Purification of the alternative sigma factor, sigma 54, from *Salmonella typhimurium* and characterization of sigma 54-holoenzyme. *J Biol Chem*, 266(29):19510–8, 1991.

[98] J. D. Puglisi and Jr. Tinoco, I. Absorbance melting curves of RNA. *Methods Enzymol*, 180:304–25, 1989.

[99] Y. Guo, L. Wang, and J. D. Gralla. A fork junction DNA-protein switch that controls promoter melting by the bacterial enhancer-dependent sigma factor. *Embo J*, 18(13):3736–45, 1999.

[100] V. Weiss, F. Claverie-Martin, and B. Magasanik. Phosphorylation of nitrogen regulator I of *Escherichia coli* induces strong cooperative binding to DNA essential for activation of transcription. *Proc Natl Acad Sci U S A*, 89(11):5088–92, 1992.

[101] H. C. Birnboim and J. Doly. A rapid alkaline extraction procedure for screening recombinant plasmid DNA. *Nucleic Acids Res*, 7(6):1513–23, 1979.

[102] M. McClelland and M. Nelson. The effect of site-specific DNA methylation on restriction endonucleases and DNA modification methyltransferases–a review. *Gene*, 74(1):291–304, 1988.

[103] A. Schulz. *Regulation der Transkription aus der Distanz: Untersuchungen an einem prokaryotischen Promoter-Enhancer-System.* PhD thesis, Universität Heidelberg, 2000.

[104] A. Schulz, N. Mucke, J. Langowski, and K. Rippe. Scanning force microscopy of *Escherichia coli* RNA polymerase.sigma54 holoenzyme complexes with DNA in buffer and in air. *J Mol Biol*, 283(4):821–36, 1998.

[105] Cantor and Schimmel. *Biophysical Chemistry*, volume 2. W. H. Freeman and Company, New York, 1980.

[106] Jr. Record, M. T., M. L. Lohman, and P. De Haseth. Ion effects on ligand-nucleic acid interactions. *J Mol Biol*, 107(2):145–58, 1976.

[107] T. M. Lohman and D. P. Mascotti. Thermodynamics of ligand-nucleic acid interactions. *Methods Enzymol*, 212:400–24, 1992.

[108] J. R. Lakowicz. *Principles of fluorescence spectroscopy.* Plenum Press, New York, London, 1983.

[109] G. Binnig, C. F. Quate, and C. Gerber. Atomic force microscope. *Physical Review Letters*, 56(9):930–933, 1986.

[110] C. Bustamante, C. Rivetti, and D. J. Keller. Scanning force microscopy under aqueous solutions. *Curr Opin Struct Biol*, 7(5):709–16, 1997.

[111] F. W. Sevenich, J. Langowski, V. Weiss, and K. Rippe. DNA binding and oligomerization of NtrC studied by fluorescence anisotropy and fluorescence correlation spectroscopy. *Nucleic Acids Res*, 26(6):1373–81, 1998.

[112] T. Heyduk and J. C. Lee. Application of fluorescence energy transfer and polarization to monitor *Escherichia coli* cAMP receptor protein and lac promoter interaction. *Proc Natl Acad Sci U S A*, 87(5):1744–8, 1990.

[113] T. Heyduk, J. C. Lee, Y. W. Ebright, E. E. Blatter, Y. Zhou, and R. H. Ebright. CAP interacts with RNA polymerase in solution in the absence of promoter DNA. *Nature*, 364(6437):548–9, 1993.

[114] V. LeTilly and C. A. Royer. Fluorescence anisotropy assays implicate protein-protein interactions in regulating trp repressor DNA binding. *Biochemistry*, 32(30):7753–8, 1993.

[115] C. R. Guest, R. A. Hochstrasser, C. G. Dupuy, D. J. Allen, S. J. Benkovic, and D. P. Millar. Interaction of DNA with the Klenow fragment of DNA polymerase I studied by time-resolved fluorescence spectroscopy. *Biochemistry*, 30(36):8759–70, 1991.

[116] R. J. Reedstrom, M. P. Brown, A. Grillo, D. Roen, and C. A. Royer. Affinity and specificity of trp repressor-DNA interactions studied with fluorescent oligonucleotides. *J Mol Biol*, 273(3):572–85, 1997.

[117] M. Boyer, N. Poujol, E. Margeat, and C. A. Royer. Quantitative characterization of the interaction between purified human estrogen receptor alpha and DNA using fluorescence anisotropy. *Nucleic Acids Res*, 28(13):2494–502, 2000.

[118] D. F. Senear, J. B. Ross, and T. M. Laue. Analysis of protein and DNA-mediated contributions to cooperative assembly of protein-DNA complexes. *Methods*, 16(1):3–20, 1998.

[119] Jr. Record, M. T., W. Zhang, and C. F. Anderson. Analysis of effects of salts and uncharged solutes on protein and nucleic acid equilibria and processes: a practical guide to recognizing and interpreting polyelectrolyte effects, Hofmeister effects, and osmotic effects of salts. *Adv Protein Chem*, 51:281–353, 1998.

[120] K. E. Klose, D. S. Weiss, and S. Kustu. Glutamate at the site of phosphorylation of nitrogen-regulatory protein NTRC mimics aspartyl-phosphate and activates the protein. *Journal of Molecular Biology*, 232:67–78, 1993.

[121] D. A. Sanders, Castro Bl Gillece, A. L. Burlingame, and De Jr Koshland. Phosphorylation site of NtrC, a protein phosphatase whose covalent intermediate activates transcription. *Journal of Bacteriology*, 174(15):5117–5122, 1992.

[122] K. Rippe, N. Mucke, and A. Schulz. Association states of the transcription activator protein NtrC from *E. coli* determined by analytical ultracentrifugation. *J Mol Biol*, 278(5):915–33, 1998.

[123] S. K. Vogel, A. Schulz, and K. Rippe. Binding affinity of *Escherichia coli* RNA polymerase*sigma54 holoenzyme for the *glnap2*, *nif*h and *nif*l promoters. *Nucleic Acids Res*, 30(18):4094–101, 2002.

[124] G. Brahms, S. Brahms, and B. Magasanik. A sequence-induced superhelical DNA segment serves as transcriptional enhancer. *J Mol Biol*, 246(1):35–42, 1995.

[125] P. Chen and L. J. Reitzer. Active contribution of two domains to cooperative DNA binding of the enhancer-binding protein nitrogen regulator I

(NtrC) of *Escherichia coli*: stimulation by phosphorylation and the binding of ATP. *J Bacteriol*, 177(9):2490–6, 1995.

[126] W. R. McClure. Rate-limiting steps in RNA chain initiation. *Proc Natl Acad Sci U S A*, 77(10):5634–8, 1980.

[127] R. Dixon, R. R. Eady, G. Espin, S. Hill, M. Iaccarino, D. Kahn, and M. Merrick. Analysis of regulation of *Klebsiella pneumoniae* nitrogen fixation (*nif*) gene cluster with gene fusions. *Nature*, 286(5769):128–32, 1980.

[128] D. S. Weiss, K. E. Klose, T. R. Hoover, A. K. North, S. C. Porter, A. B. Wedel, and S. Kustu. Prokaryotic transcriptional enhancers. In S. L. McKnight and K. R. Yamamoto, editors, *Transcriptional Regulation*, volume 2, pages 667–694. Cold Spring Harbor Laboratory Press, Cold Spring Harbor, NY, 1992.

[129] H. Khan, M. Buck, and R. Dixon. Deletion loop mutagenesis of the *nif*L promoter from *Klebsiella pneumoniae*: role of the -26 to -12 region in promoter function. *Gene*, 45(3):281–8, 1986.

[130] S. L. Shaner, P. Melancon, K. S. Lee, R. R. Burgess, and M. T. Record, Jr. Ion effects on the aggregation and DNA-binding reactions of *Escherichia coli* RNA polymerase. *Cold Spring Harb Symp Quant Biol*, 47 Pt 1:463–72, 1983.

[131] H. S. Strauss, R. R. Burgess, and Jr. Record, M. T. Binding of *Escherichia coli* ribonucleic acid polymerase holoenzyme to a bacteriophage T7 promoter-containing fragment: evaluation of promoter binding constants as a function of solution conditions. *Biochemistry*, 19(15):3504–15, 1980.

[132] S. Cayley, B. A. Lewis, H. J. Guttman, and Jr. Record, M. T. Characterization of the cytoplasm of *Escherichia coli* K-12 as a function of external osmolarity. Implications for protein-DNA interactions in vivo. *J Mol Biol*, 222(2):281–300, 1991.

[133] Y. Kao-Huang, A. Revzin, A. P. Butler, P. O'Conner, D. W. Noble, and P. H. von Hippel. Nonspecific DNA binding of genome-regulating proteins as a biological control mechanism: measurement of DNA-bound *Escherichia coli* lac repressor *in vivo*. *Proc Natl Acad Sci U S A*, 74(10):4228–32, 1977.

[134] P. J. Schlax, M. W. Capp, and Jr. Record, M. T. Inhibition of transcription initiation by lac repressor. *J Mol Biol*, 245(4):331–50, 1995.

[135] T. R. Hoover, E. Santero, S. Porter, and S. Kustu. The integration host factor stimulates interaction of RNA polymerase with NIFA, the transcriptional activator for nitrogen fixation operons. *Cell*, 63(1):11–22, 1990.

[136] A. K. Cheema, N. R. Choudhury, and H. K. Das. A- and T-tract-mediated intrinsic curvature in native DNA between the binding site of the upstream activator NtrC and the *nif*LA promoter of *Klebsiella pneumoniae* facilitates transcription. *J Bacteriol*, 181(17):5296–302, 1999.

[137] J. A. Molina-Lopez, F. Govantes, and E. Santero. Geometry of the process of transcription activation at the sigma 54-dependent *nif*H promoter of *Klebsiella pneumoniae*. *J Biol Chem*, 269(41):25419–25, 1994.

[138] T. Ellenberger and A. Landy. A good turn for DNA: the structure of integration host factor bound to DNA. *Structure*, 5(2):153–157, 1997.

[139] P. A. Rice. Making DNA do a U-turn: IHF and related proteins. *Curr Opin Struct Biol*, 7(1):86–93, 1997.

[140] P. A. Rice, S. Yang, K. Mizuuchi, and H. A. Nash. Crystal structure of an IHF-DNA complex: a protein-induced DNA U-turn. *Cell*, 87(7):1295–1306, 1996.

[141] M. Carmona, F. Claverie-Martin, and B. Magasanik. DNA bending and the initiation of transcription at sigma 54-dependent bacterial promoters. *Proc Natl Acad Sci U S A*, 94(18):9568–72, 1997.

[142] F. Claverie-Martin and B. Magasanik. Positive and negative effects of DNA bending on activation of transcription from a distant site. *J Mol Biol*, 227(4):996–1008, 1992.

[143] S. Austin, N. Henderson, and R. Dixon. Requirements for transcriptional activation in vitro of the nitrogen-regulated *gln*A and *nif*LA promoters from *Klebsiella pneumoniae*: dependence on activator concentration. *Mol Microbiol*, 1(1):92–100, 1987.

[144] G. Bertoni, N. Fujita, A. Ishihama, and V. de Lorenzo. Active recruitment of sigma54-RNA polymerase to the Pu promoter of *Pseudomonas putida*: role of IHF and alphaCTD. *Embo J*, 17(17):5120–8, 1998.

[145] M. Carmona, V. de Lorenzo, and G. Bertoni. Recruitment of rna polymerase is a rate-limiting step for the activation of the sigma(54) promoter Pu of *Pseudomonas putida*. *J Biol Chem*, 274(47):33790–4, 1999.

[146] W. Cannon, M. T. Gallegos, P. Casaz, and M. Buck. Amino-terminal sequences of sigmaN (sigma54) inhibit RNA polymerase isomerization. *Genes Dev*, 13(3):357–70, 1999.

[147] J. T. Wang, A. Syed, and J. D. Gralla. Multiple pathways to bypass the enhancer requirement of sigma 54 RNA polymerase: roles for DNA and protein determinants. *Proc Natl Acad Sci U S A*, 94(18):9538–43, 1997.

[148] M. Buck and W. Cannon. Mutations in the RNA polymerase recognition sequence of the *Klebsiella pneumoniae nif*H promoter permitting transcriptional activation in the absence of NifA binding to upstream activator sequences. *Nucleic Acids Res*, 17(7):2597–612, 1989.

[149] W. V. Cannon, R. Kreutzer, H. M. Kent, E. Morett, and M. Buck. Activation of the *Klebsiella pneumoniae nif*u promoter: identification of multiple and overlapping upstream NifA binding sites. *Nucleic Acids Res*, 18(7):1693–701, 1990.

[150] S. Whitehall, S. Austin, and R. Dixon. DNA supercoiling response of the sigma54-dependent *Klebsiella pneumoniae nif*L promoter *in vitro*. *J Mol Biol*, 225(3):591–607, 1992.

[151] V. Bondarenko, Y. Liu, A. Ninfa, and V. M. Studitsky. Action of prokaryotic enhancer over a distance does not require continued presence of promoter-bound sigma 54 subunit. *Nucleic Acids Res*, 30(3):636–42., 2002.

[152] Y. Liu, V. Bondarenko, A. Ninfa, and V. M. Studitsky. DNA supercoiling allows enhancer action over a large distance. *Proc Natl Acad Sci U S A*, 98(26):14883–8, 2001.

[153] J. F. Marko and E. D. Siggia. Fluctuations and supercoiling of DNA. *Science*, 265(5171):506–8, 1994.

[154] K. V. Klenin, M. D. Frank-Kamenetskii, and J. Langowski. Modulation of intramolecular interactions in superhelical DNA by curved sequences: a monte carlo simulation study. *Biophysical Journal*, 68(1):81–88, 1995.

[155] H. Jian, T. Schlick, and A. Vologodskii. Internal motion of supercoiled DNA: brownian dynamics simulations of site juxtaposition. *J Mol Biol*, 284(2):287–96, 1998.

[156] B. Révet, S. Brahms, and G. Brahms. Binding of the transcription activator NRI (NTRC) to a supercoiled DNA segment imitates association with the natural enhancer: An electron microscopic investigation. *Proceedings of the National Academy of Sciences of the USA*, 92:7535–7539, 1995.

[157] T. Cremer and C. Cremer. Chromosome territories, nuclear architecture and gene regulation in mammalian cells. *Nat Rev Genet*, 2(4):292–301, 2001.

[158] T. A. Knoch. Towards a holistic understanding of the human genome by determination and integration of its sequential and three-dimensional organization. In E. Krause, W. Jäger, and M. Resch, editors, *High Performance Computing in Science and Engineering*, pages 421–440. Springer Berlin-Heidelberg-New York, 2003.

[159] K. Rippe. Simultaneous binding of two DNA duplexes to the NtrC-enhancer complex studied by two-color fluorescence cross-correlation spectroscopy. *Biochemistry*, 39(9):2131–2139, 2000.

[160] C. Wyman, I Rombel, A. K. North, C. Bustamante, and S. Kustu. Unusual oligomerization required for activity of a bacterial enhancer-binding protein. *Science*, 275:1658–1661, 1997.

[161] M. R. Atkinson, N. Pattaramanon, and A. J. Ninfa. Governor of the *gln*Ap2 promoter of *Escherichia coli*. *Mol Microbiol*, 46(5):1247–57, 2002.

[162] R. Dixon. Tandem promoters determine regulation of the *Klebsiella pneumoniae* glutamine synthetase (*gln*a) gene. *Nucleic Acids Res*, 12(20):7811–30, 1984.

[163] R. Bueno, G. Pahel, and B. Magasanik. Role of *gln*B and *gln*D gene products in regulation of the *gln*ALG operon of *Escherichia coli*. *J Bacteriol*, 164(2):816–22, 1985.

[164] F. Claverie-Martin and B. Magasanik. Role of integration host factor in the regulation of the *gln*Hp2 promoter of *Escherichia coli*. *Proc Natl Acad Sci U S A*, 88(5):1631–5, 1991.

[165] M. R. Atkinson, T. A. Blauwkamp, V. Bondarenko, V. Studitsky, and A. J. Ninfa. Activation of the *gln*A, *gln*K, and nac promoters as *Escherichia coli* undergoes the transition from nitrogen excess growth to nitrogen starvation. *J Bacteriol*, 184(19):5358–63, 2002.

Appendix D

Index

Index